# Backprojection Methods

Peter Shearer

*IGPP/SIO/U.C. San Diego*

September 9, 2009

*Earthquake Research Institute*

# Migration in Reflection Seismology

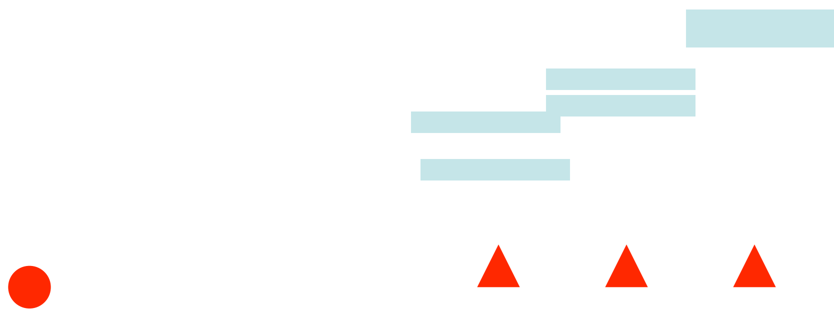

Assume point scatterers

For each pixel in image, sum values from each trace at time of predicted source-to-scatterer-to-receiver travel time

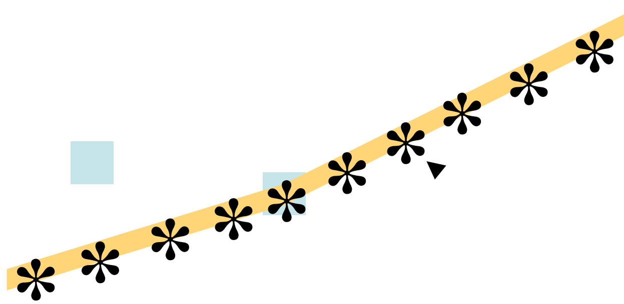

Complete image is sum of individual point scatterers

"Exploding reflector" model

# Source Imaging Using Back-projection

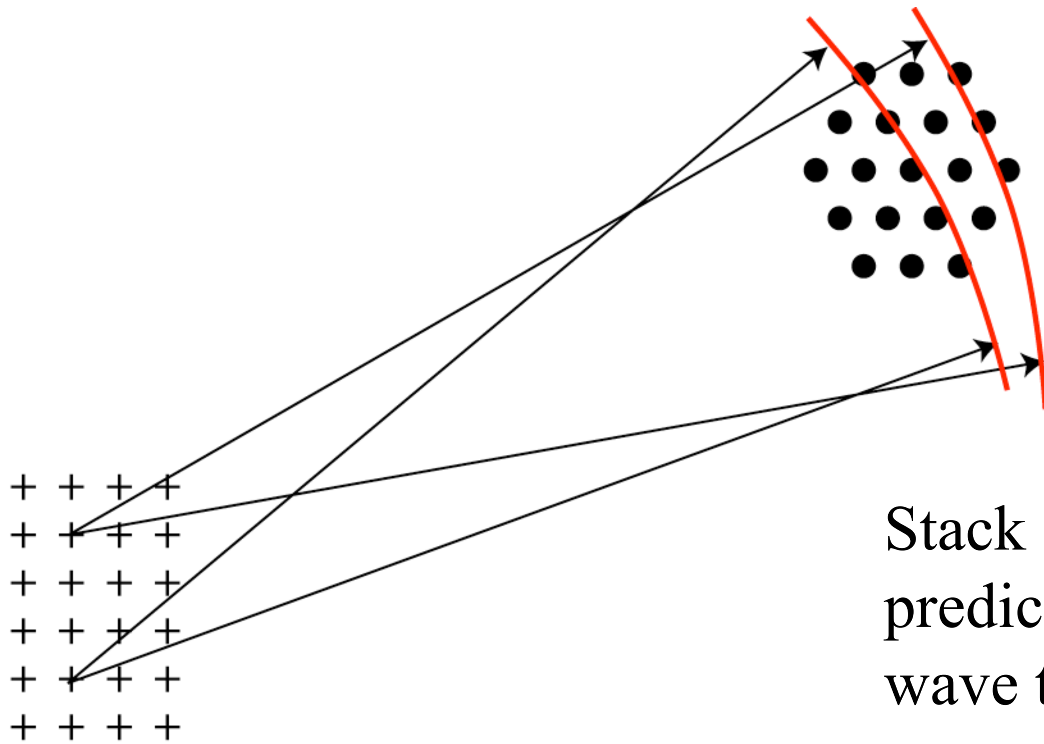

Stack along predicted P-wave travel time curves

Assume grid of possible source locations

# Seismic imaging of the 2004 Sumatra-Andaman and Parkfield earthquakes

Peter Shearer, Miaki Ishii & Bettina Allmann

*IGPP, U.C. San Diego*

Miaki Ishii

Bettina Allmann

# Two very different earthquakes

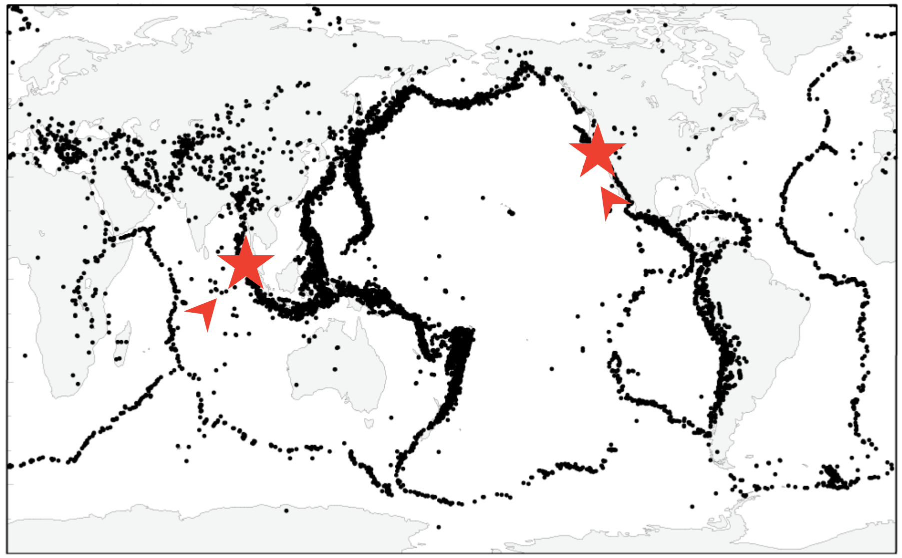

12/25/04 Sumatra-Andaman

- Mw 9.15 (largest since ‘64)
- 1300 km long
- Subduction zone thrust
- 230,000 deaths

9/28/04 Parkfield, California

- Mw 6.0
- 20 km long
- Strike-slip on San Andreas
- 0 deaths

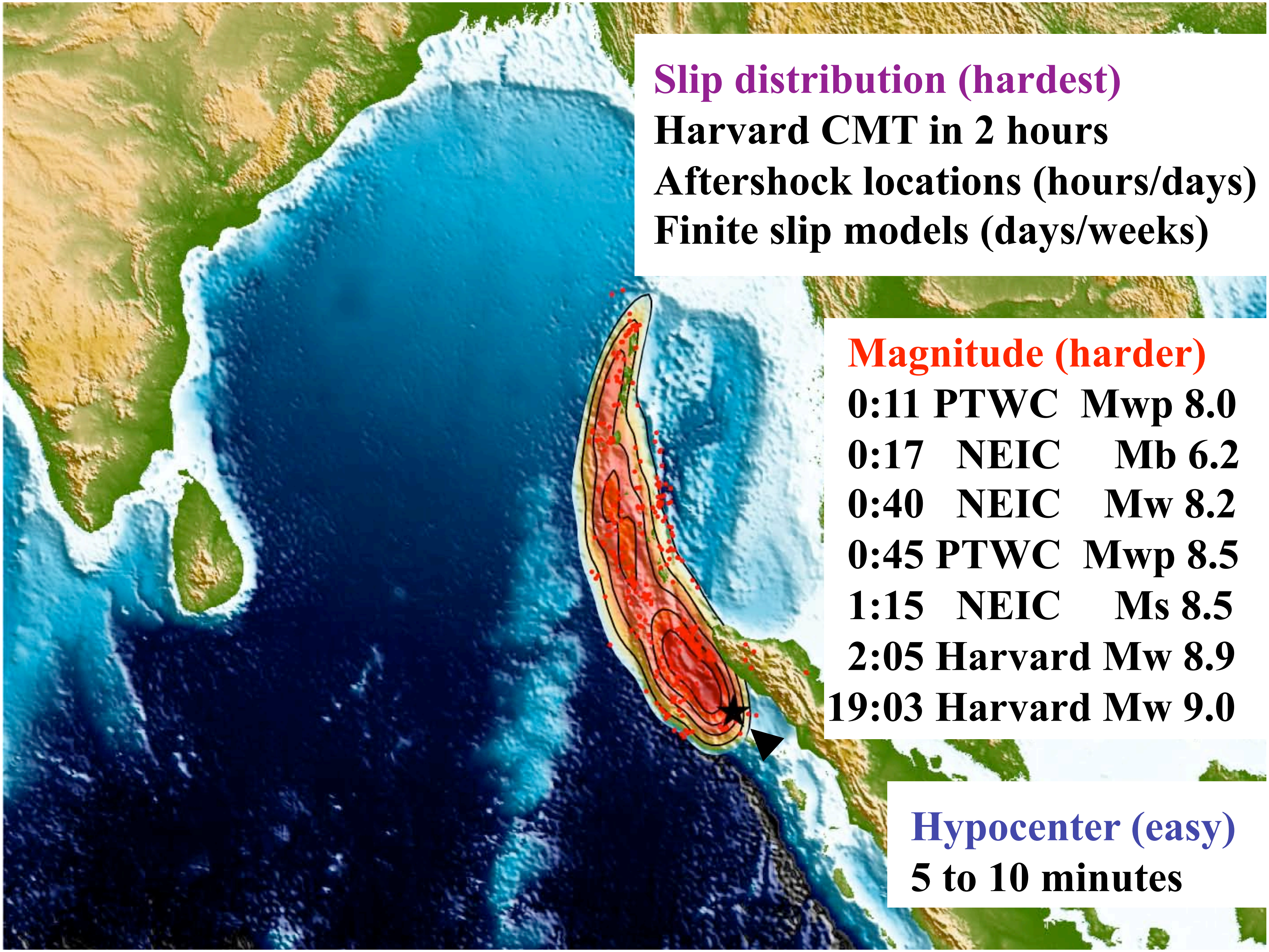
Slip distribution (hardest)
Harvard CMT in 2 hours
Aftershock locations (hours/days)
Finite slip models (days/weeks)
Magnitude (harder)
0:11 PTWC Mwp 8.0
0:17 NEIC Mb 6.2
0:40 NEIC Mw 8.2
0:45 PTWC Mwp 8.5
1:15 NEIC Ms 8.5
2:05 Harvard Mw 8.9
19:03 Harvard Mw 9.0
Hypocenter (easy)
5 to 10 minutes

# Finite source inversion

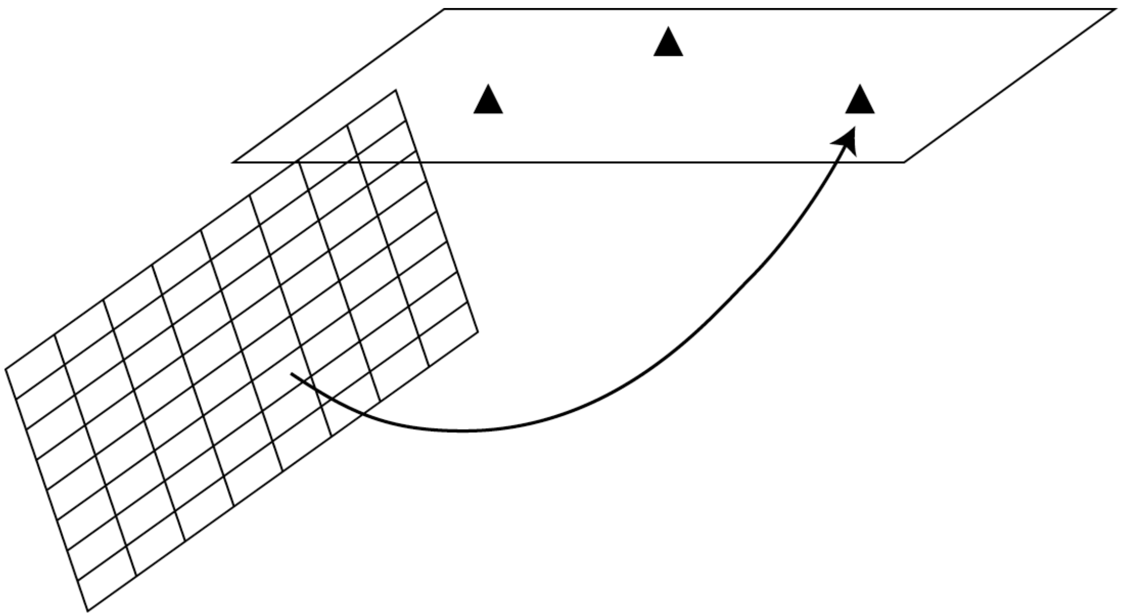

data

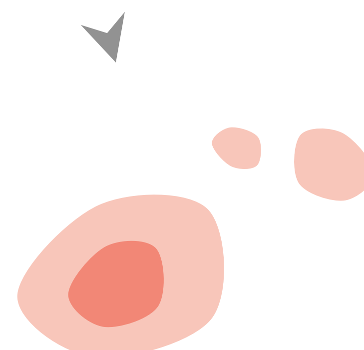

Slip model

- Assume specific fault geometry & gridding
- Compute Green's function (synthetic seismogram) from each grid point to each station
- Set up and solve inverse problem for time-space slip model that predicts observed seismograms
- Only stable at relatively long periods

# How long do seismic waves take to cross the globe?

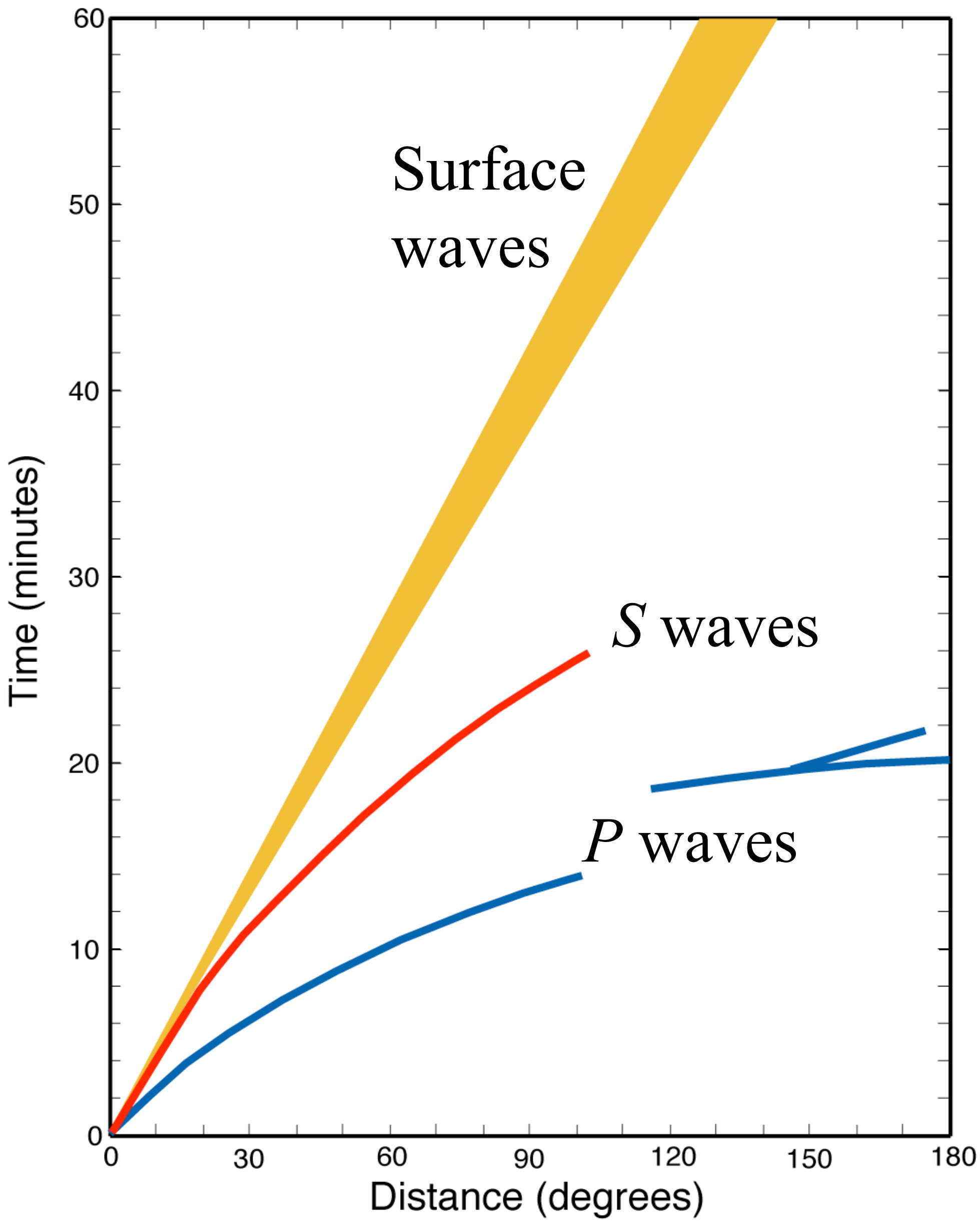


- *P* (compressional) waves are fastest and arrive first
  - cover half the globe in 13 minutes
- *S* (shear) waves arrive second
- Surface waves are slowest and arrive last
  - cover half the globe in 45 minutes

# *P* waves from two big earthquakes

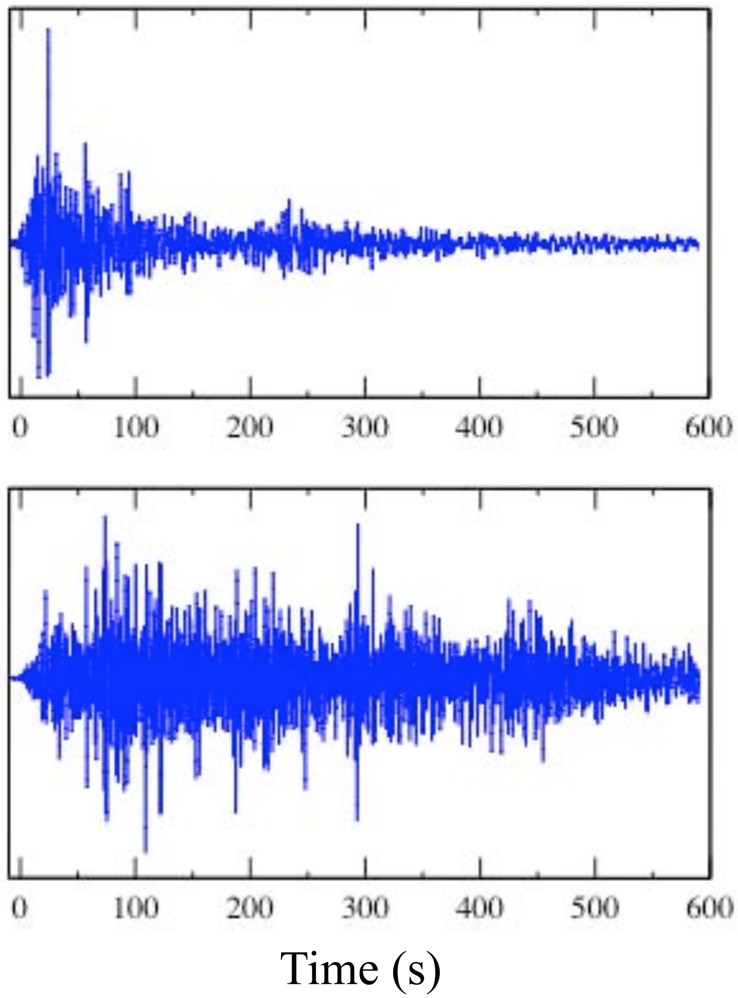


23 December 2004
MacQuarie Island
$M_W$ 8.1

26 December 2004
Northern Sumatra
$M_W$ 9.0

Records from Japanese station AGMH

# Back-projection to image earthquake rupture

Japanese Hi-Net array of 700 stations

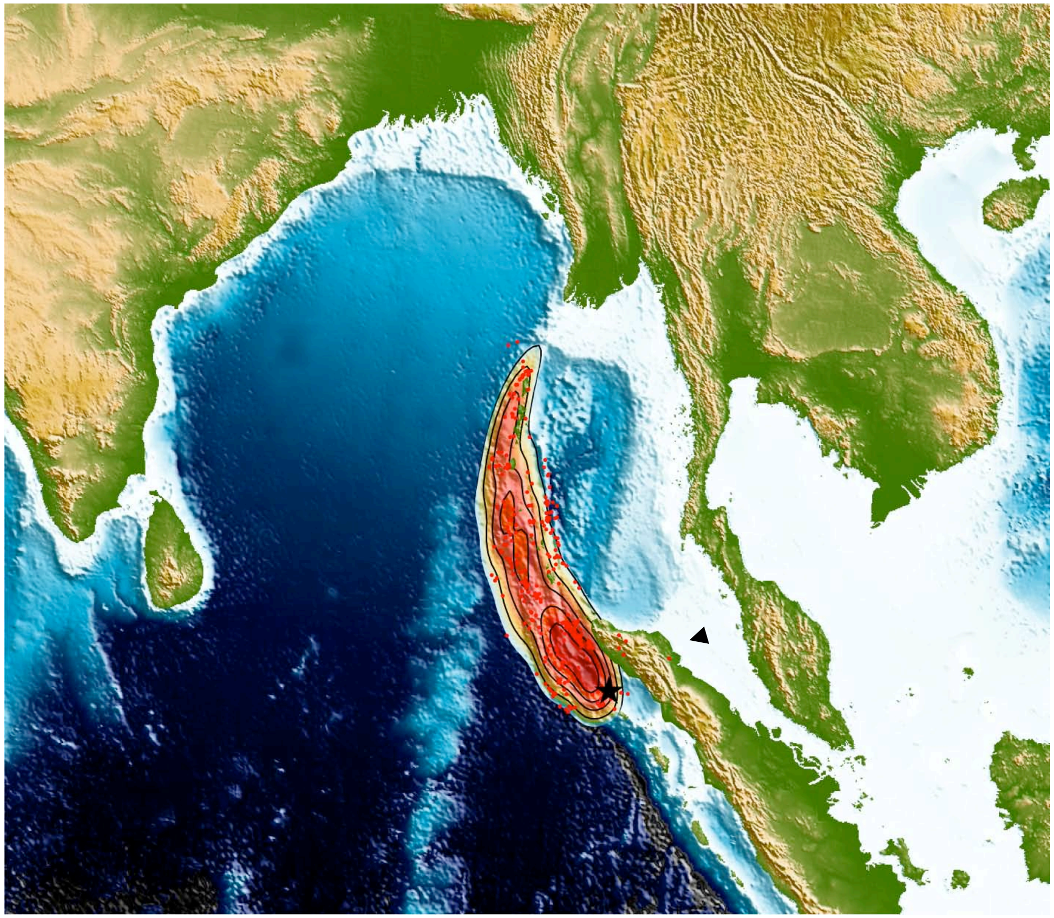

2004 Sumatra-Andaman earthquake

from *Ishii et al*. (2005)

# Traditional array processing

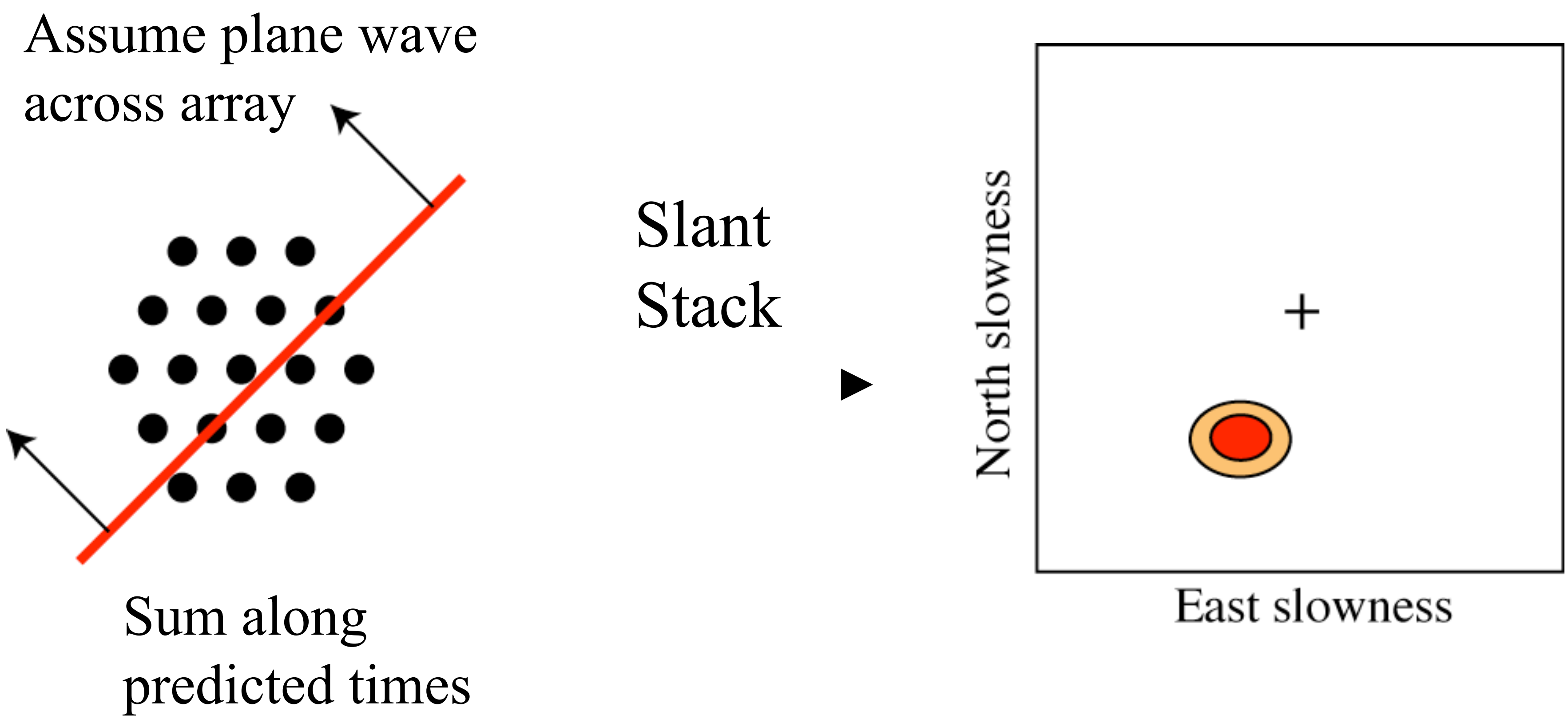

# Curved wavefront complications

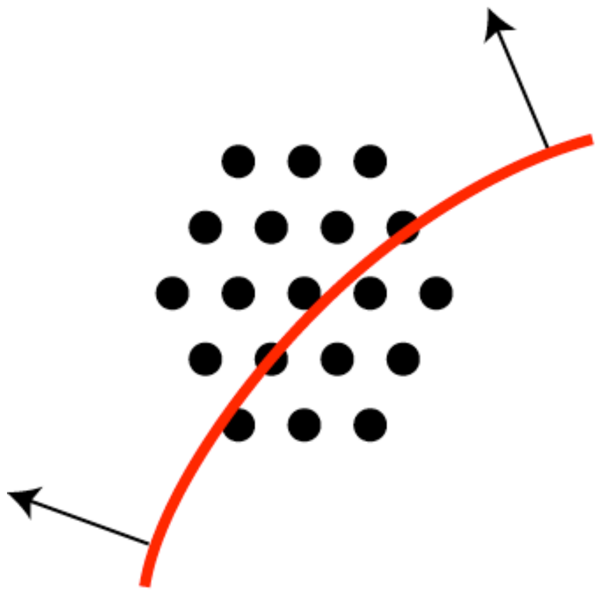

Slant
Stack

►

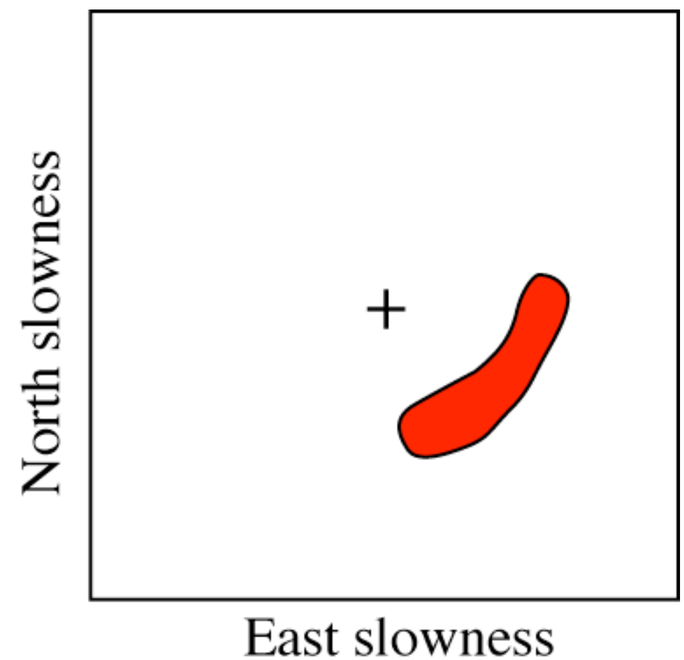


Plane wave assumption produces blurred image of source

# Direct Back-projection

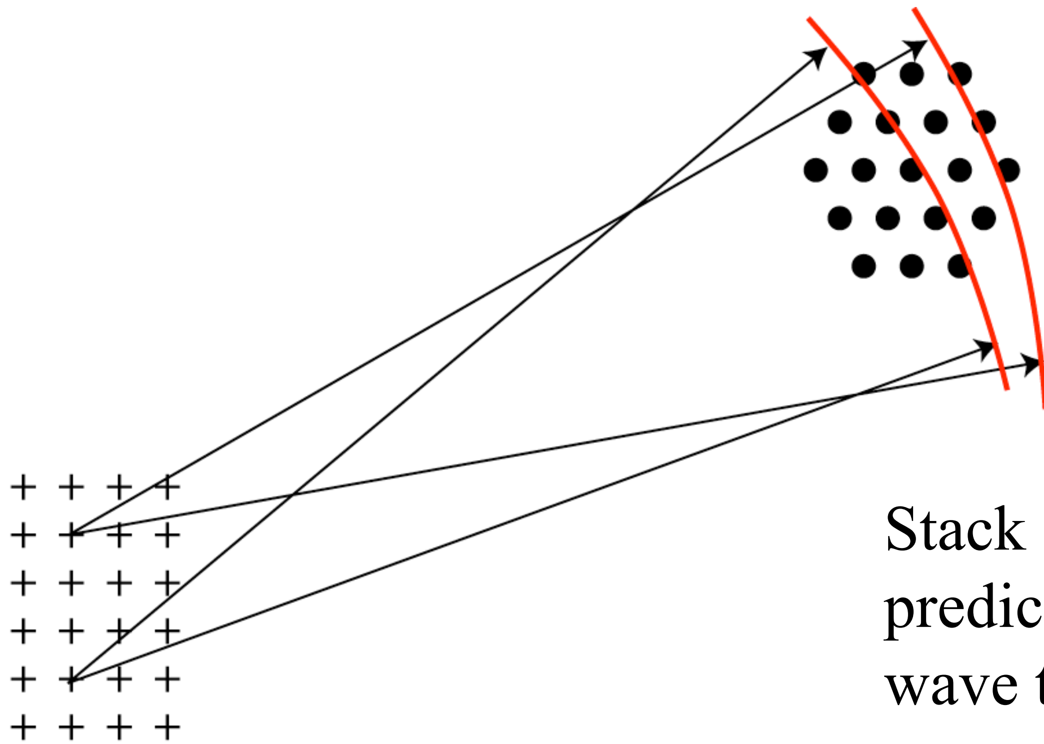

Stack along predicted P-wave travel time curves

Assume grid of possible source locations

# Problem: Incoherent stacking from time shifts from 3-D structure

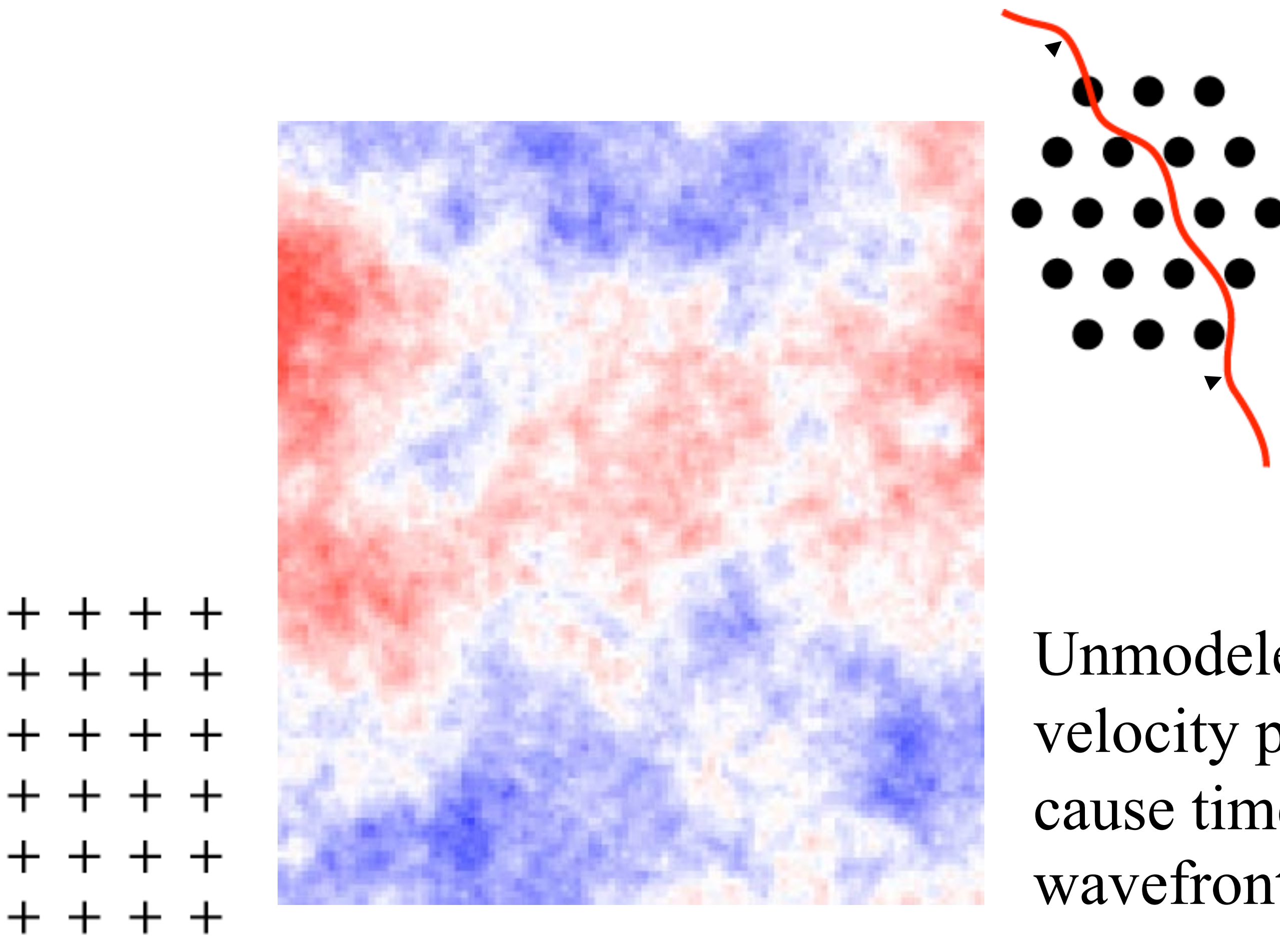

Unmodeled 3-D velocity perturbations cause time shifts in wavefront

# Sumatra earthquake *P*-waves

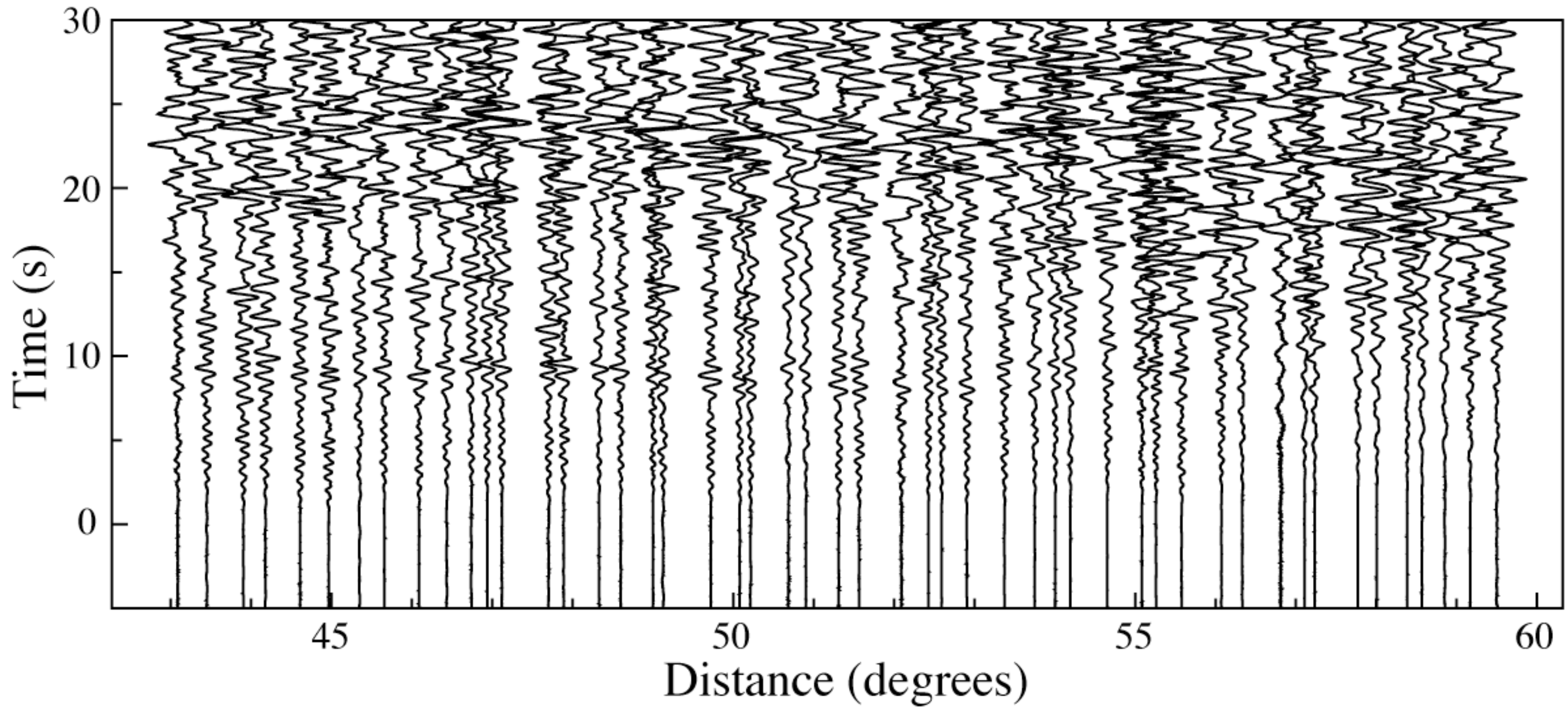


Aligned on theoretical (iasp91) *P*-wave travel times

# Migration in Reflection Seismology

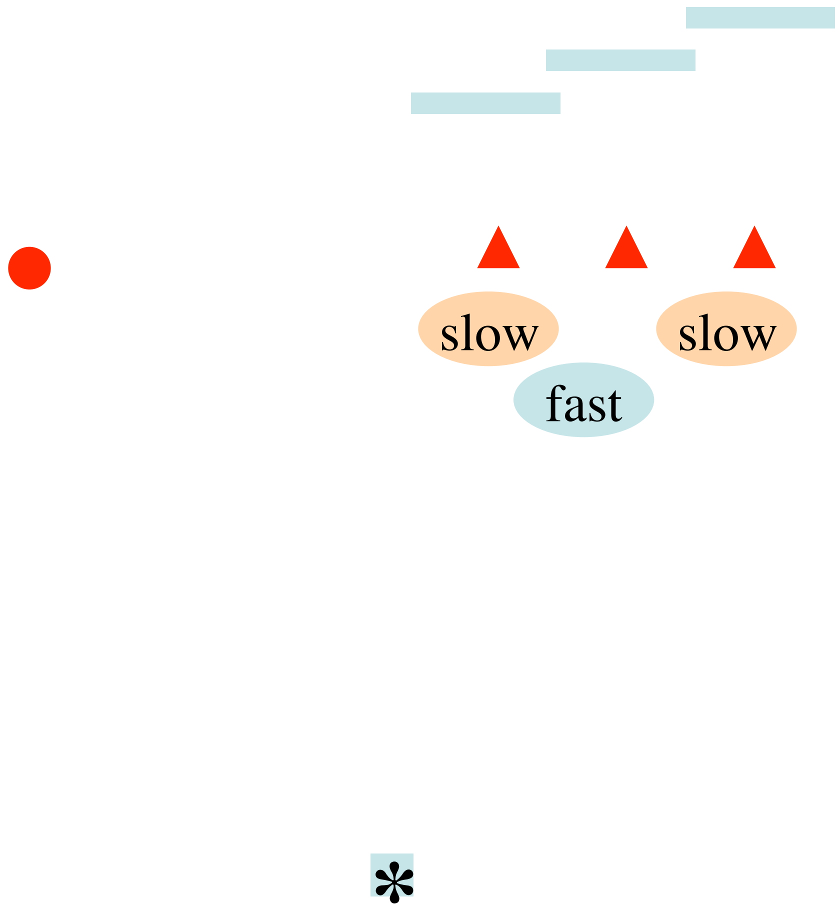


Problem:

Time shifts from 3-D structure can destroy stack coherence

Solution:

Statics corrections (station terms)

# Align *P*-waves with cross-correlation

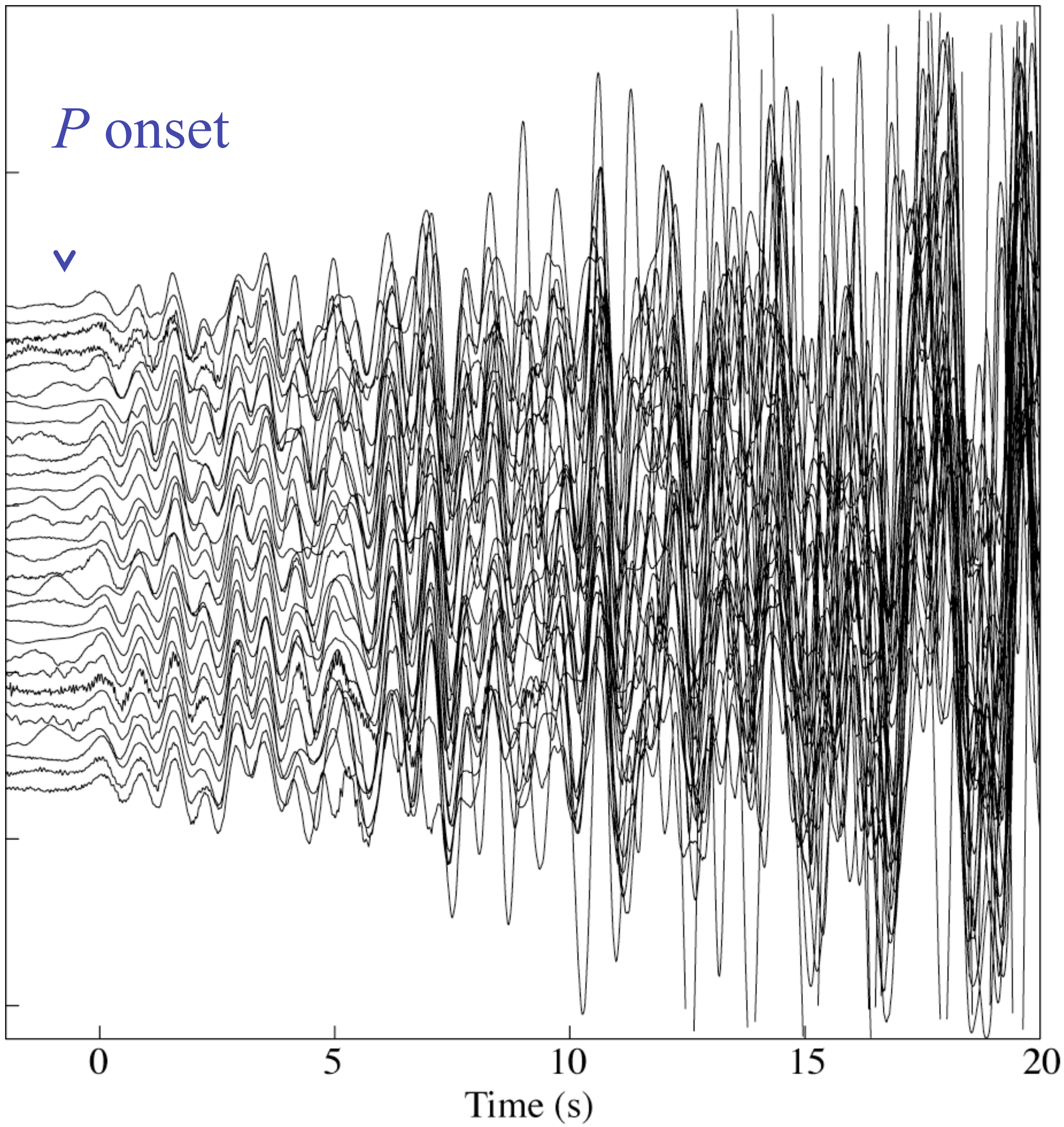

# Method forces coherent stack at hypocenter

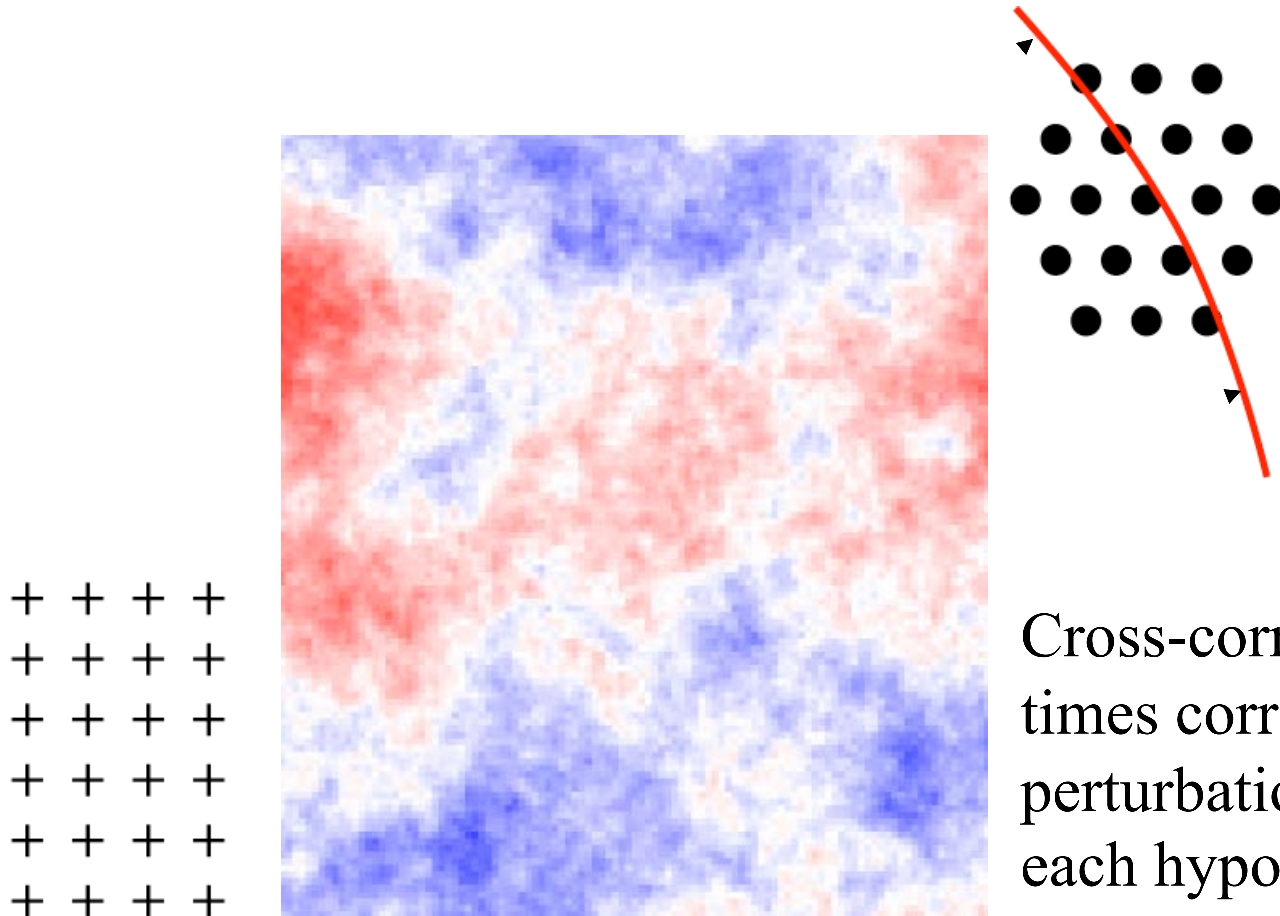

Cross-correlation times correct for perturbations along each hypocenter-station ray path

# But coherence not guaranteed for sources offset from hypocenter

Time shifts here not identical to hypocenter shifts

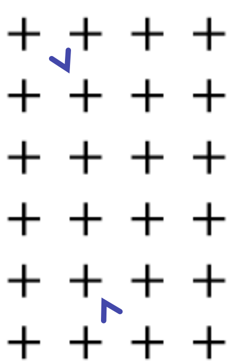

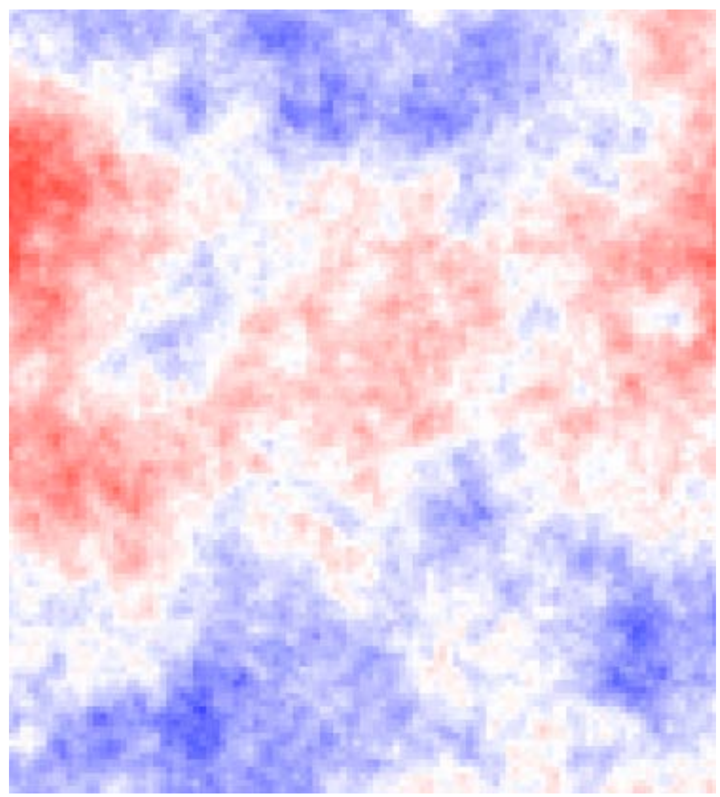

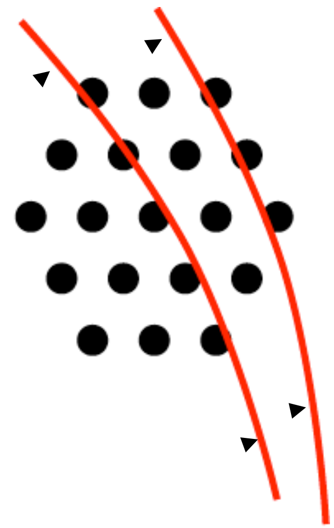

Calibrated time corrections at hypocenter

# Stacks at different source points

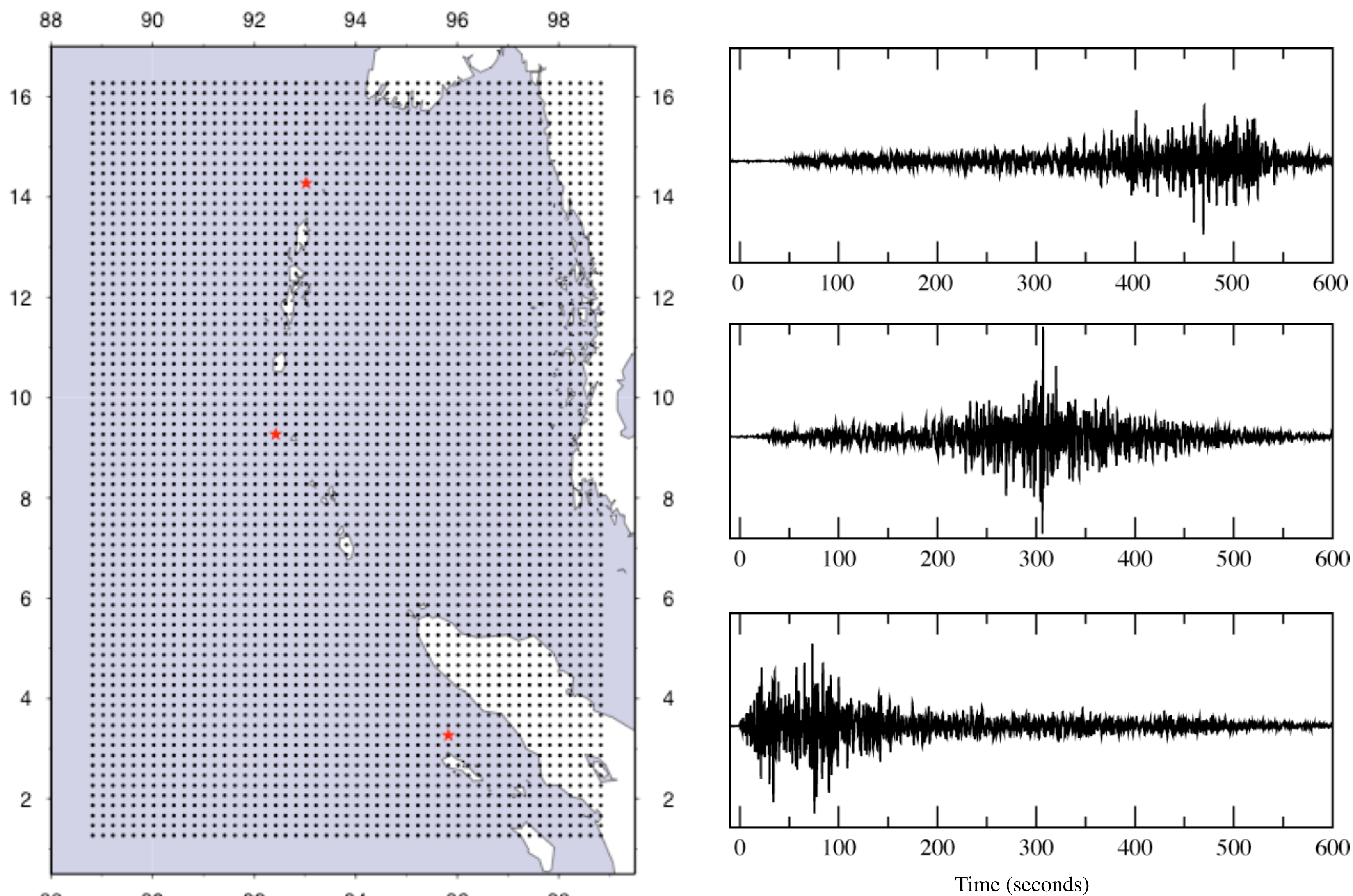


from *Ishii et al.* (2005)

# Stacks and Time Slice (60 seconds)

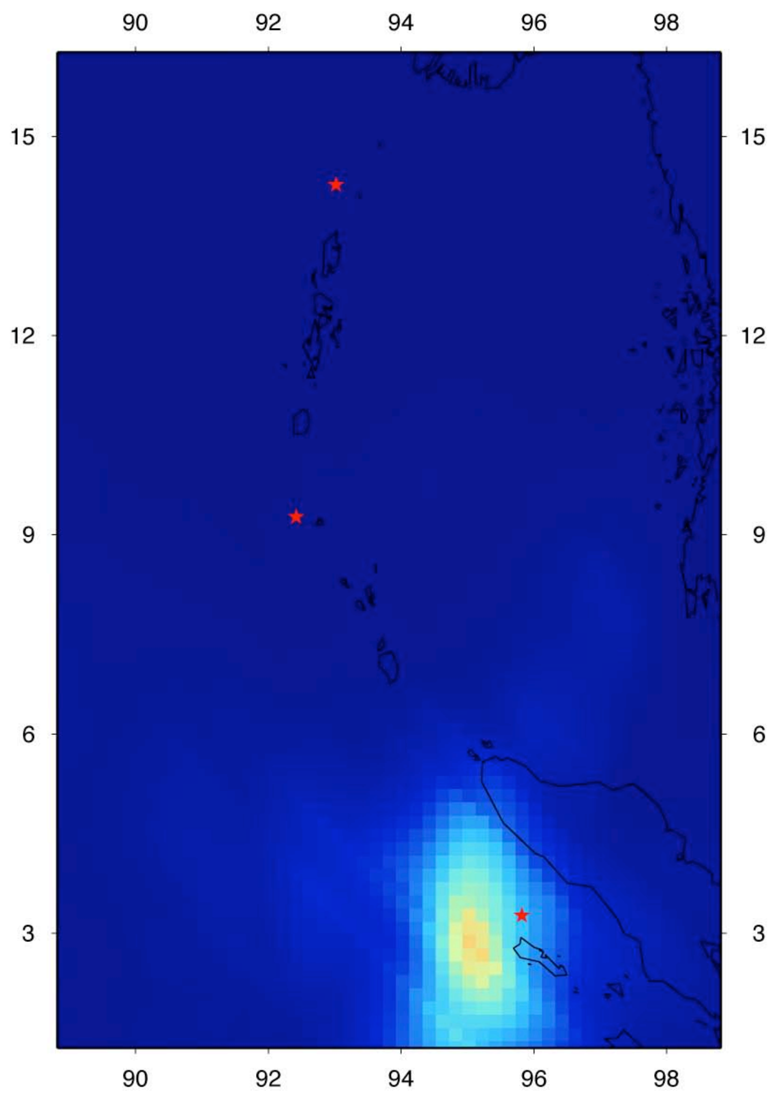


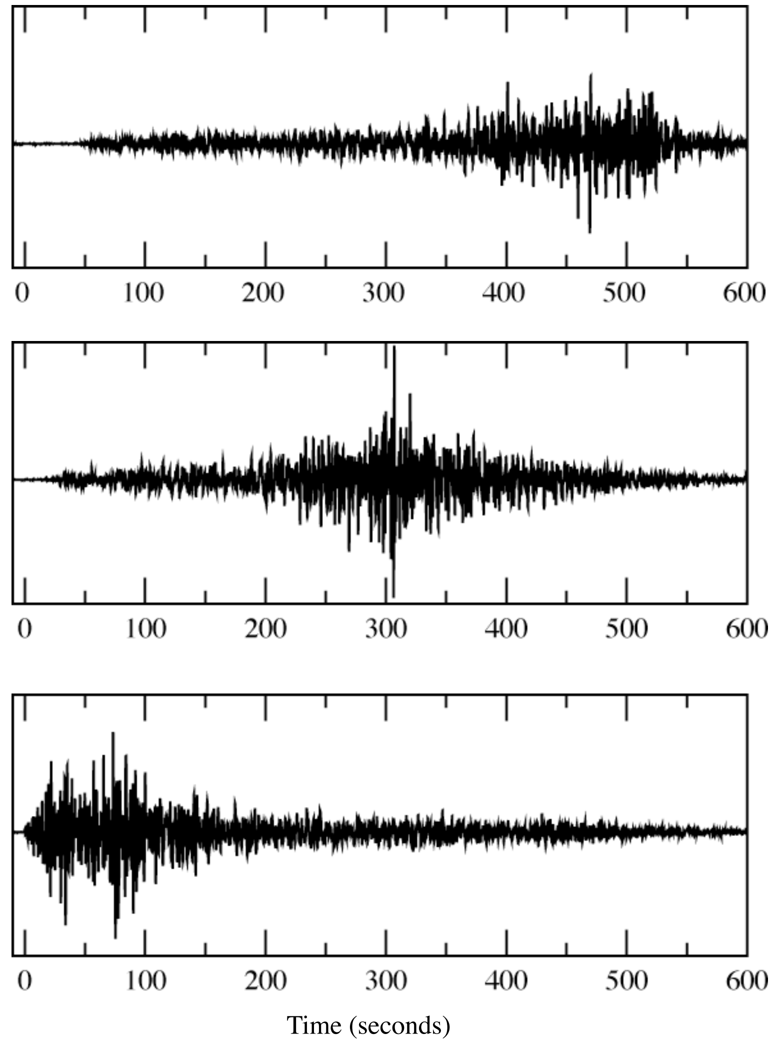

# Stacks and Time Slice (300 seconds)

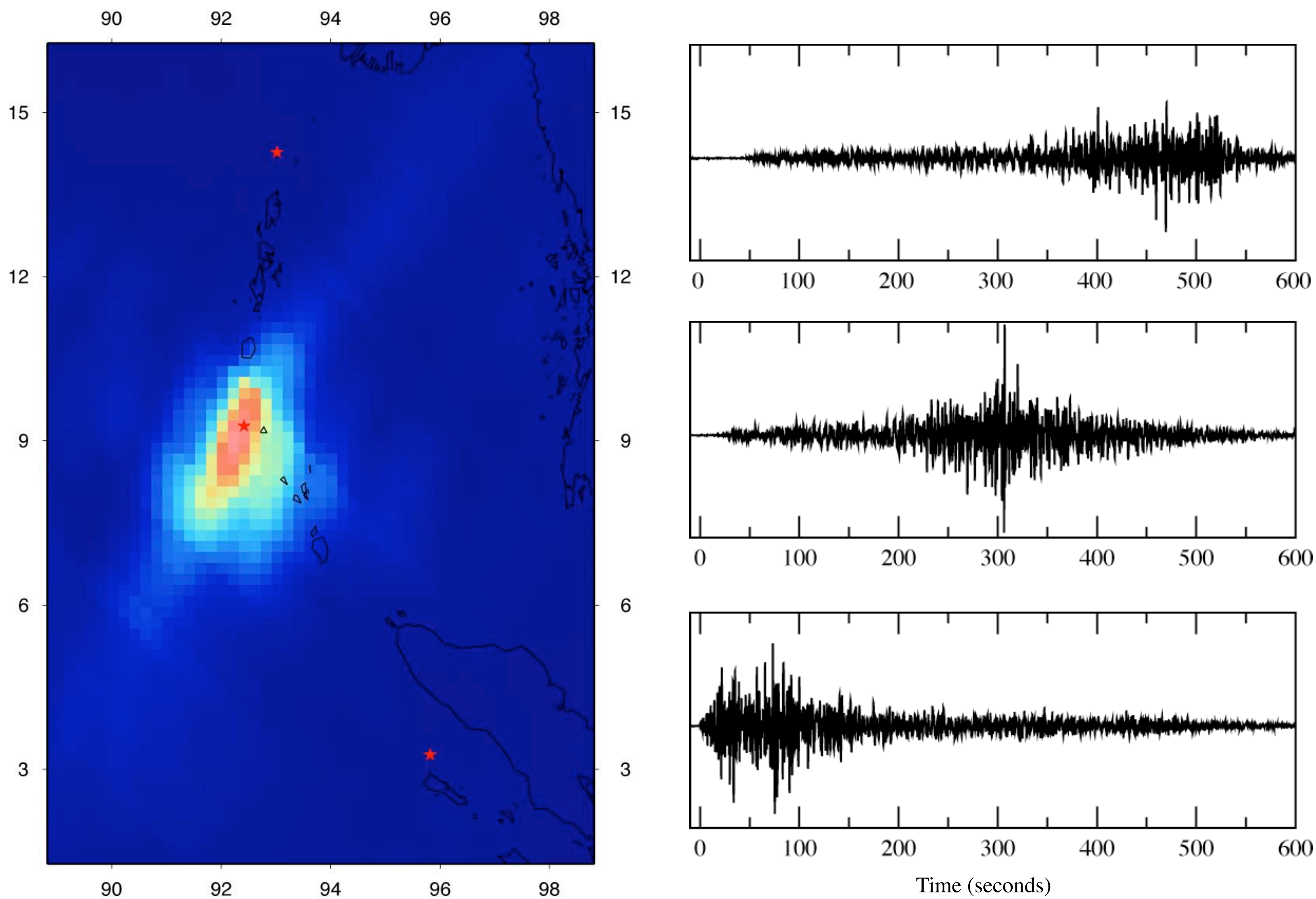

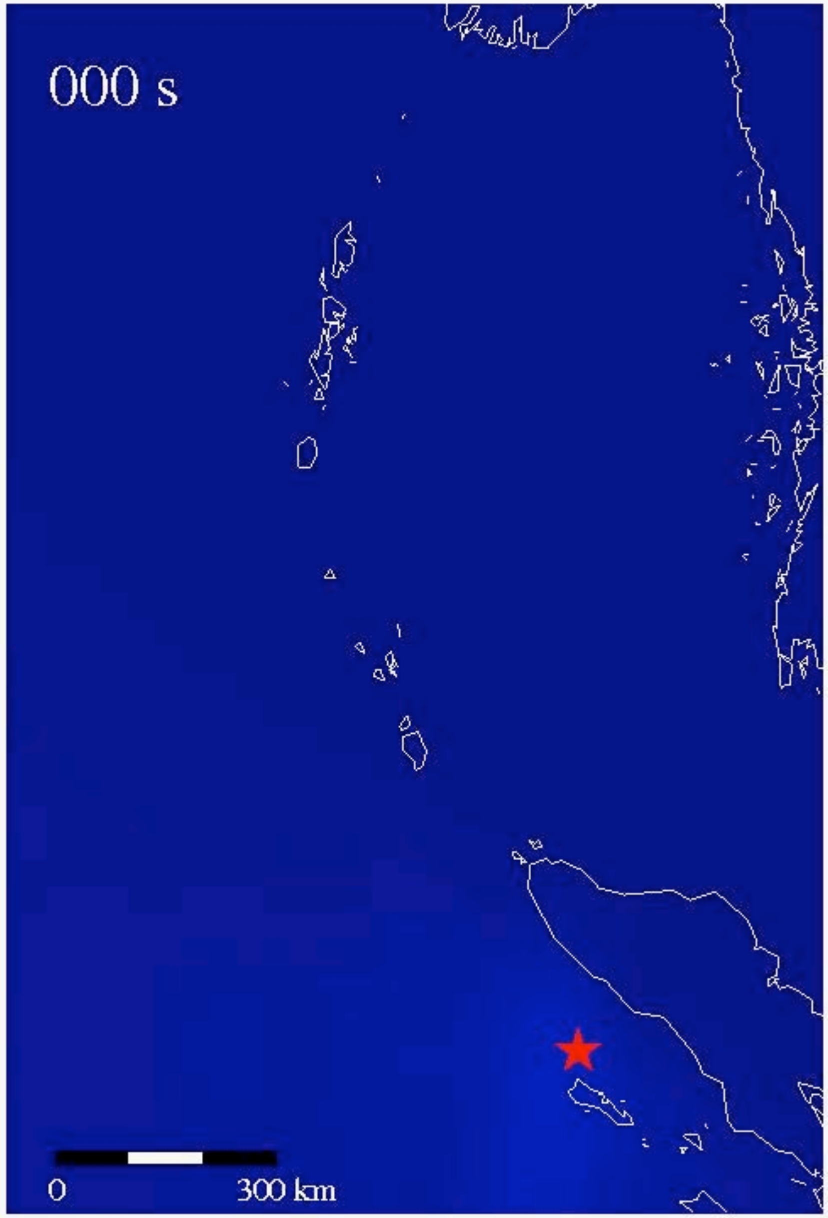
000 s
0
300 km

# Sumatra earthquake: Slow slip on northern part?

- Initial rupture models confined most slip to south
- Tide gauge record appeared to show no northern subsidence for 30 minutes after shaking
- "Tsunami and geodetic observations indicate that additional slow slip occurred in the north over a time scale of 50 minutes or longer." (*Lay et al*., 2005)
- "A surprising feature of the earthquake is that after the initial rapid rupture, subsequent slip of the plane interface occurred with decreasing speed toward the north." (*Bilham et al*., 2005)

?

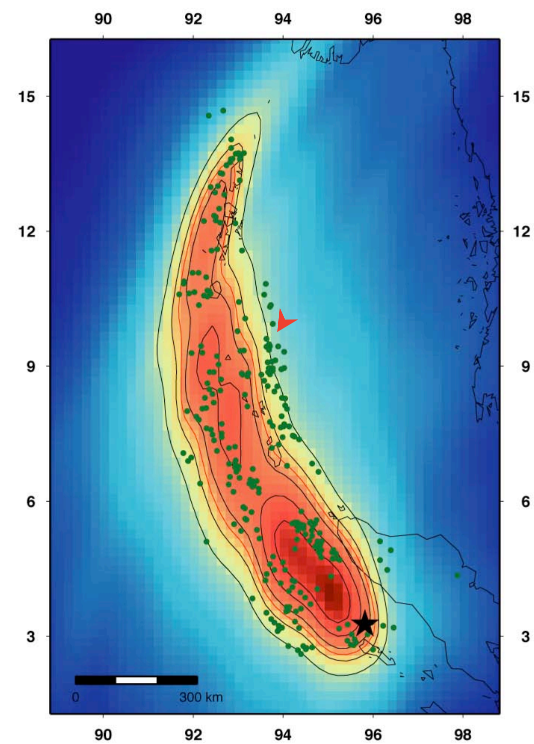

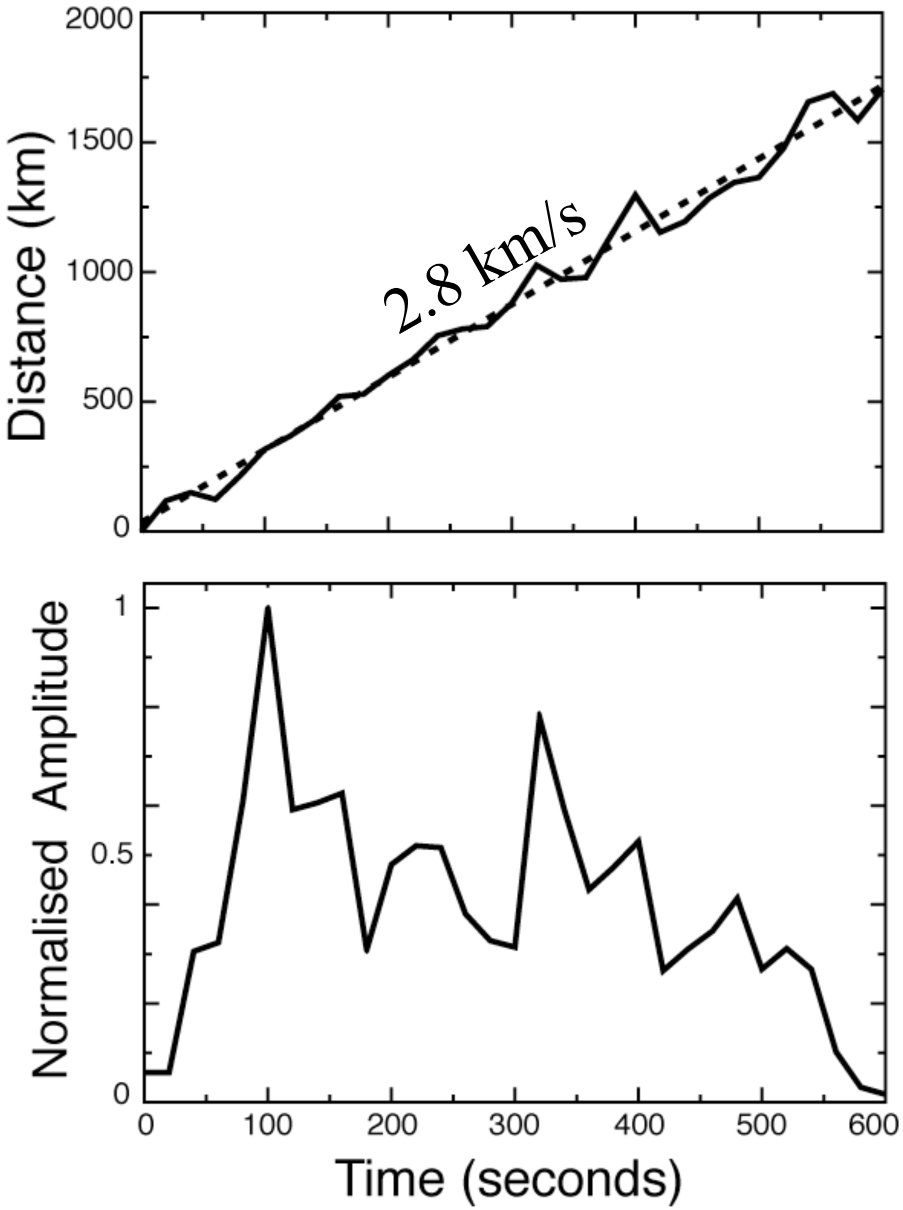


# We don't see slow slip in our model

- 2.8 km/s rupture
- Rupture does not slow to north
- Amplitude peaks near 100 and 340 s
- Total duration of ~9 minutes

# Most evidence for slow slip has now disappeared…

- Seismic rupture models now have considerable slip to north.
- Tide gauge record had 30 minute timing error (*Neetu et al.*, 2005)

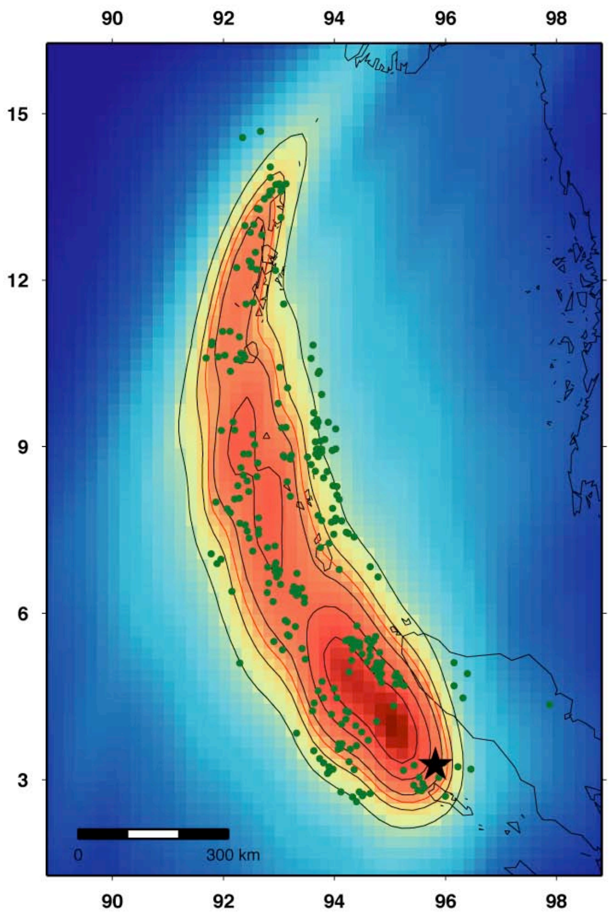


*Ishii et al.*, 2005

Harvard multiple CMT

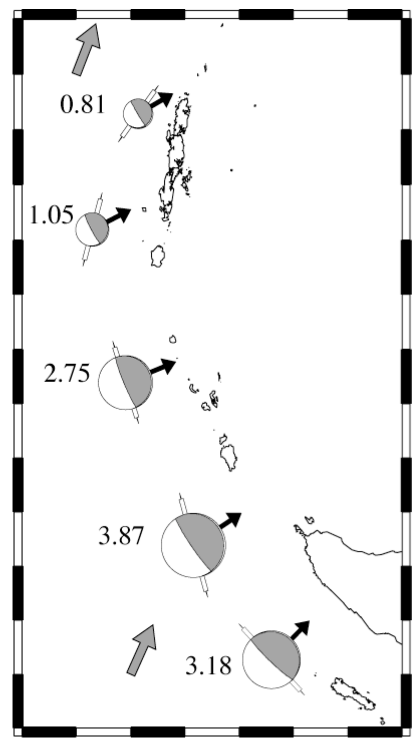


*Tsai et al.*, 2005

Coseismic GPS model

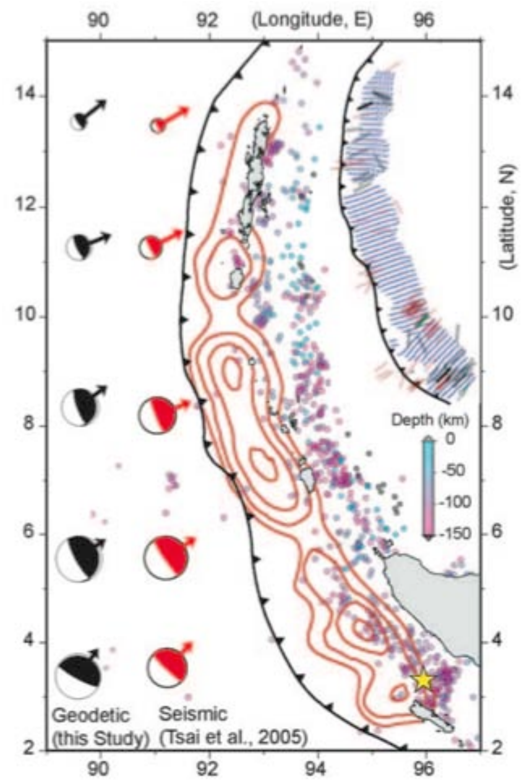


*Chlieh et al.*, 2007

# Comparison with Other Large Earthquakes

1957 Aleutians

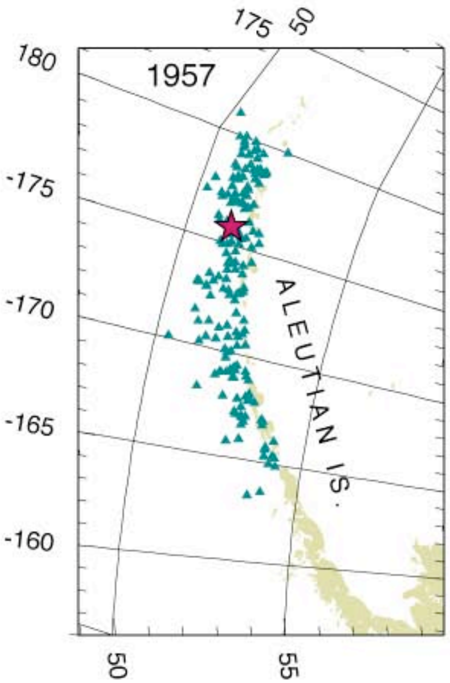


Mw=9.1

1960 Chile

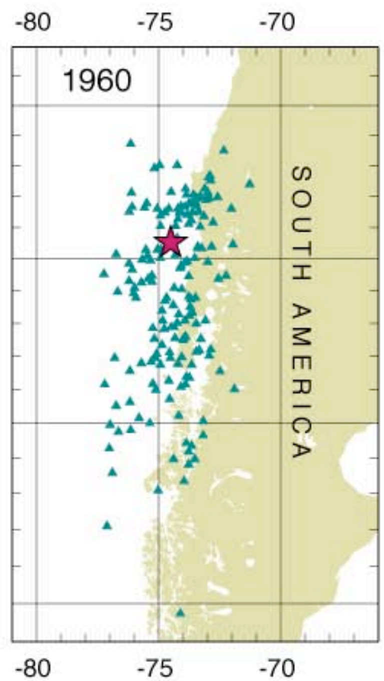


Mw=9.5

1964 Alaska

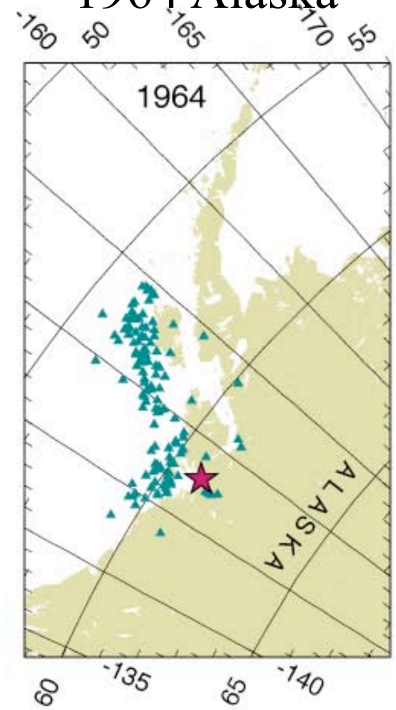


Mw=9.2

2004 Sumatra

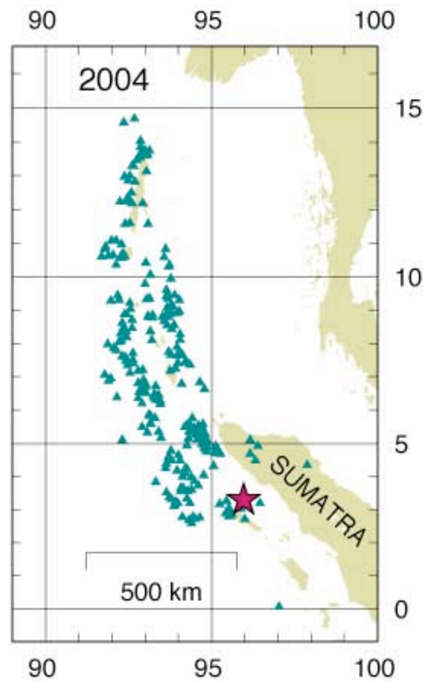


Mw=9.15?

# *P*-wave Back-Projection Method

- Suited for a global real-time system
- No assumptions needed about fault geometry
- Will give much quicker warnings about massive earthquakes than existing system
- We are working with U.S. Geological Survey scientists to implement this method

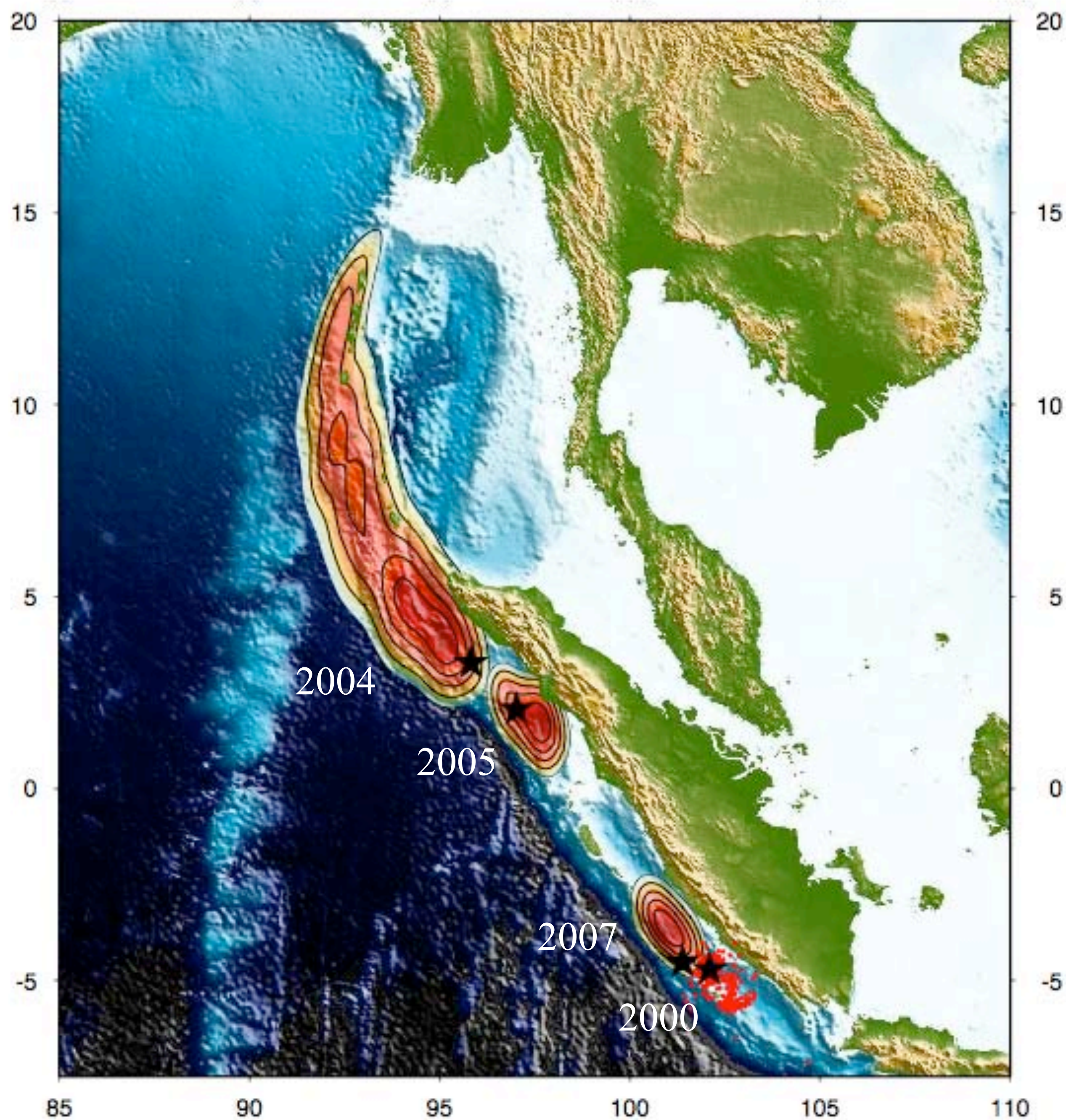

20
15
10
5
0
-5
85
90
95
100
105
110
2004
2005
2007
2000

# The 28 September 2004 M6.0 Parkfield earthquake

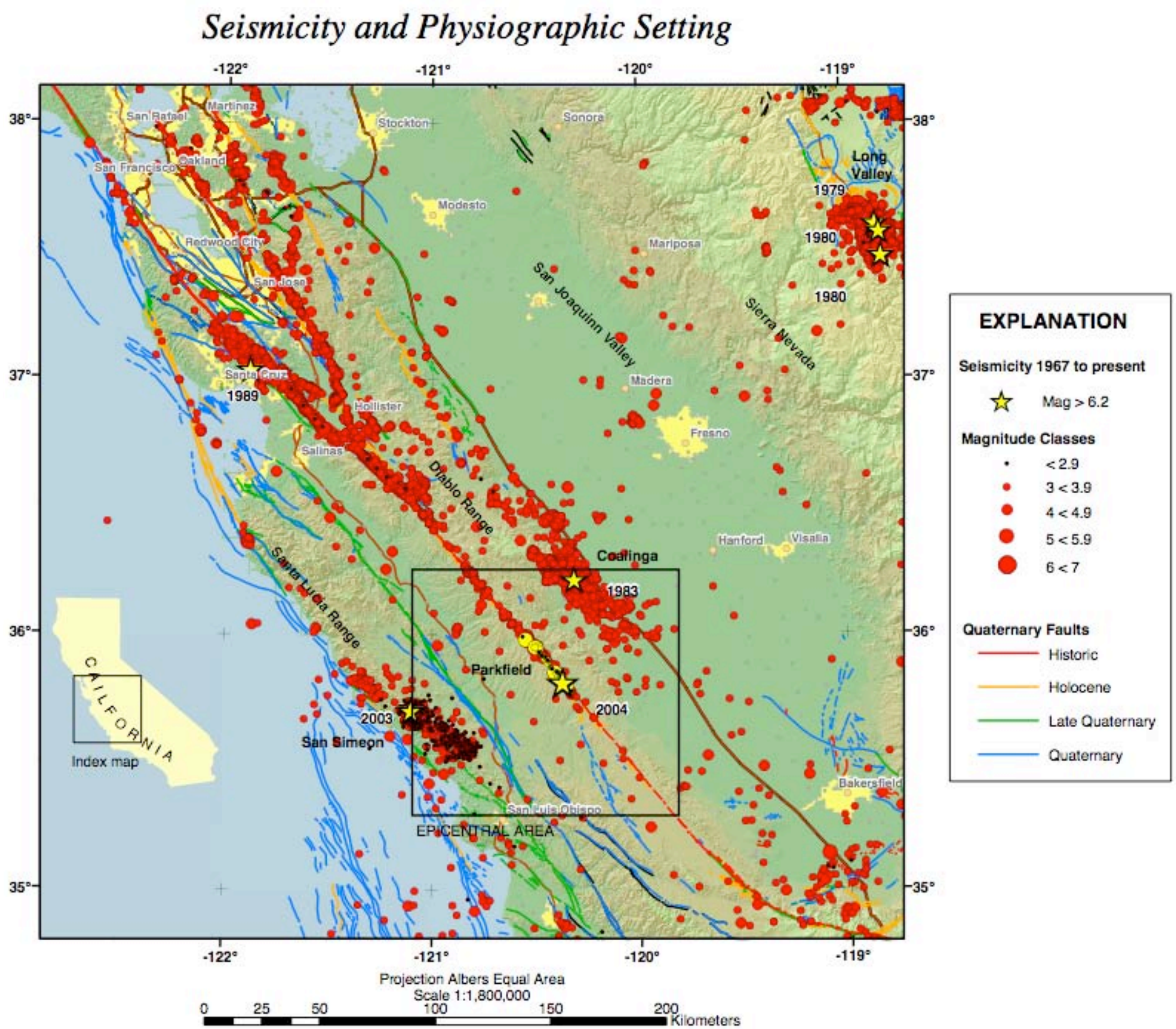


# The 2004 M6.0 Parkfield earthquake was *supposed* to have occurred before 1993….

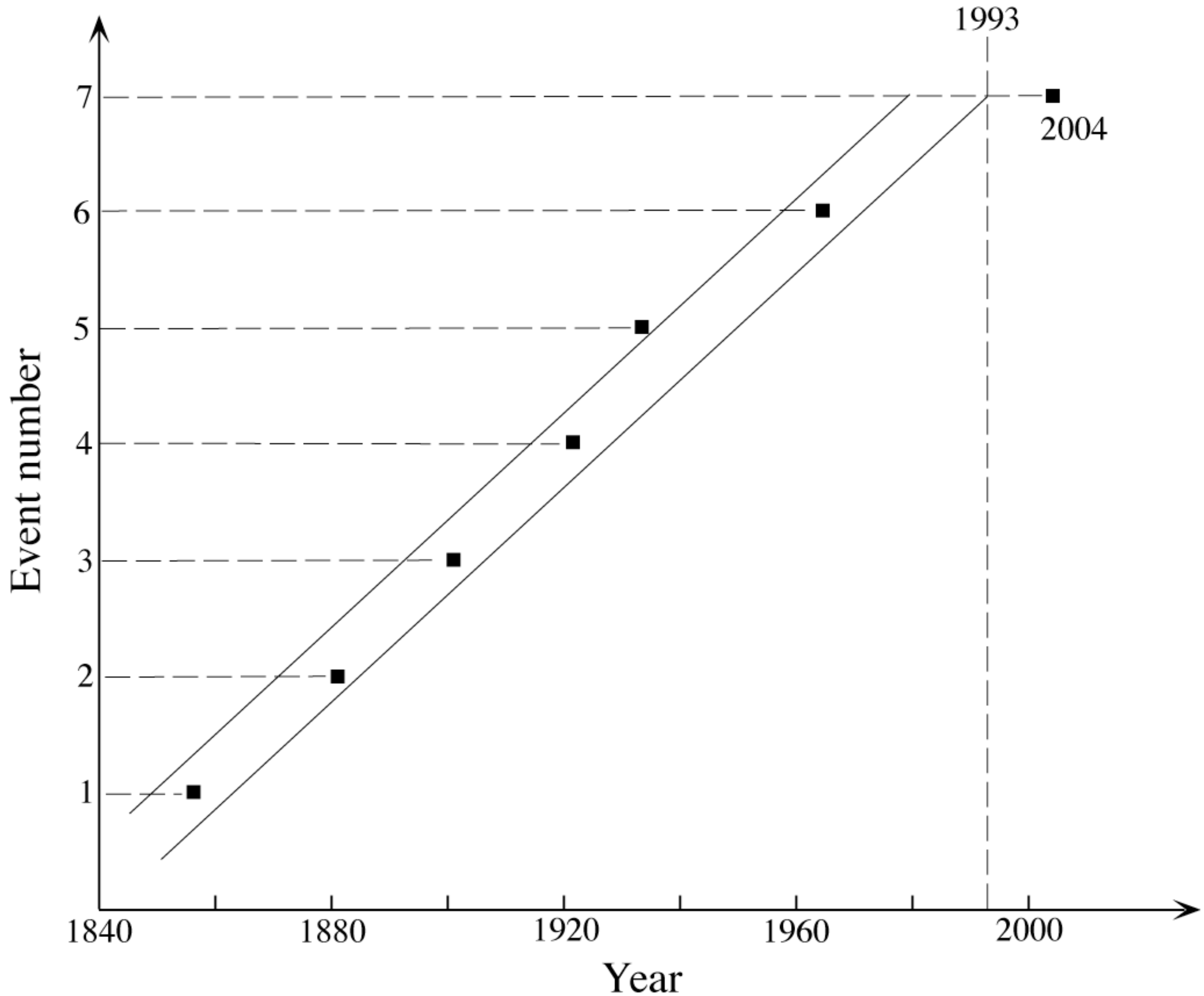

# The 2004 M6.0 Parkfield earthquake

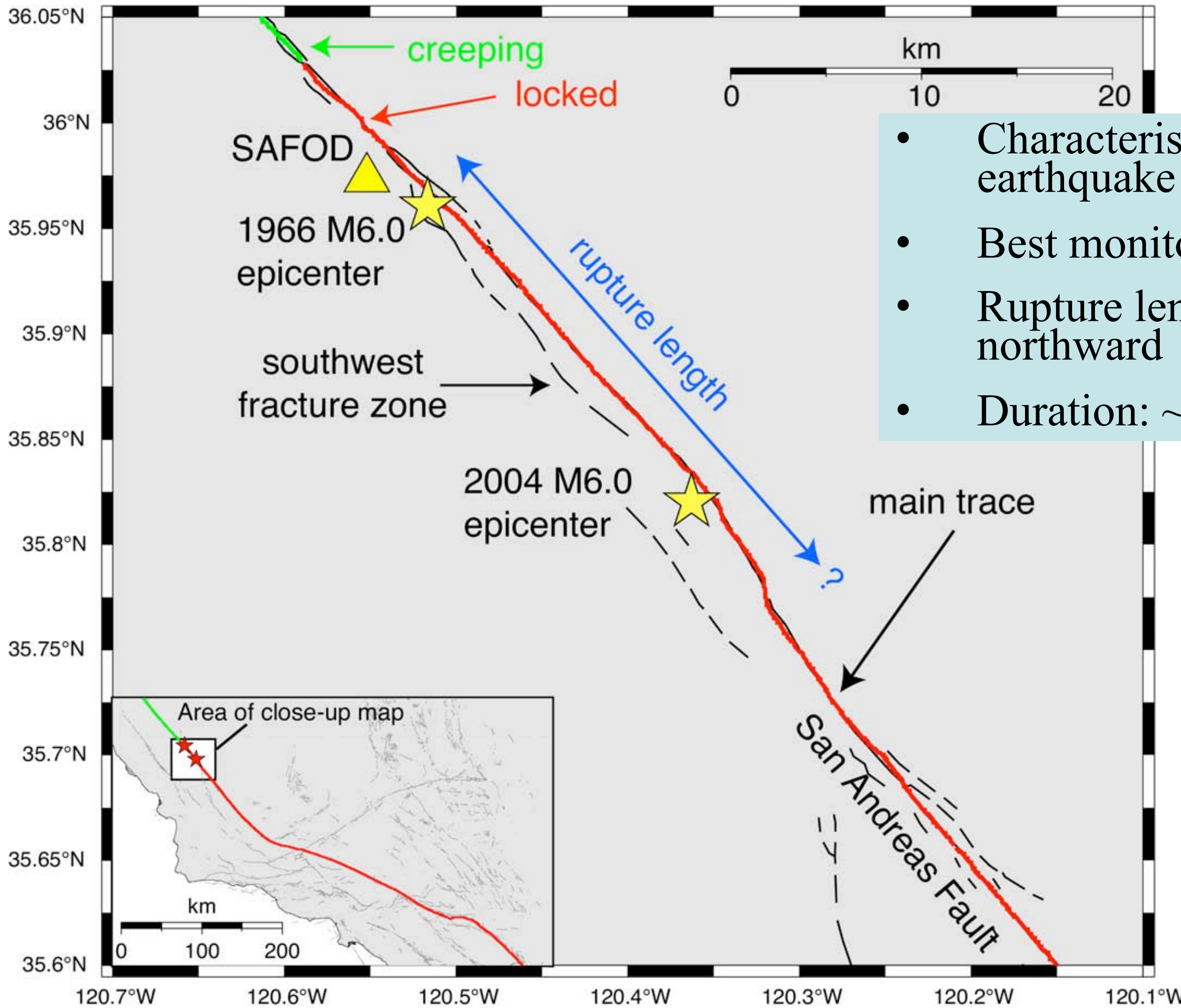


- Characteristic magnitude 6.0 earthquake
- Best monitored earthquake
- Rupture length: ~ 20 km northward
- Duration: ~ 12-14 seconds

# The 2004 M6.0 Parkfield earthquake

One example slip inversion model using combined GPS and strong-motion data

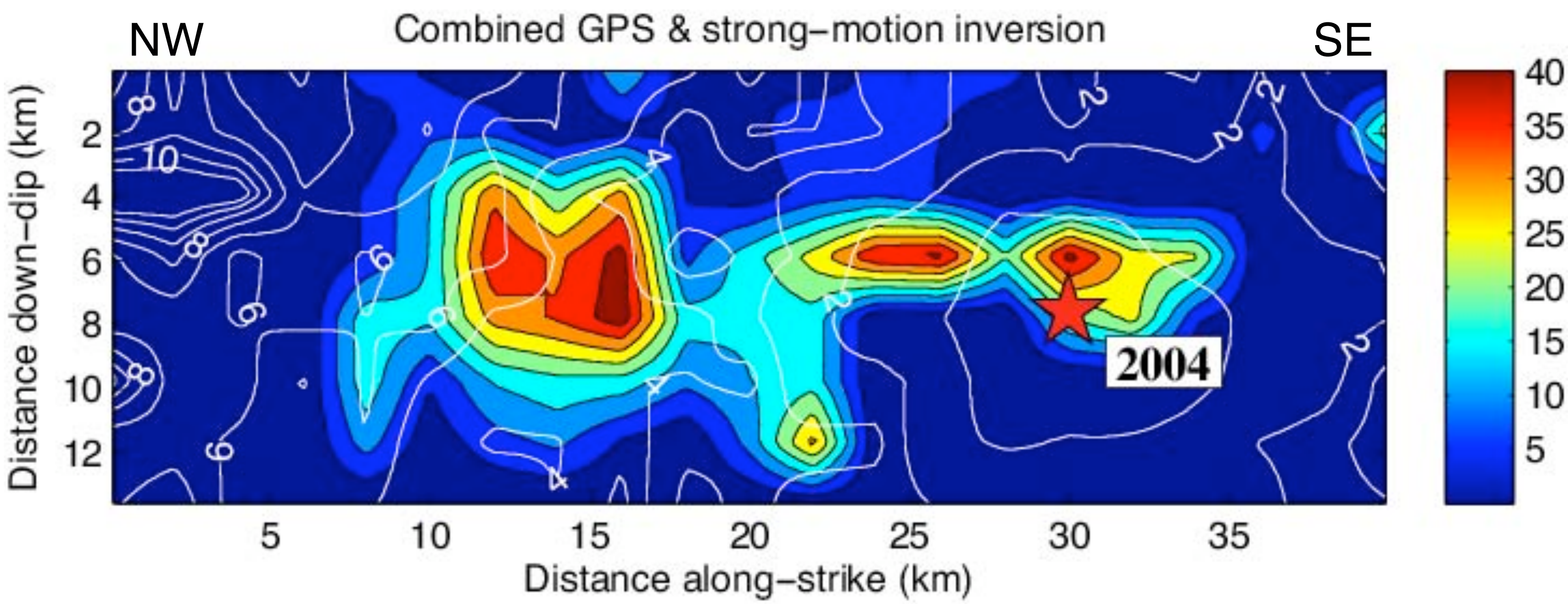


*Custodio et al. (2007, in prep.)*

# Different slip model inversions from long-period seismic and geodetic data

*Custodio et al. (2007, in prep.)*

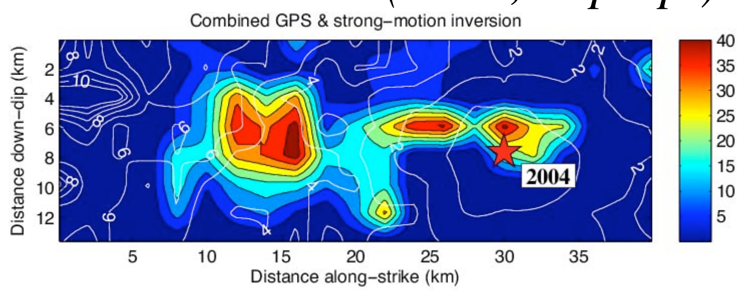


*Liu et al. (2006)*

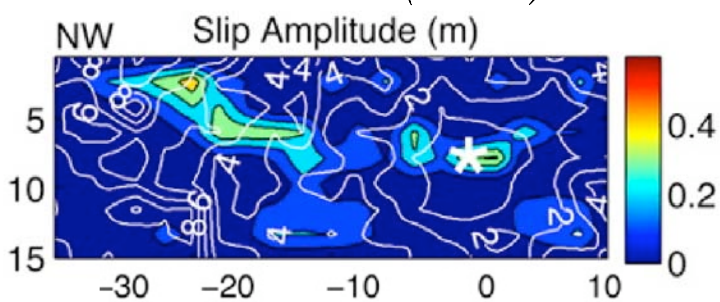


*Johanson et al. (2006)*

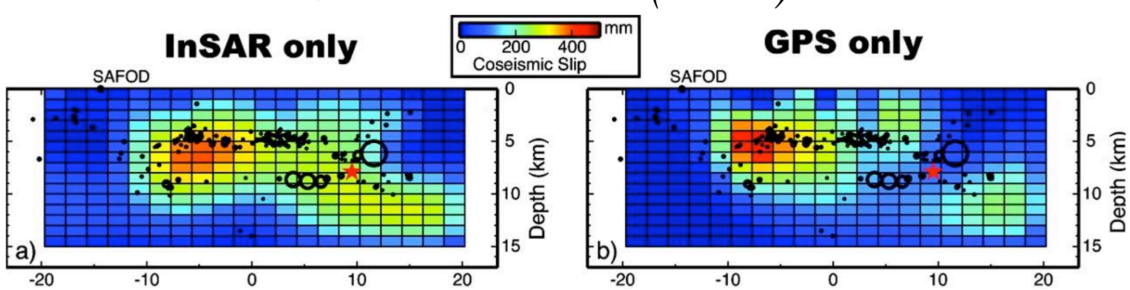


*Langbein et al. (2005)*

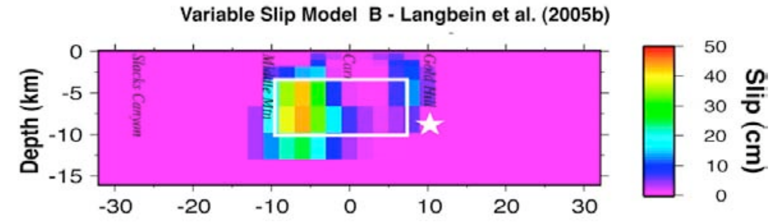


*Johnson et al. (2006)*

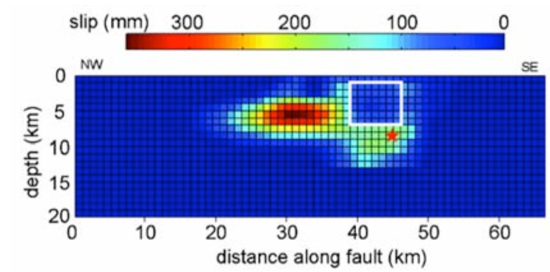


*Murray et al. (2006)*

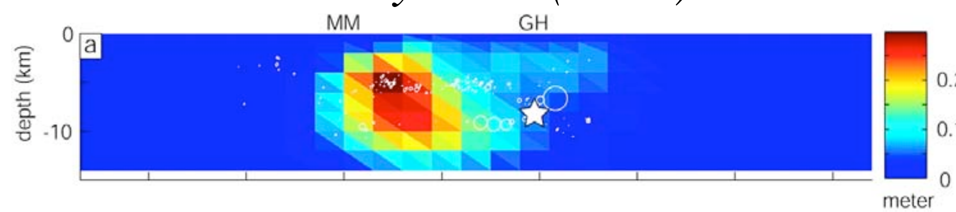


*Ji et al. (2005)*

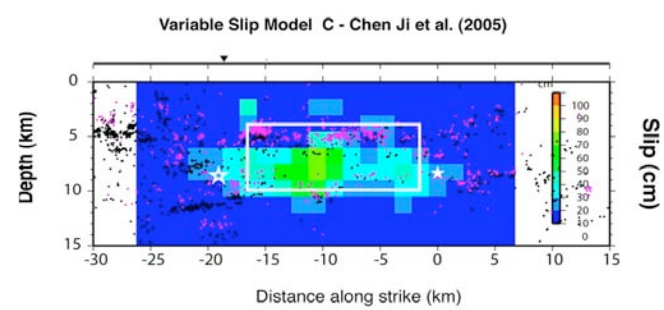

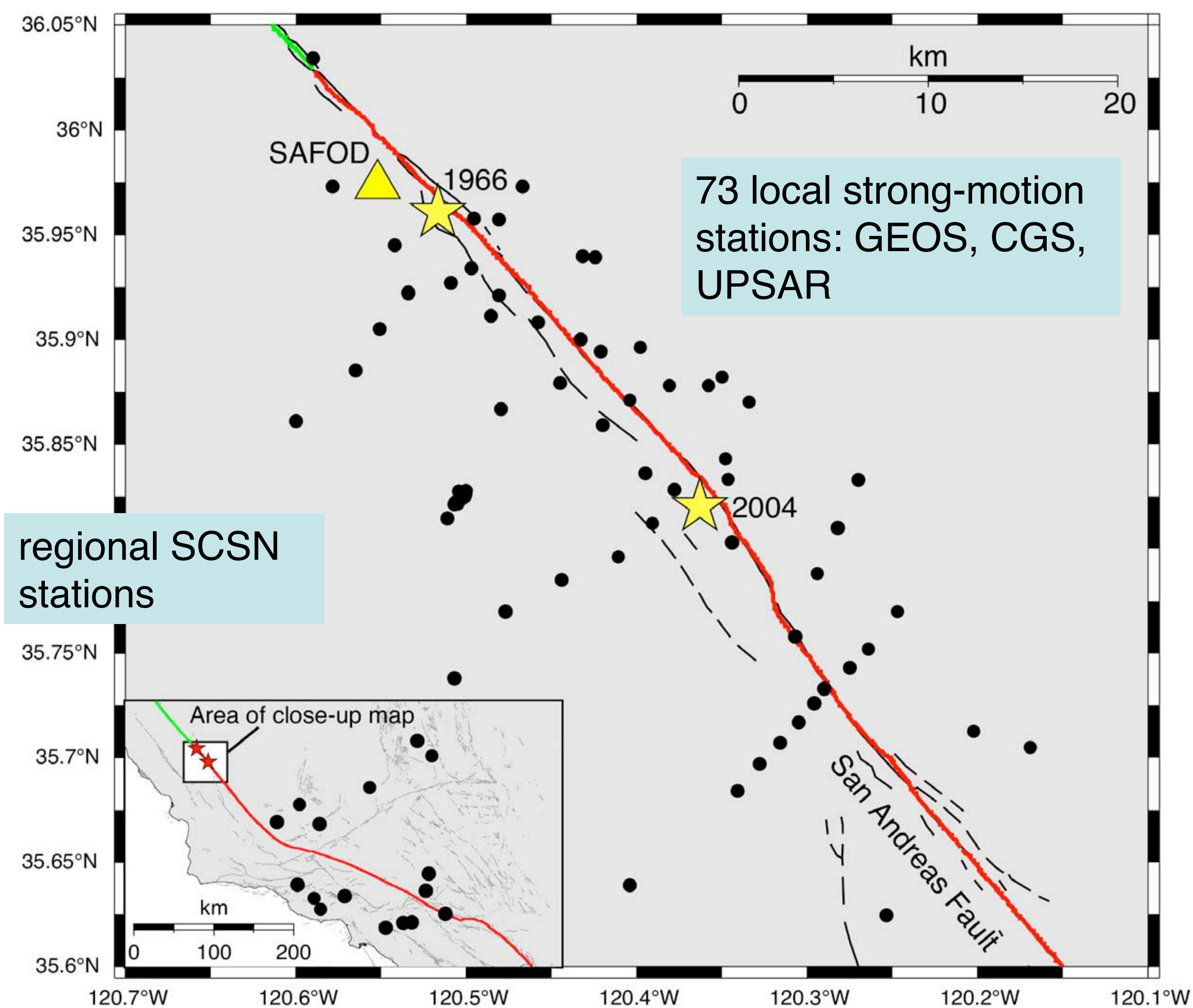

36.05°N
36°N
35.95°N
35.9°N
35.85°N
35.75°N
35.7°N
35.65°N
35.6°N
120.7°W
120.6°W
120.5°W
120.4°W
120.3°W
120.2°W
120.1°W
km
0
10
20
SAFOD
1966
2004
73 local strong-motion stations: GEOS, CGS, UPSAR
regional SCSN stations
San Andreas Fault
Area of close-up map
km
0
100
200

Traveltime difference between P01 to hypocenter and P01 to each image point: **Real station distribution**

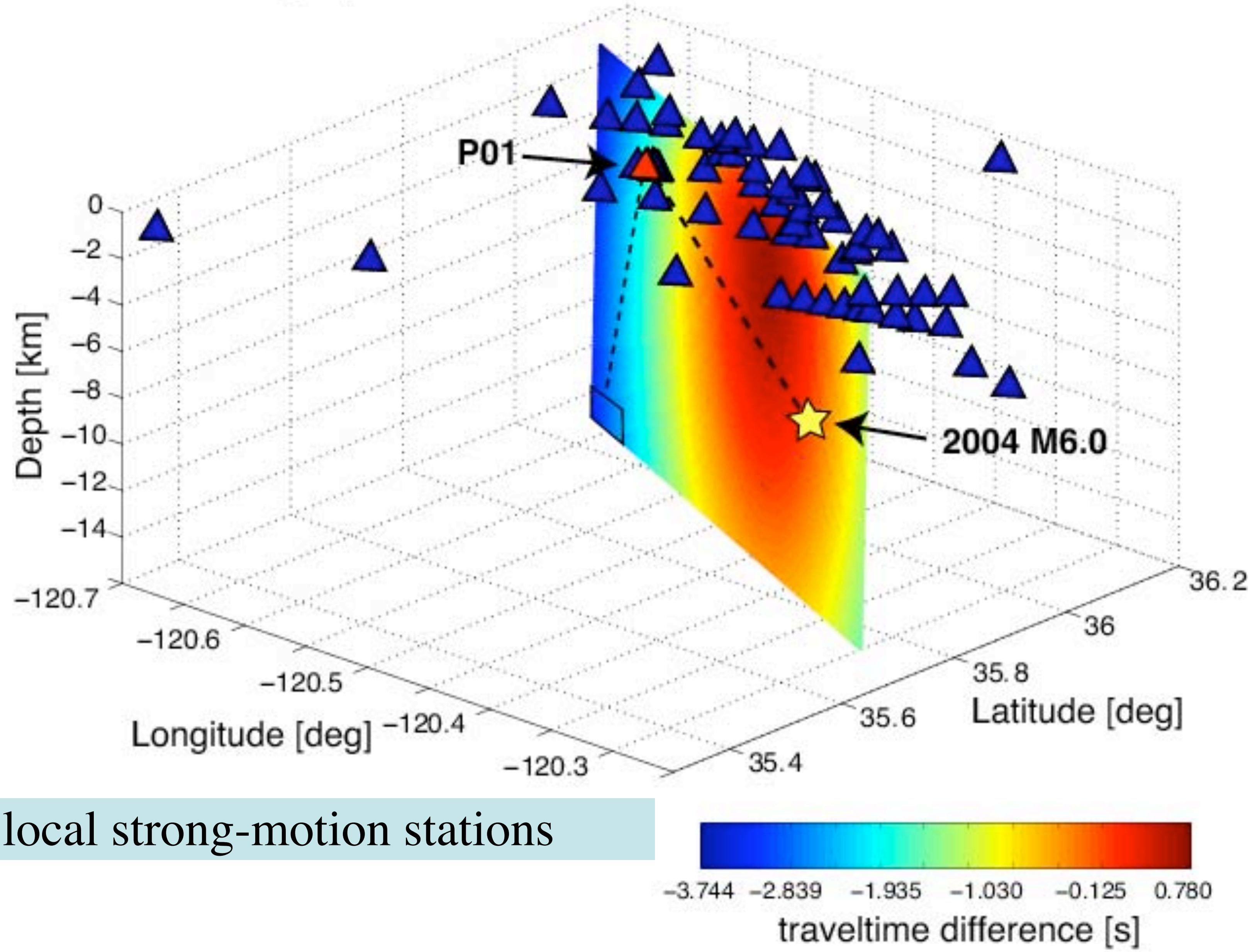


73 local strong-motion stations

# Aligned S waves

- 73 local strong-motion stations aligned using waveform cross-correlation
- Resample to 5 ms
- Bandpass filter between 2-8 Hz
- Automatic gain control (AGC) over 10 s

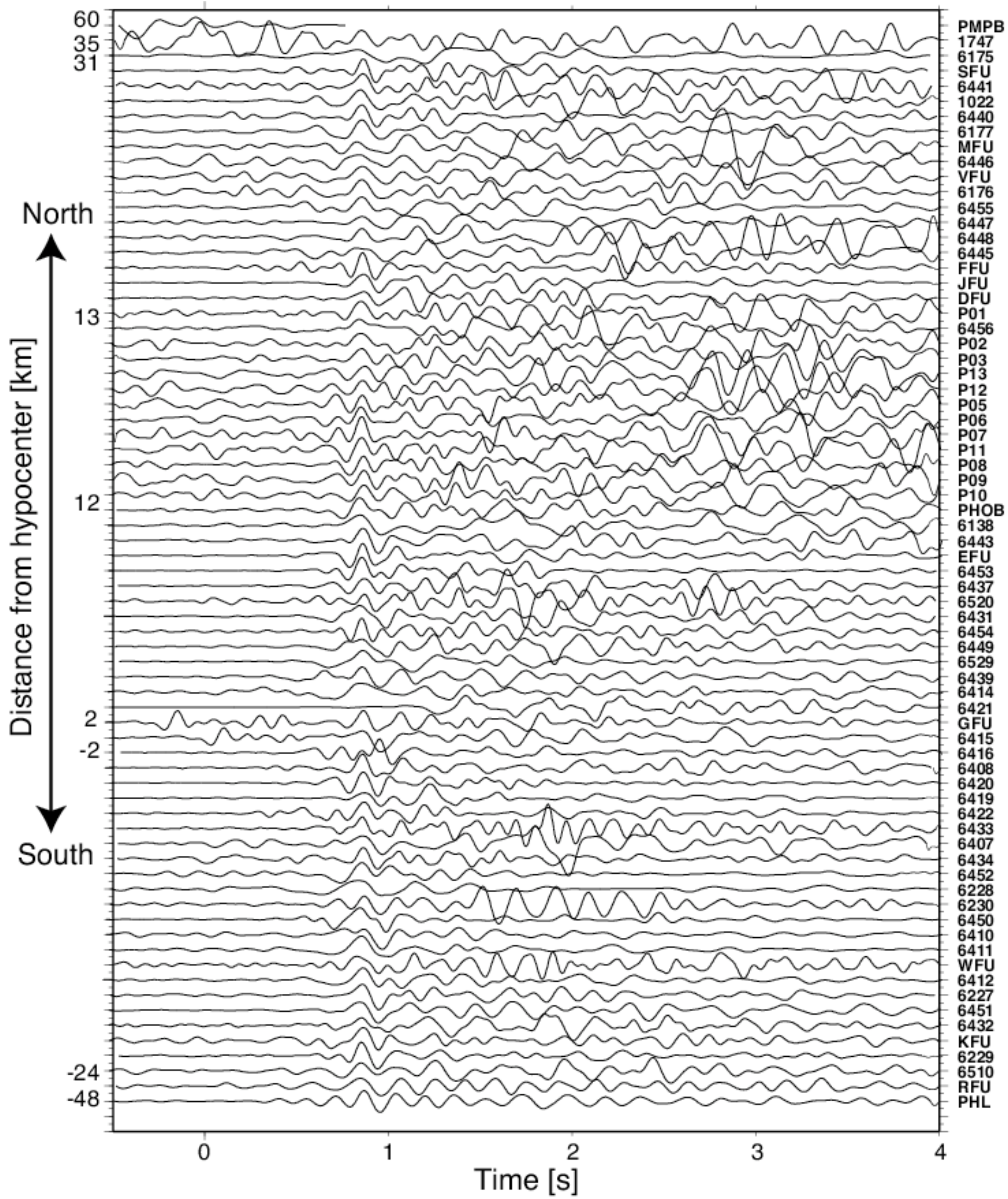

# Along fault image at 0.5 s intervals

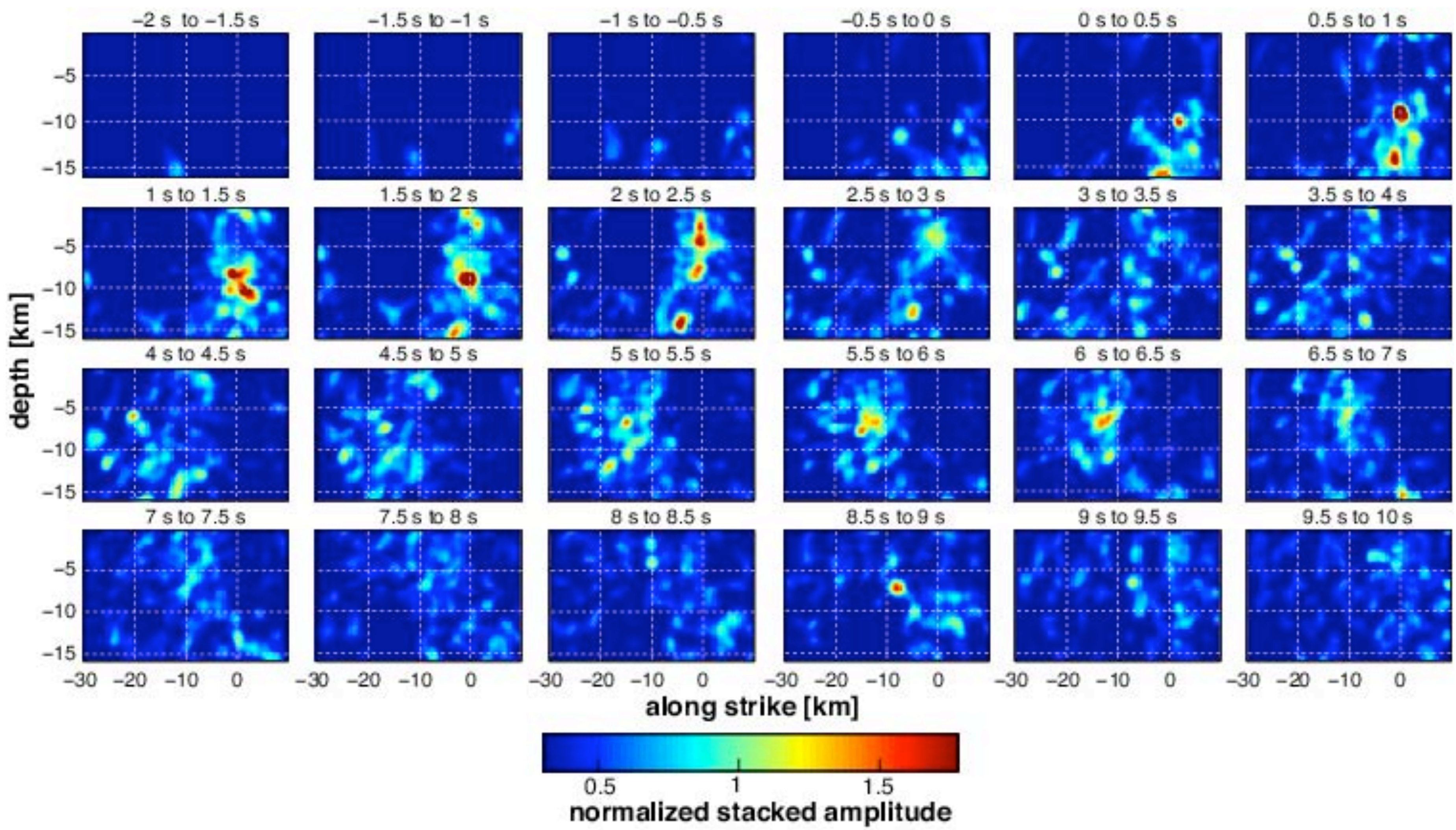

# Mute first 2 s of seismograms to reduce artifacts

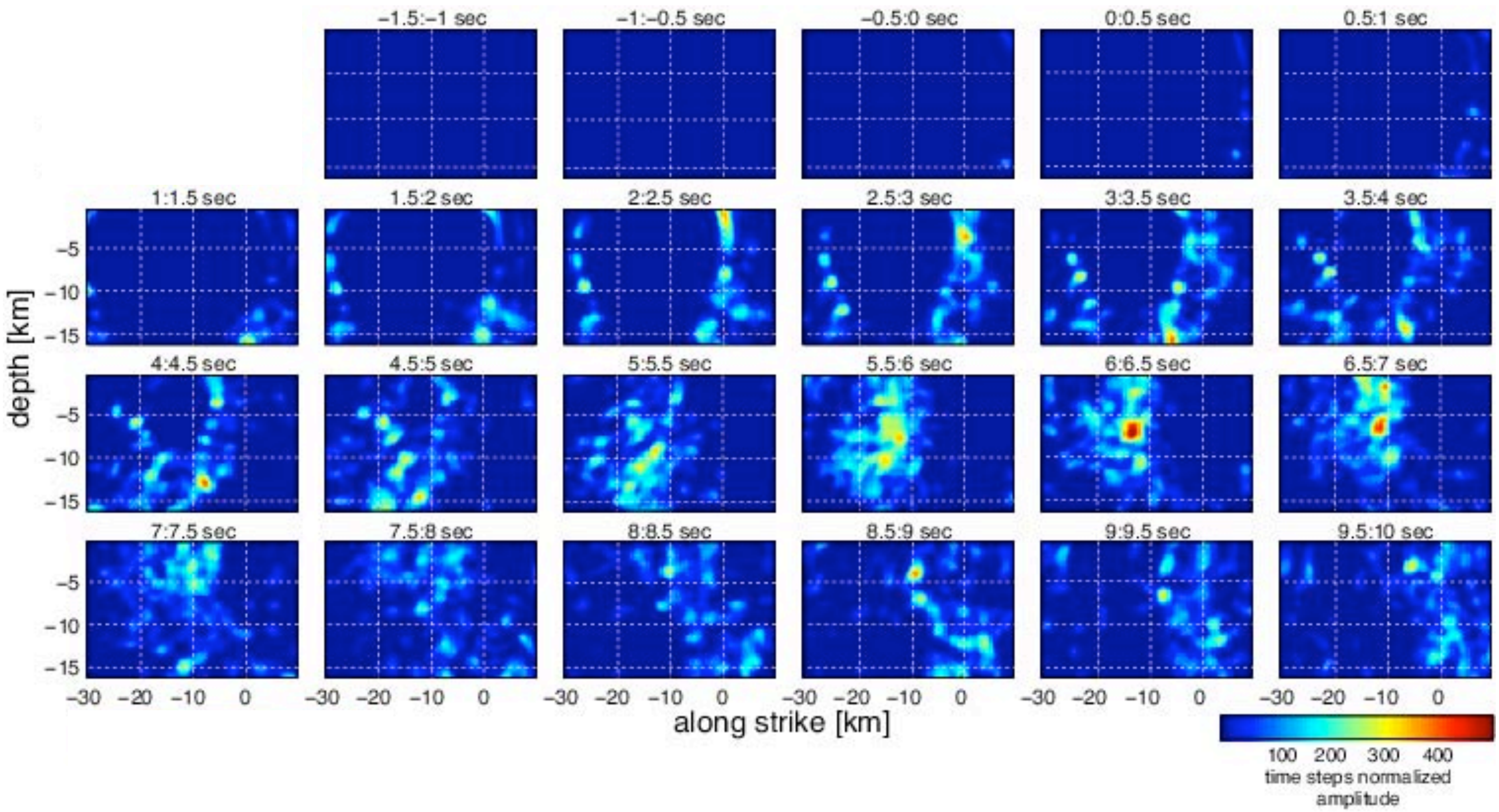

0.5 to 1.5 s

5.5 to 6.5 s

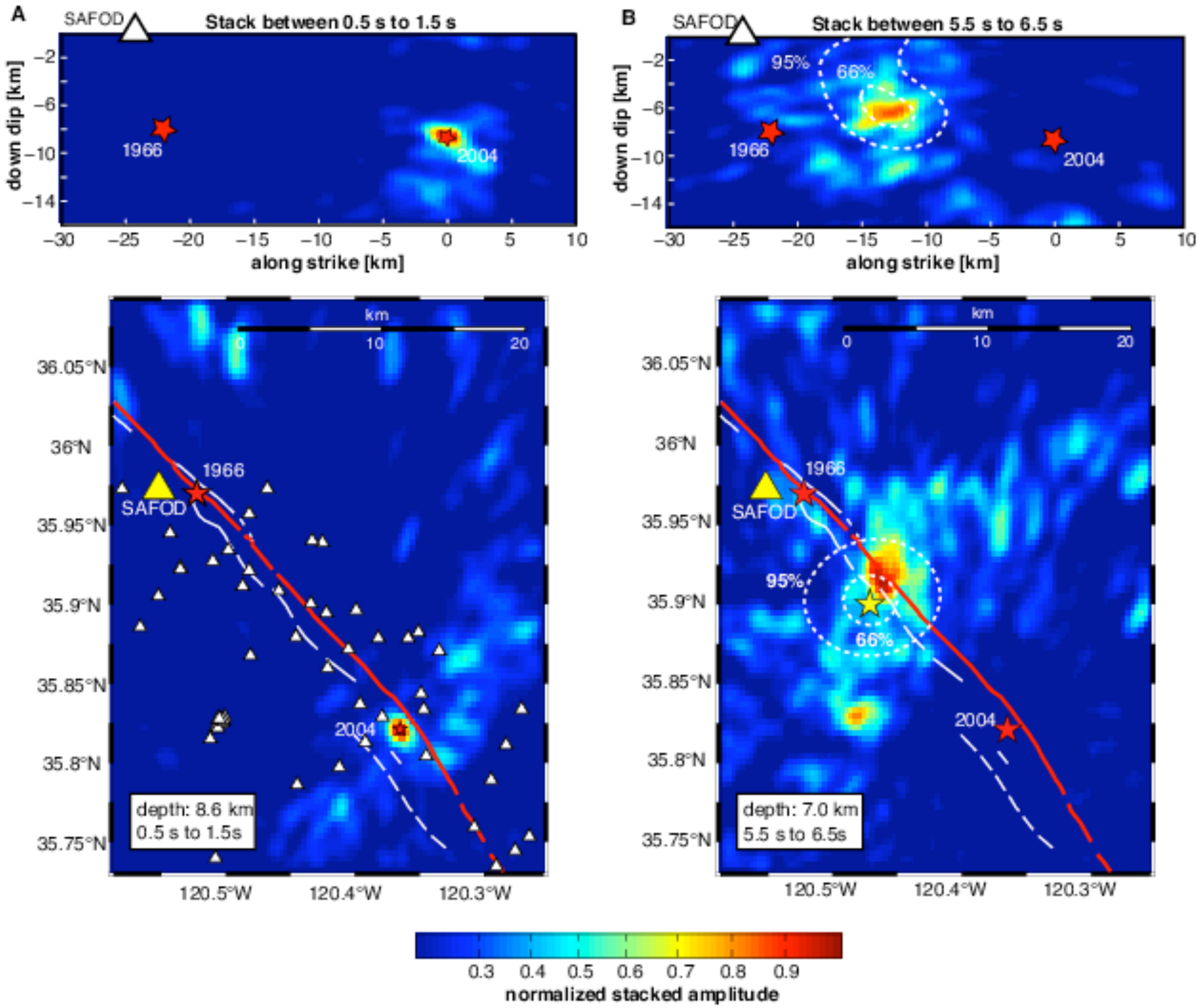

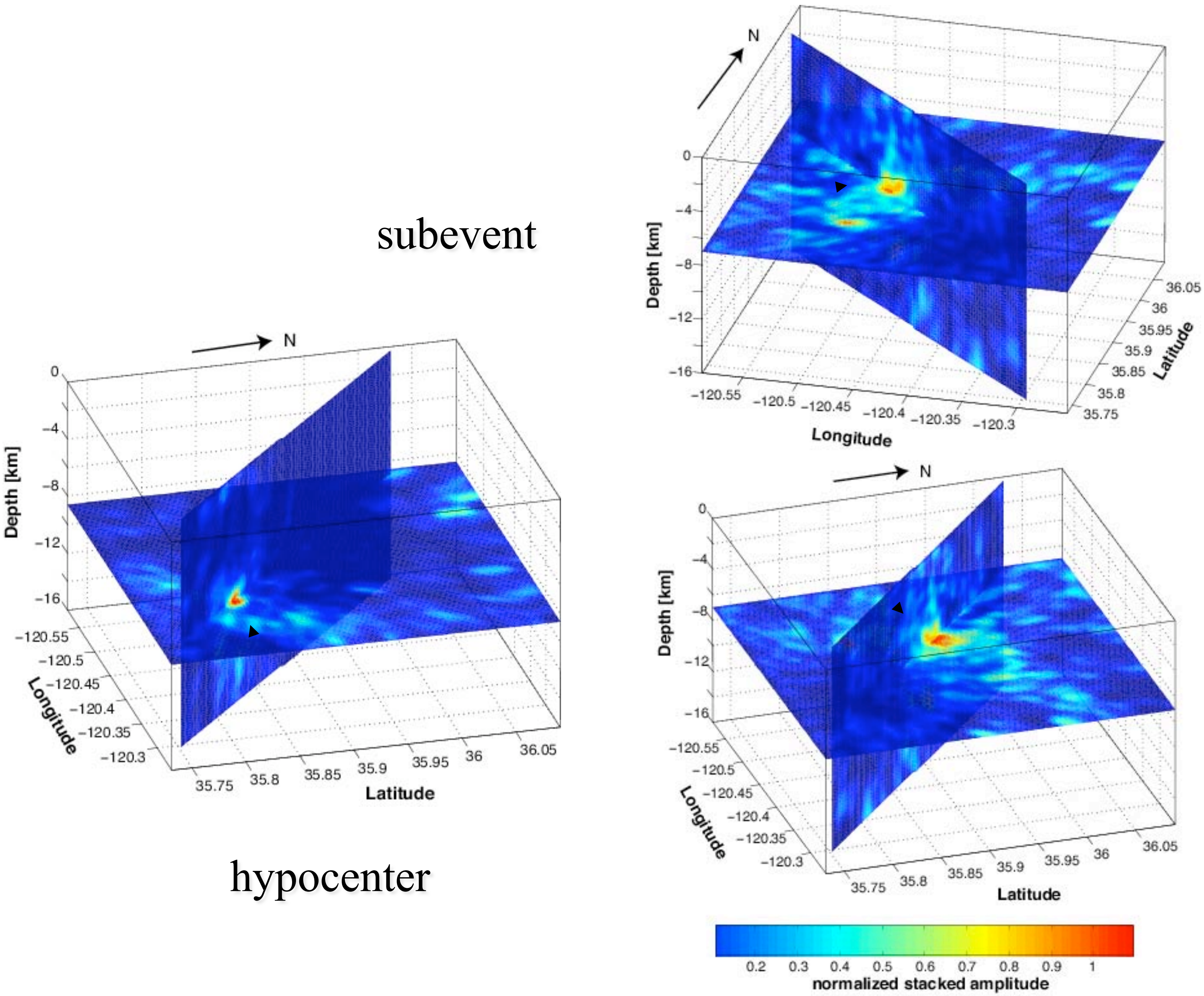

subevent
hypocenter
N
Depth [km]
Longitude
Latitude
0
-4
-8
-12
-16
-120.55
-120.5
-120.45
-120.4
-120.35
-120.3
35.75
35.8
35.85
35.9
35.95
36
36.05
0.2 0.3 0.4 0.5 0.6 0.7 0.8 0.9 1
normalized stacked amplitude

synthetic data

real data

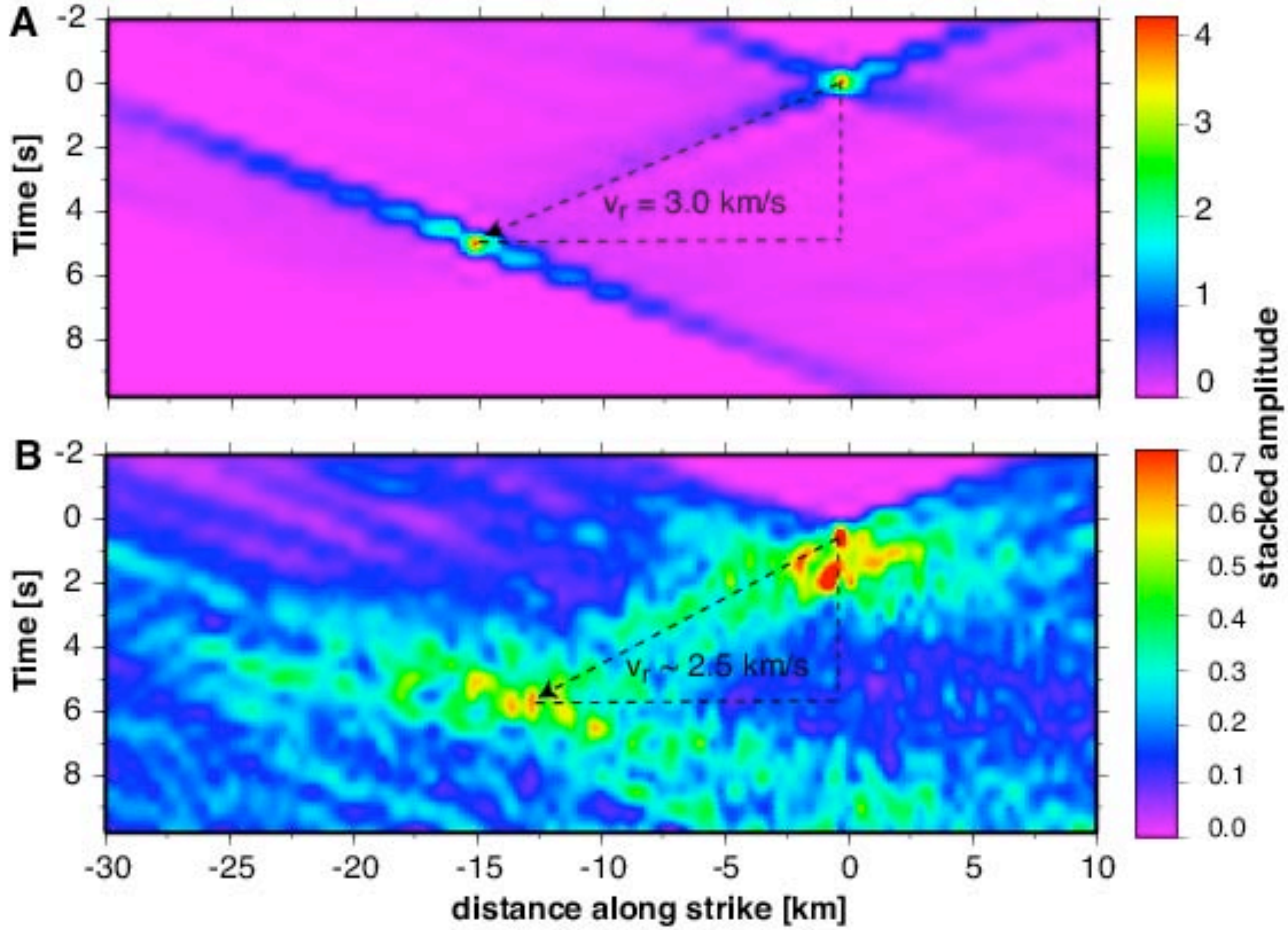

Secondary phase detected at some stations

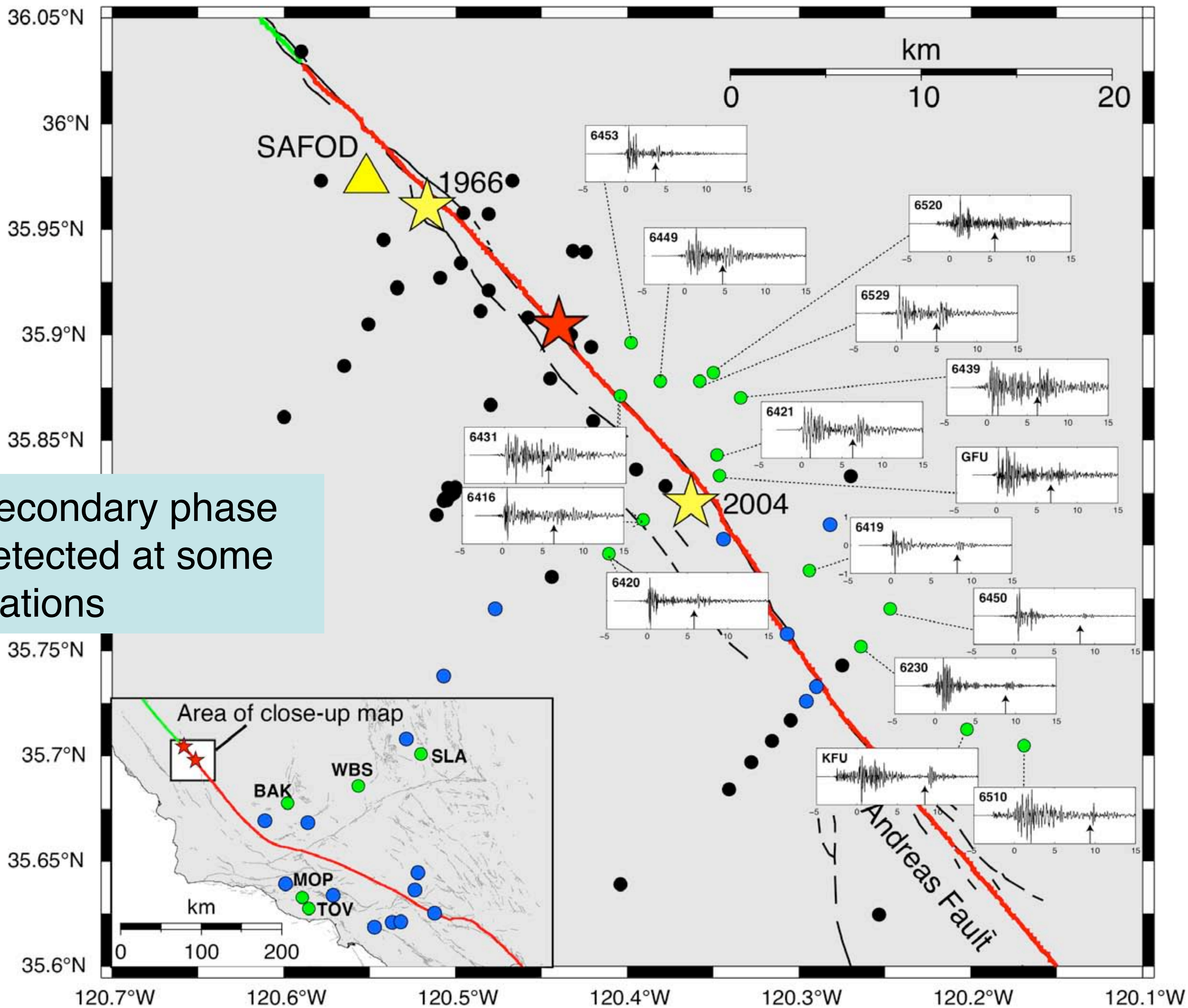

- Best 15 local CGS and GEOS stations for S picks
- Best 5 regional SCSN stations for P picks
- Bandpass filtered between 2 to 8 Hz

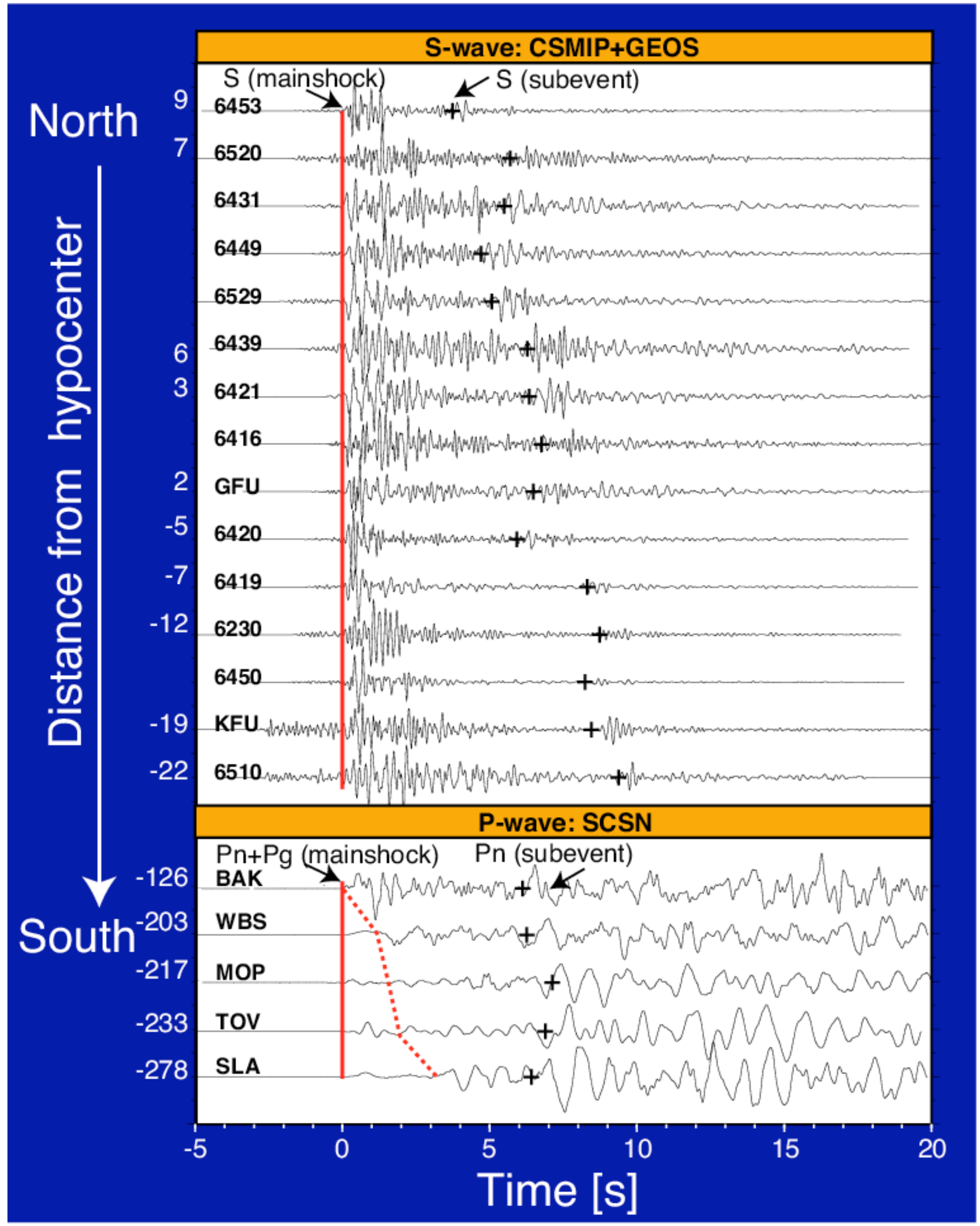

Best-fitting sub-event location:

using **combined S and P picks of local and regional stations**

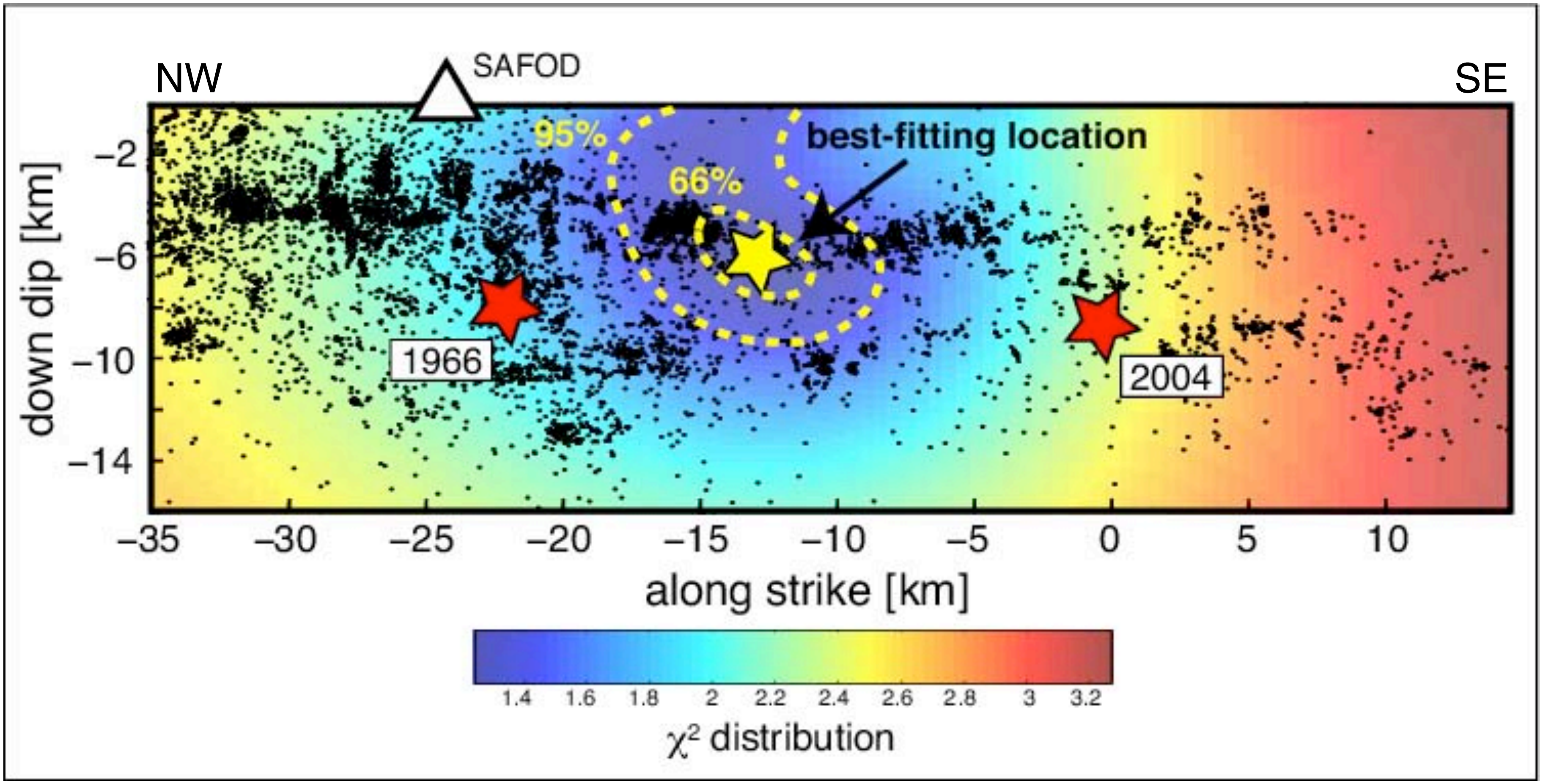


- Along strike: 12.5 km north
- Depth: 6.1 km
- Origin time: 4.945 s

➡ Rupture velocity ~ 2.5 km/s

… good fit between forward-calculated traveltime for the best-fitting hypocenter location and picks

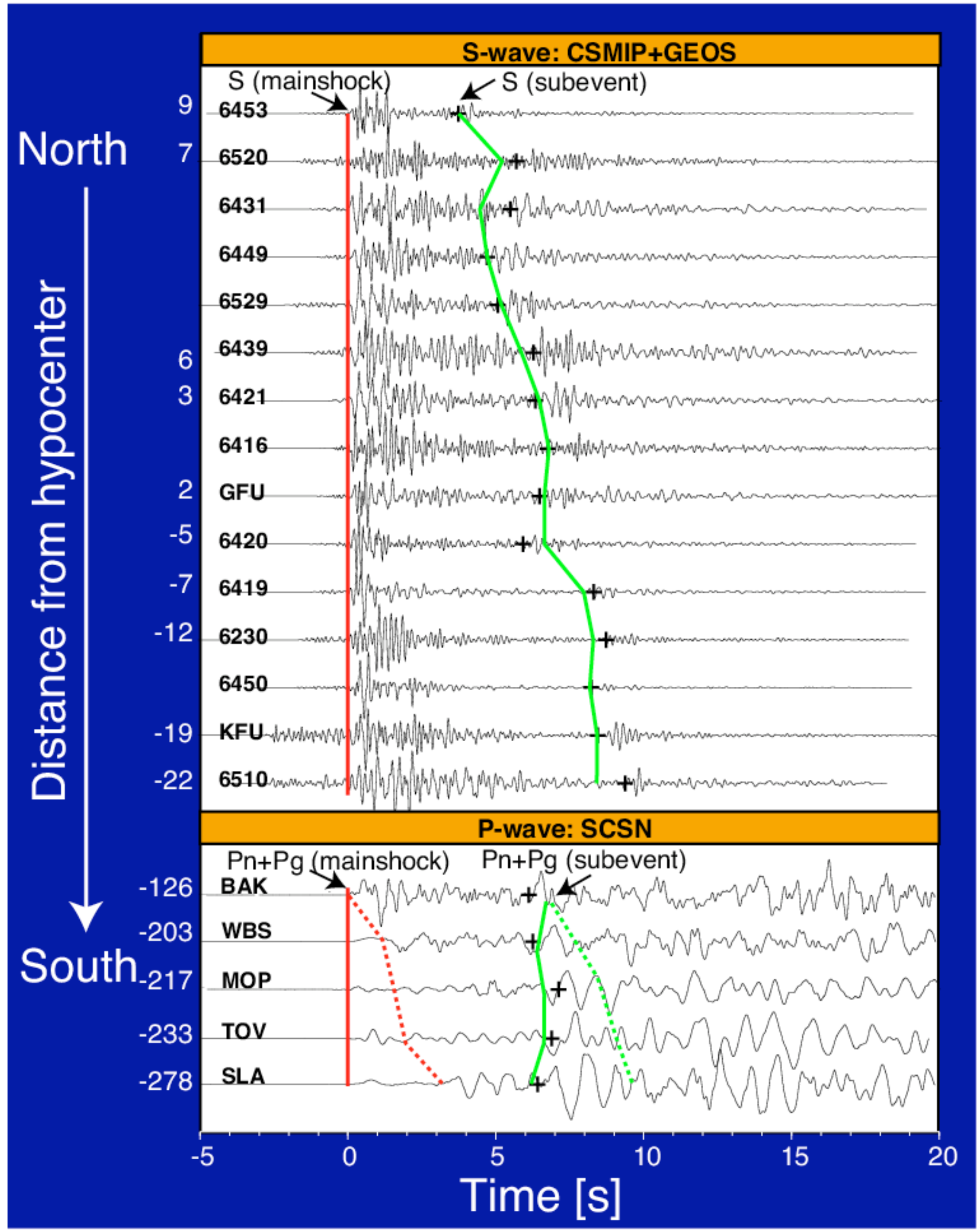

Slip model of *Liu et al. (2006)*

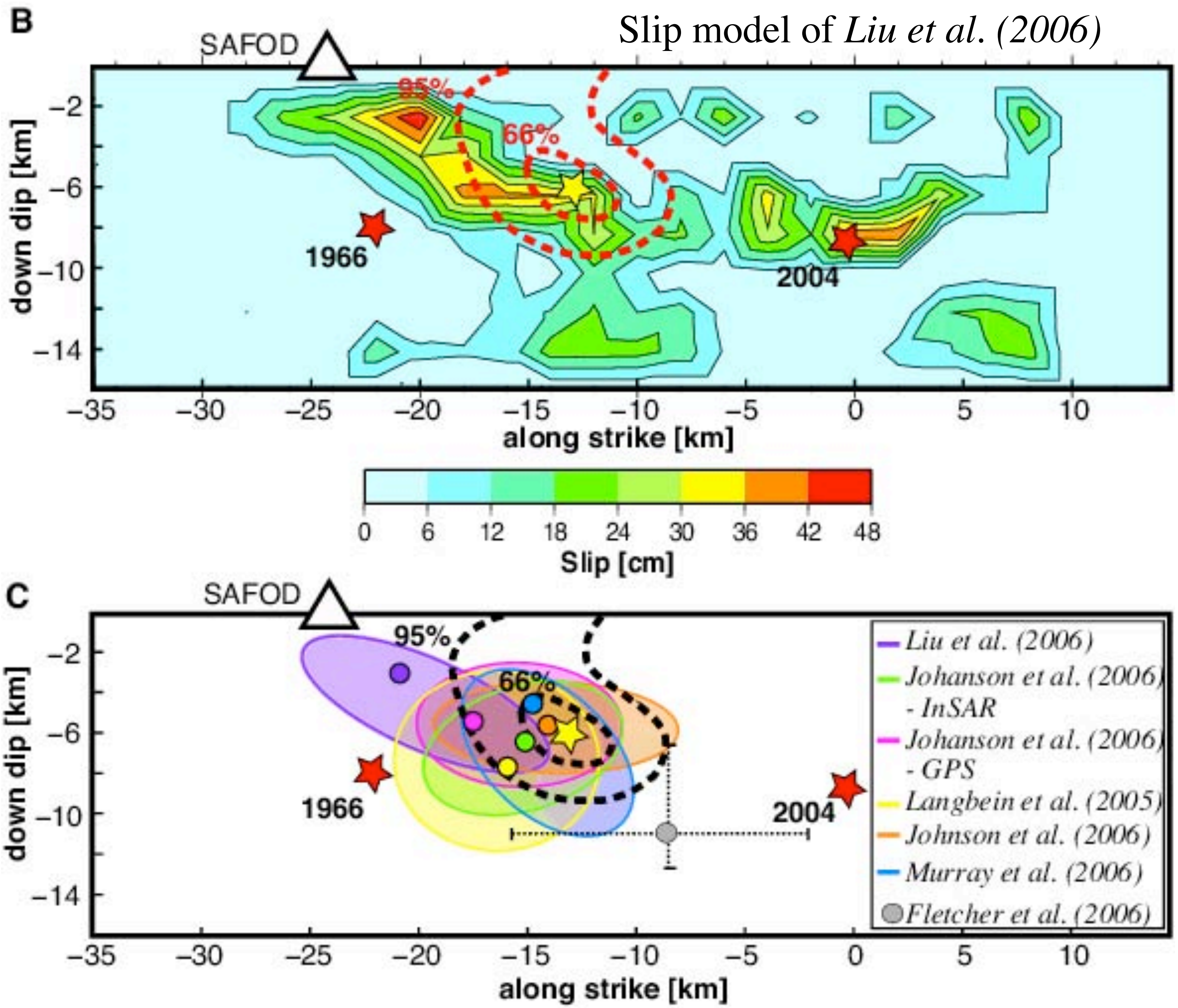

# High-frequency content of subevent … two example stations

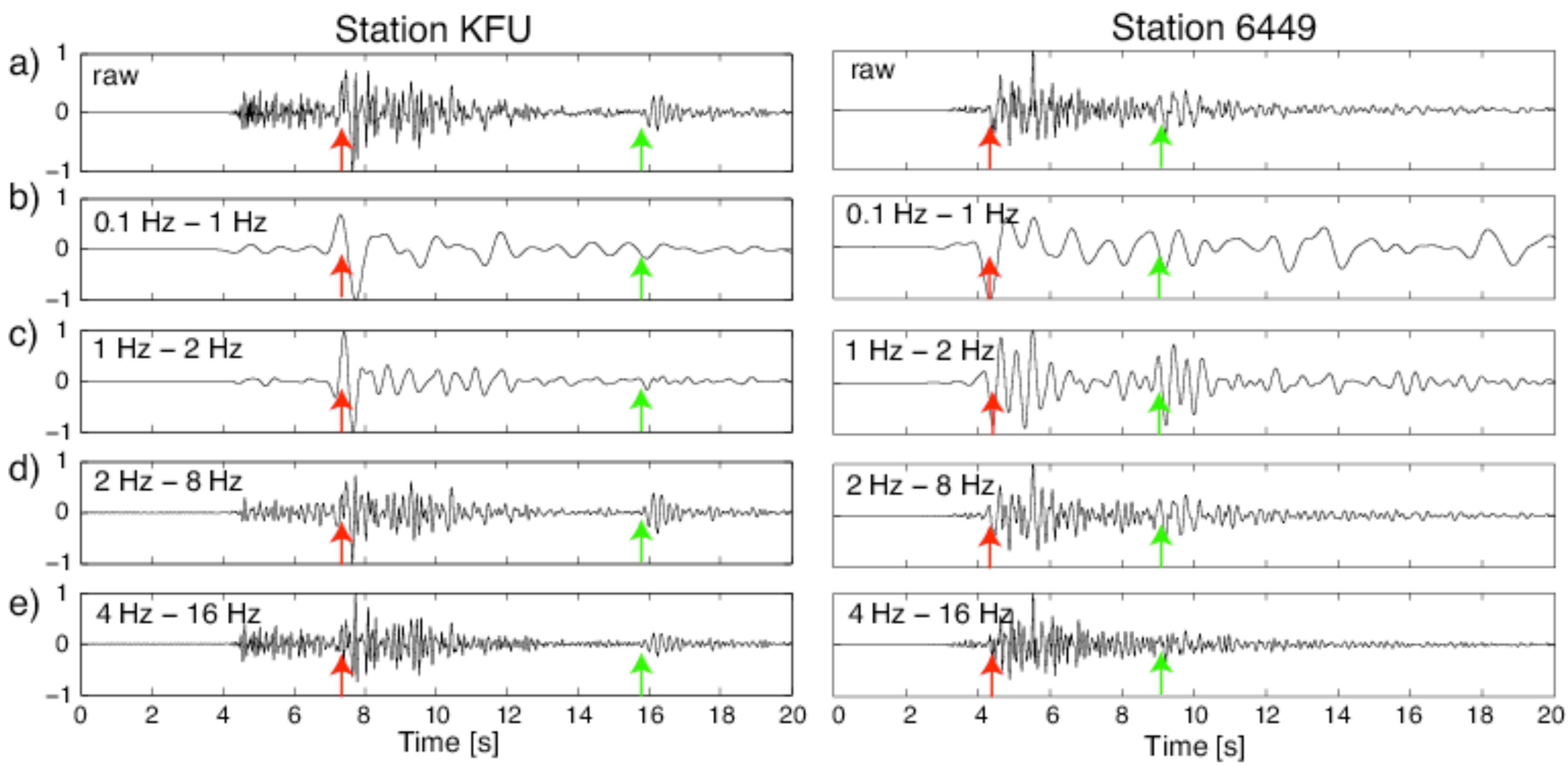

# High-frequency (HF) radiation

- HF radiation from areas of changes in slip and/ or abrupt changes in rupture velocity (e.g., *Madariaga,* 1977*; Spudich and Frazer,* 1984)
- Near the initiation point of asperities or near changes in fault geometry (*Ide*, 2002)
- Some observations indicate HF radiation is found at edges of major slip patches (*Nakayama and Takeo*, 1997*; Nakahara et al.*, 1998*)*

# Synthetic experiment

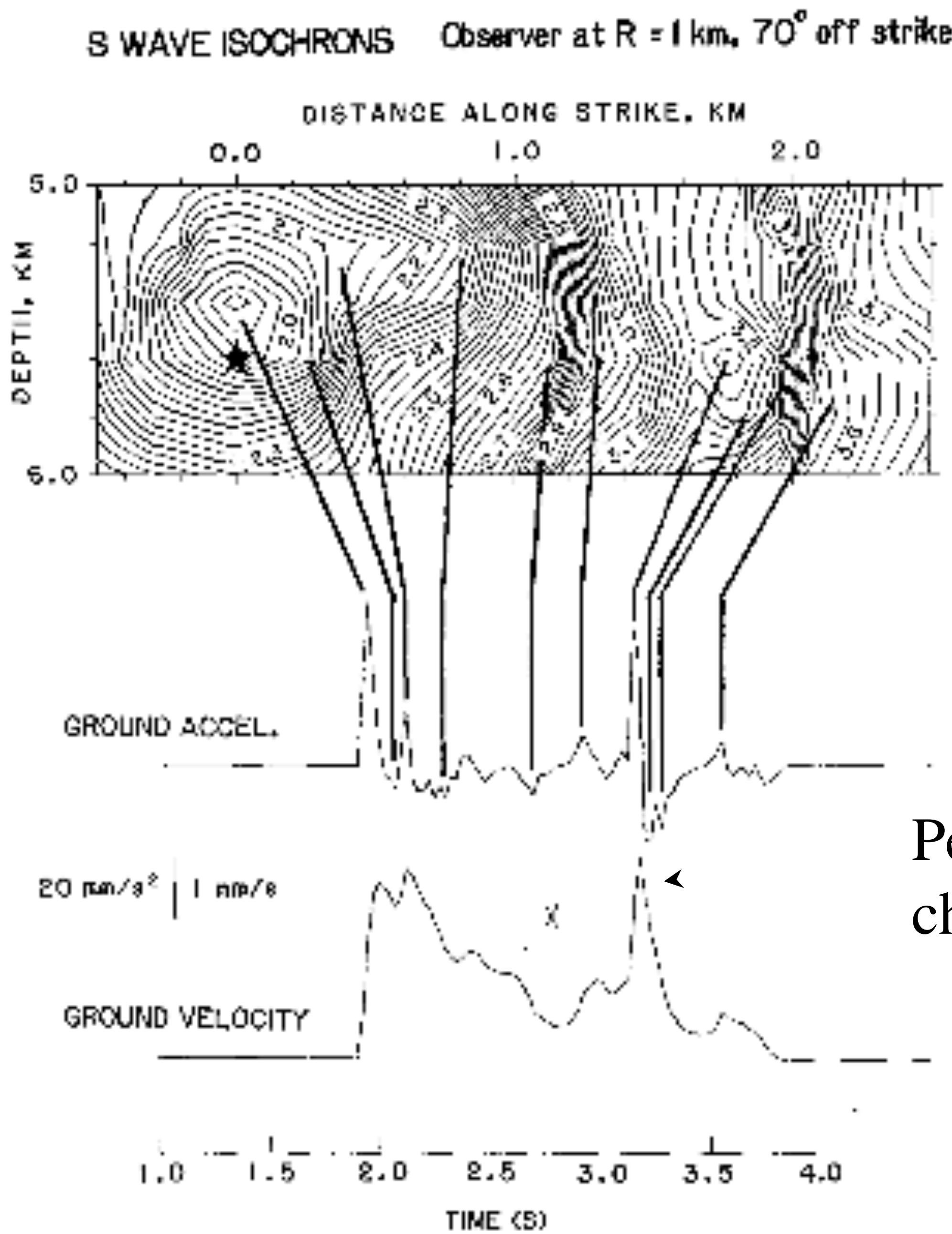


Peak in seismogram from change in rupture velocity

from *Spudich & Frazer* (1984)

# 1995 Kobe earthquake

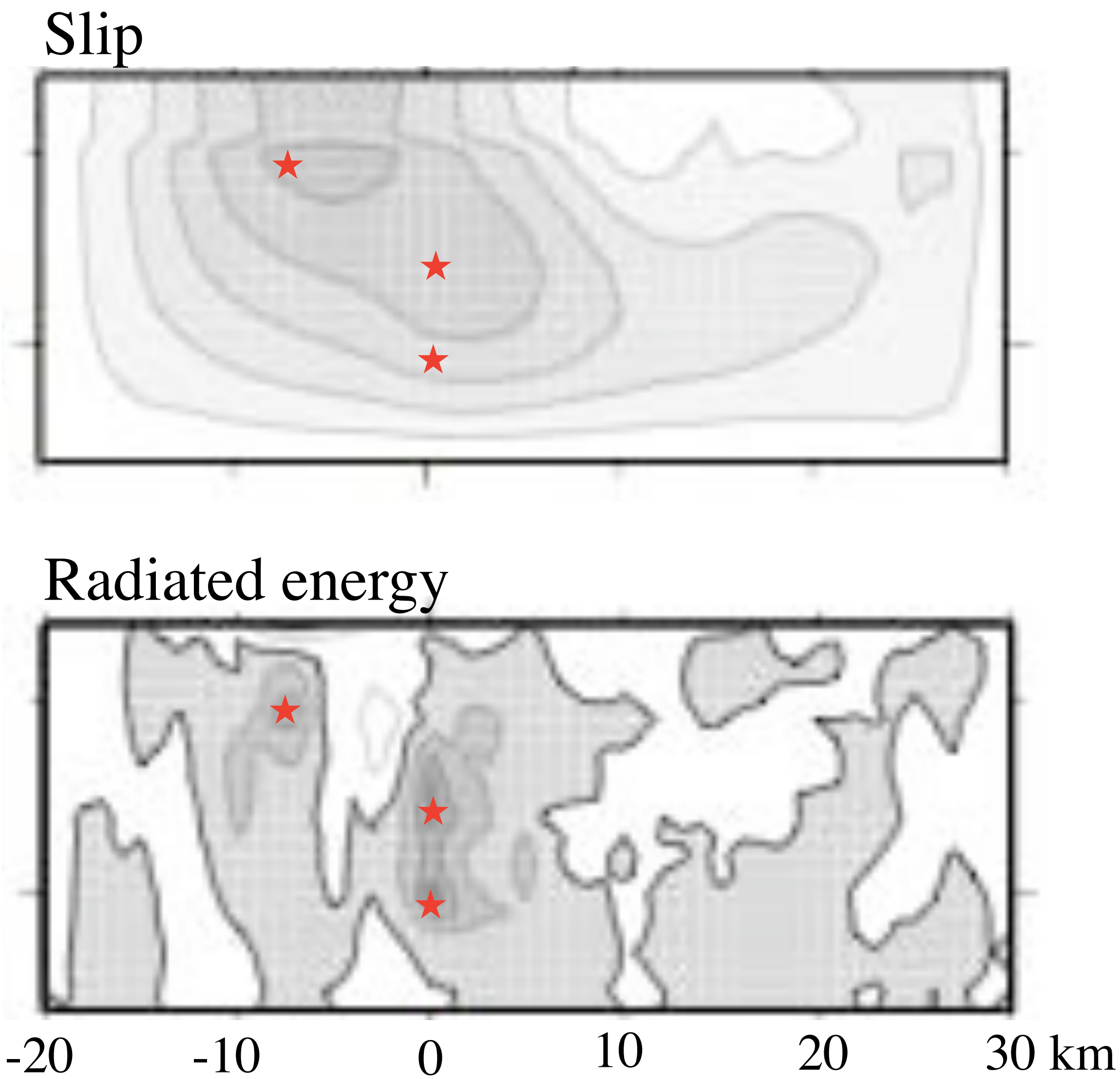


from *Ide* (2002)

# High-frequency (HF) radiation

2. Envelope inversions:  1994 Sanriku earthquake, Japan

HF energy radiation                Low-frequency slip

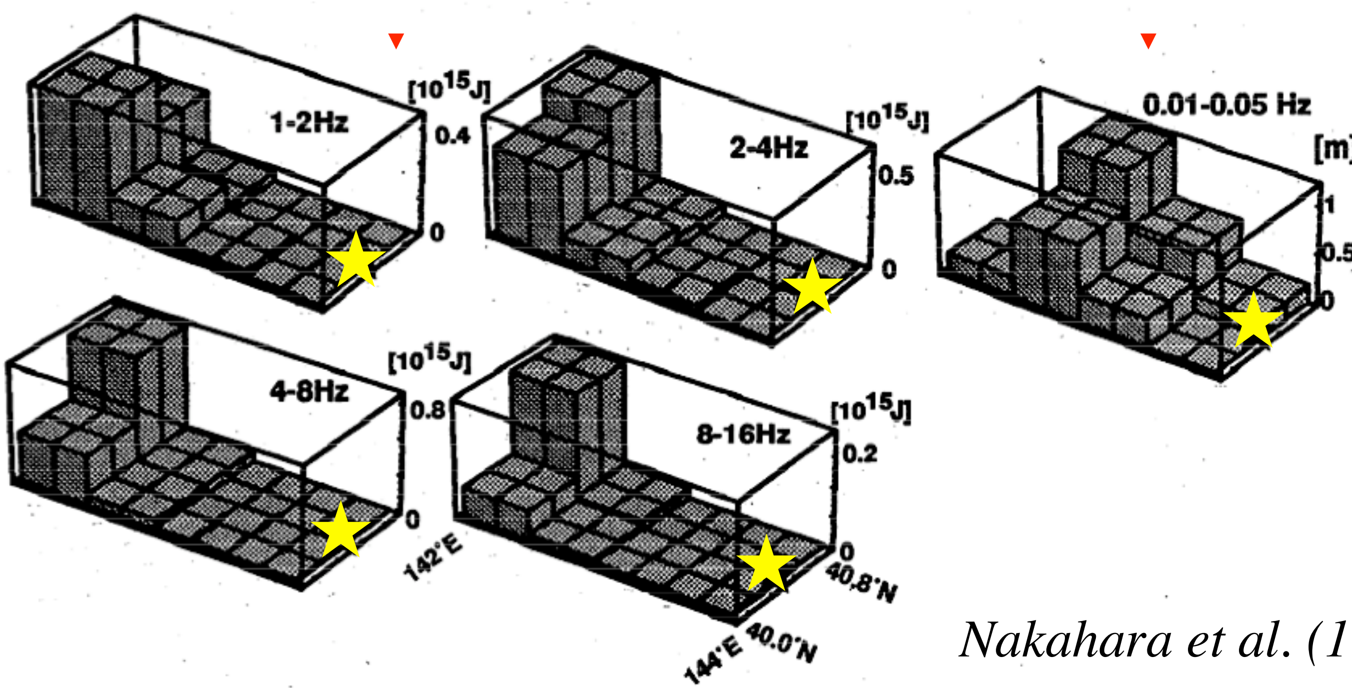


*Nakahara et al. (1998)*

- Larger slip concentrated near the center of the fault
- HF radiation from the western edge of the fault
- Similar results were found for other large earthquakes (e.g. Loma Prieta)
- Limited to equal or lower resolution than low-frequency slip inversions

# 1994 Sanriku earthquake, Japan

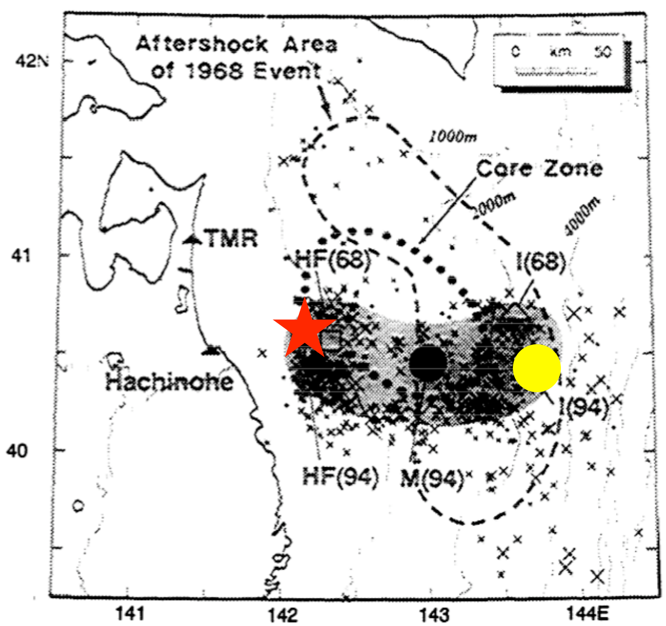


*Sato et al. (1996)*

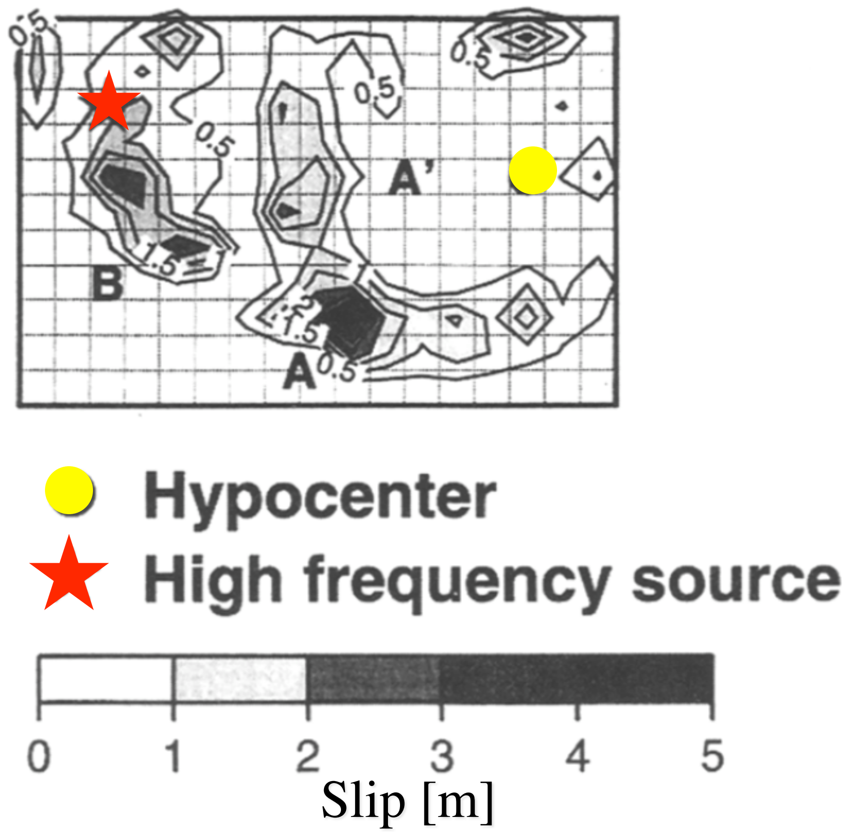


- HF radiation near the end of the rupture
- Can not resolve whether HF radiation is associated with boundary of slip patch or possibly with a stopping phase
- Restricted to 2D fault plane geometry

*Nakayama and Takeo* (1997)

# Initial slip patch radiated more seismic energy, $E_R$, than secondary slip patch

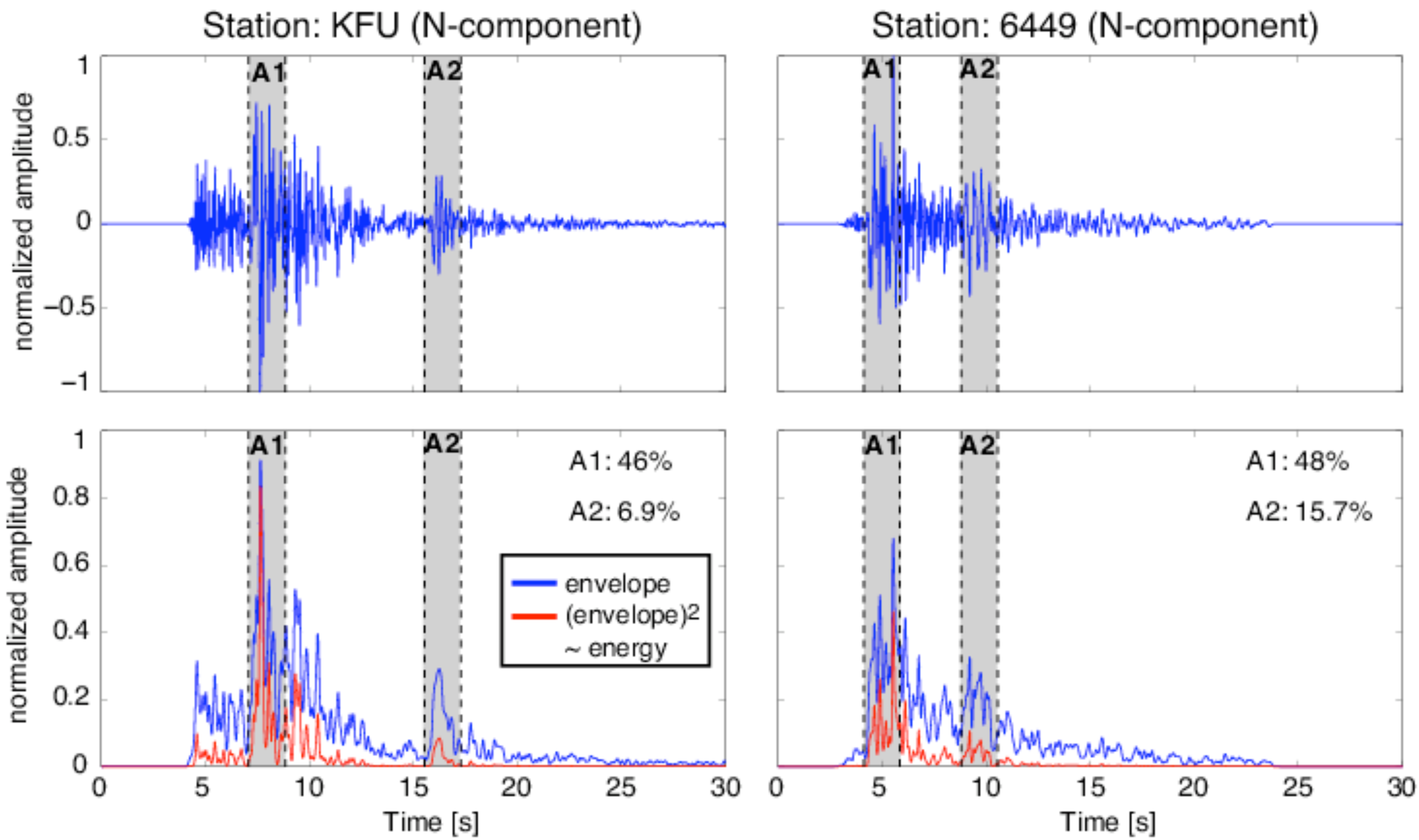

Energy-to-moment ratio (scaled energy) between primary and secondary events

$$\tilde{e} = E_R / M_0$$

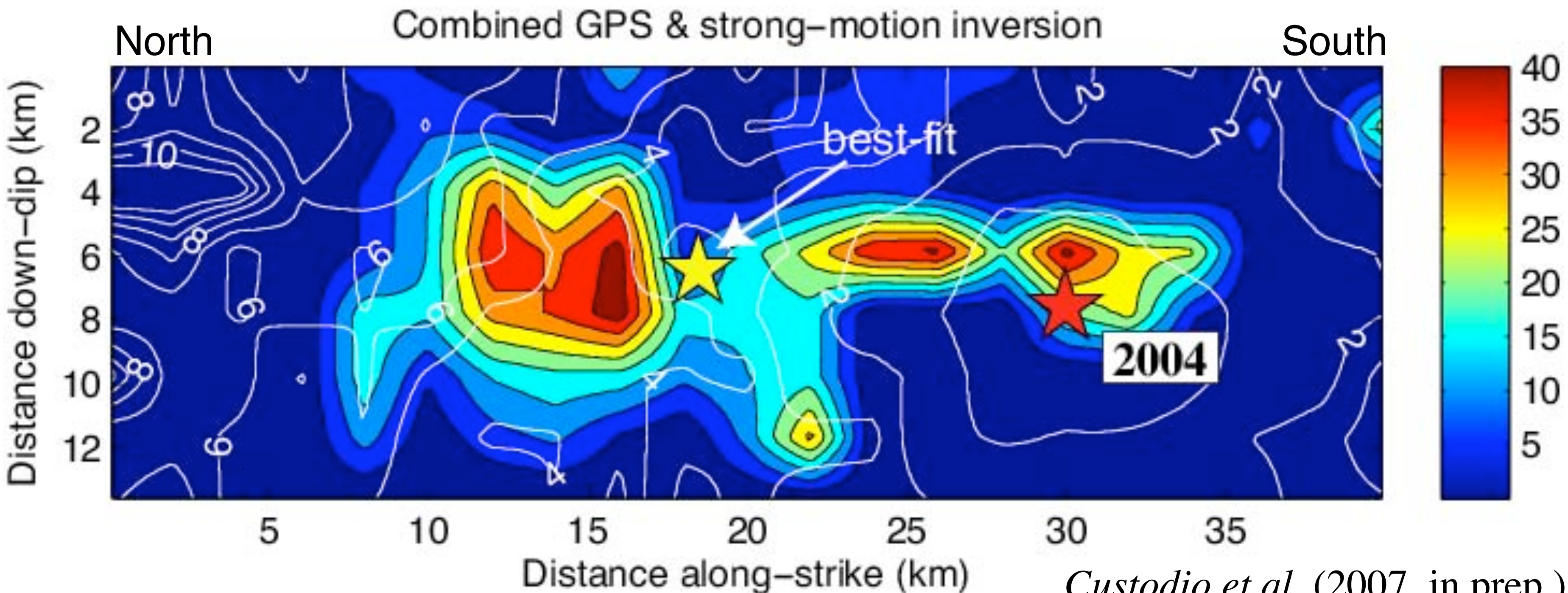


*Custodio et al*. (2007, in prep.)

**Subevent:**

- Less energy $E_s$
- Larger area $A$
- Similar displacement $D$

➡ Smaller scaled energy, likely lower stress drop

# Comparison to small earthquake stress drops Δσ

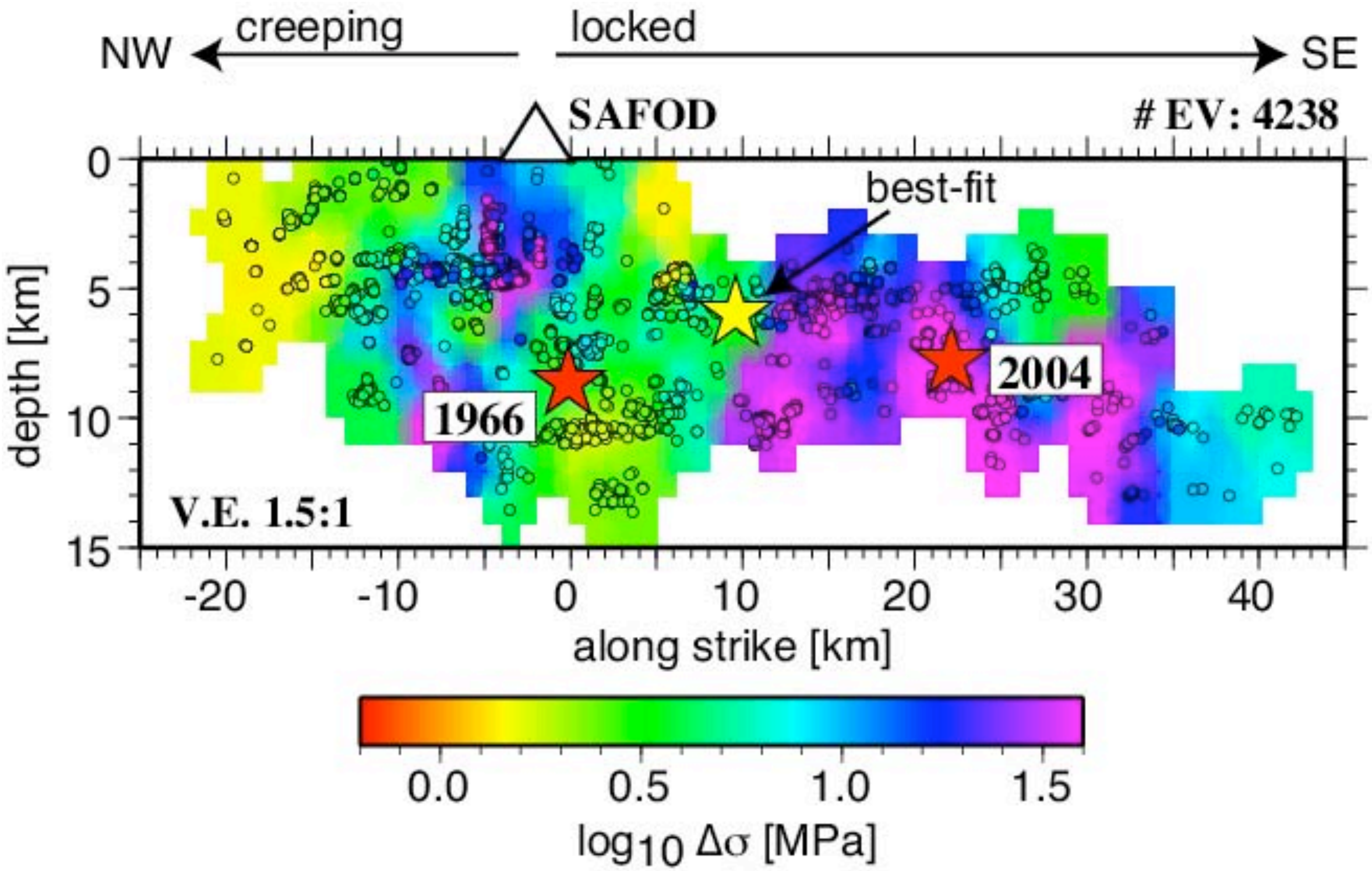


➡ Northern slip patch is located in low stress drop region

Sumatra

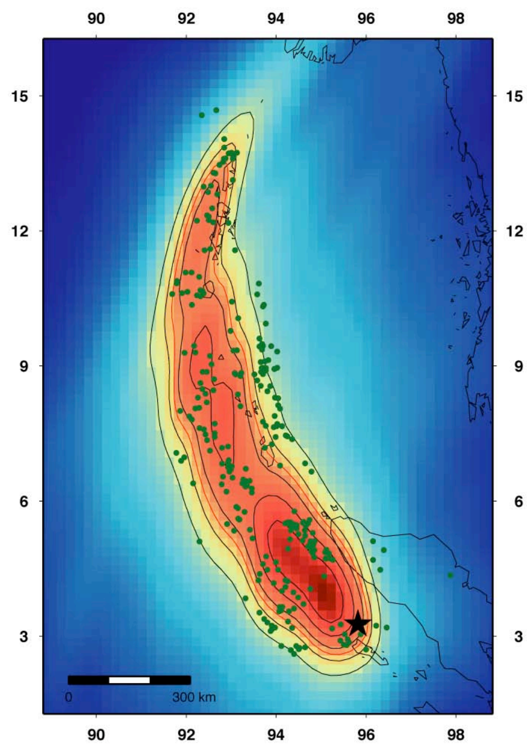


Parkfield

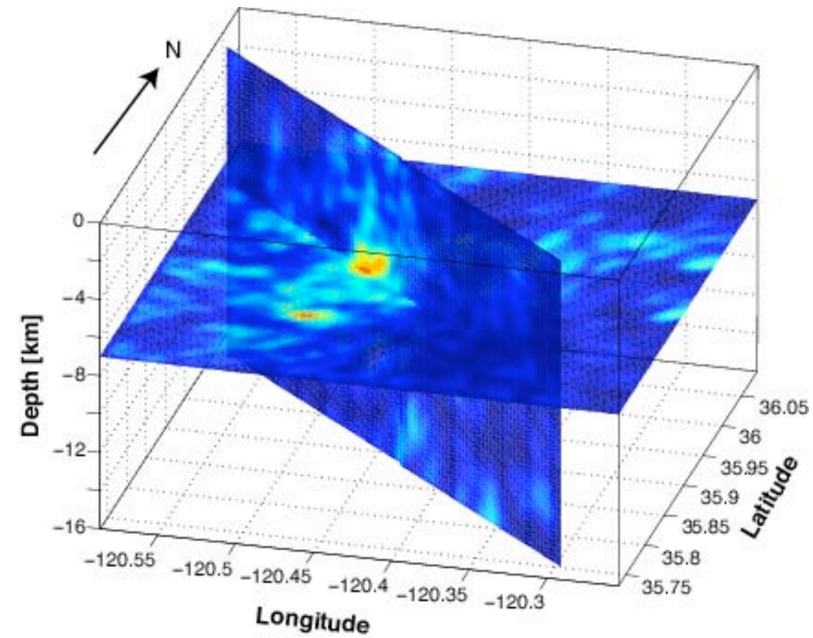


- Back-projection is promising new tool to examine high-frequency radiation from earthquake ruptures
- Complementary to low-frequency seismic slip modeling
- Will help to learn about rupture dynamics

# Resolving supershear rupture using P-wave back-projection imaging

Peter Shearer and Kris Walker

*IGPP, U.C. San Diego*

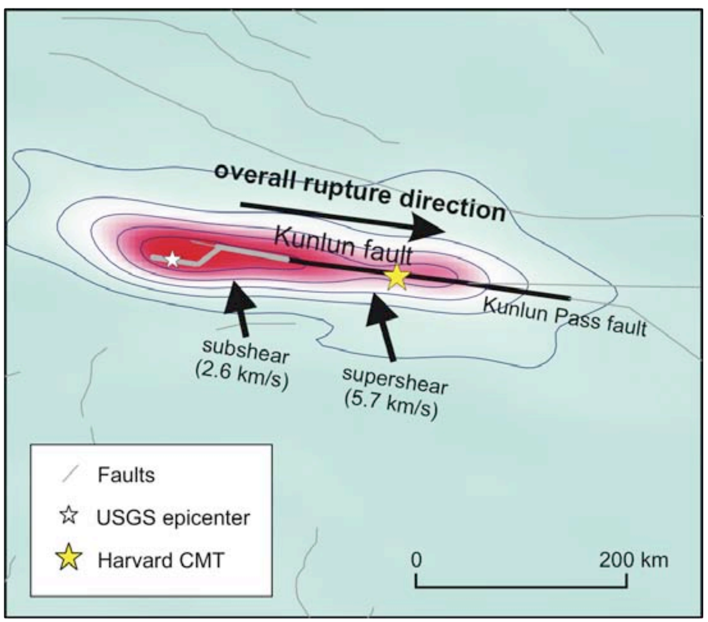


Kris Walker

# Two large strike-slip earthquakes

Kokoxili (Kunlun fault, Tibet), 2001, Mw 7.8

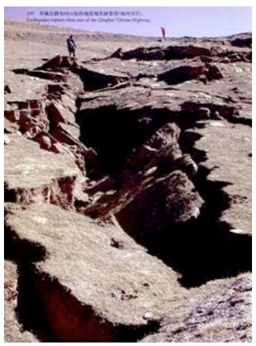

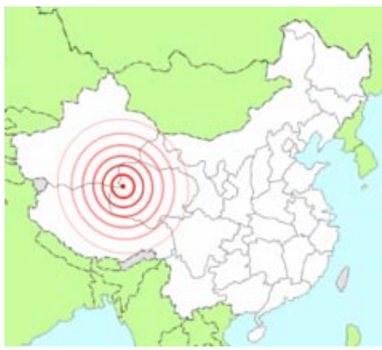

Denali (Alaska), 2002, Mw 7.9

Rupture velocity estimates for these events vary widely, but some studies have indicated *super-shear* velocities (faster than S-wave speed)

# Kokoxili Waveforms

Best backprojection results obtained using western subset of global stations

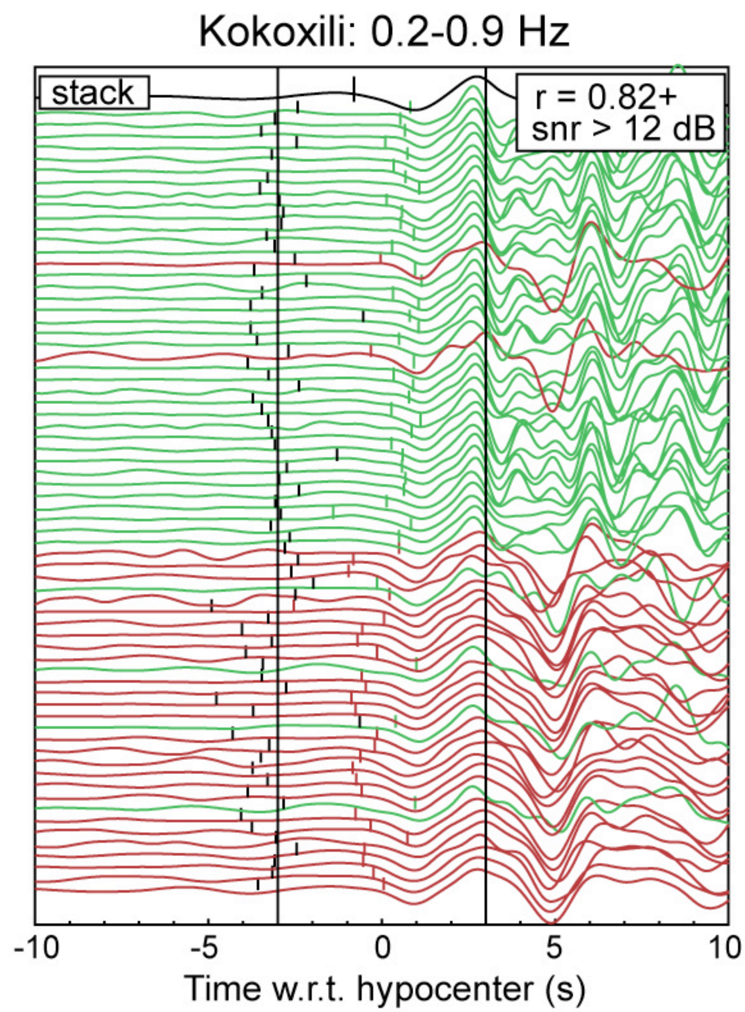


traces for European stations plotted in red

# Kokoxili Waveforms

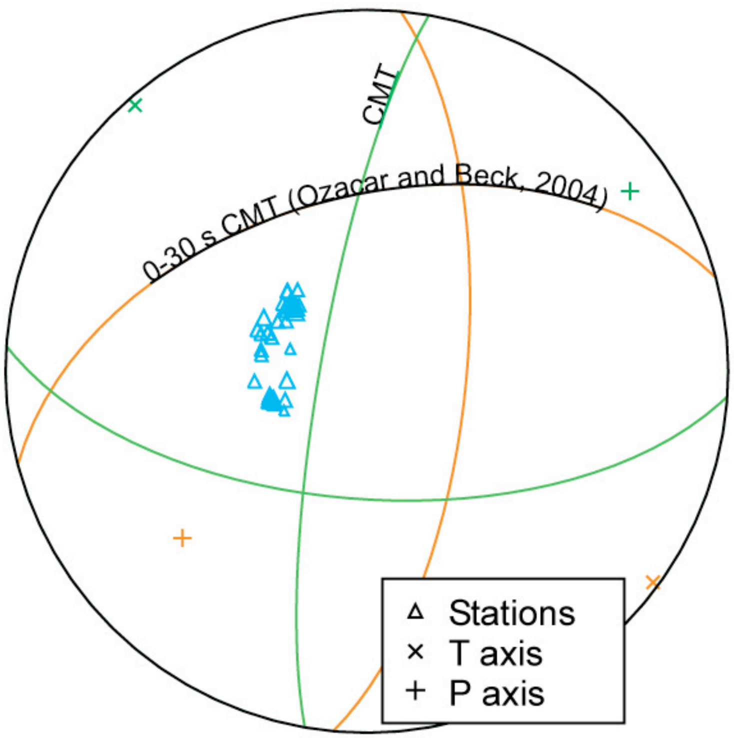


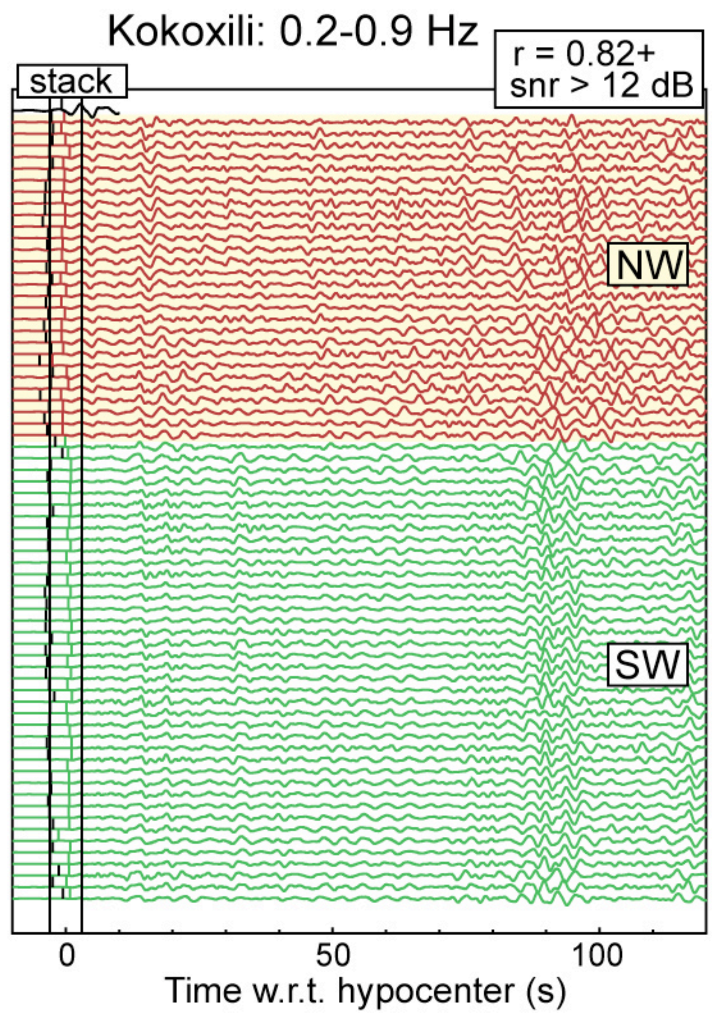


Cross-correlation did not identify polarity flips, which is consistent with CMT solutions

# Post-Processing $S(x,y,t)^2$ -> $S(x,y,t)_i^2$: Cube Integrator

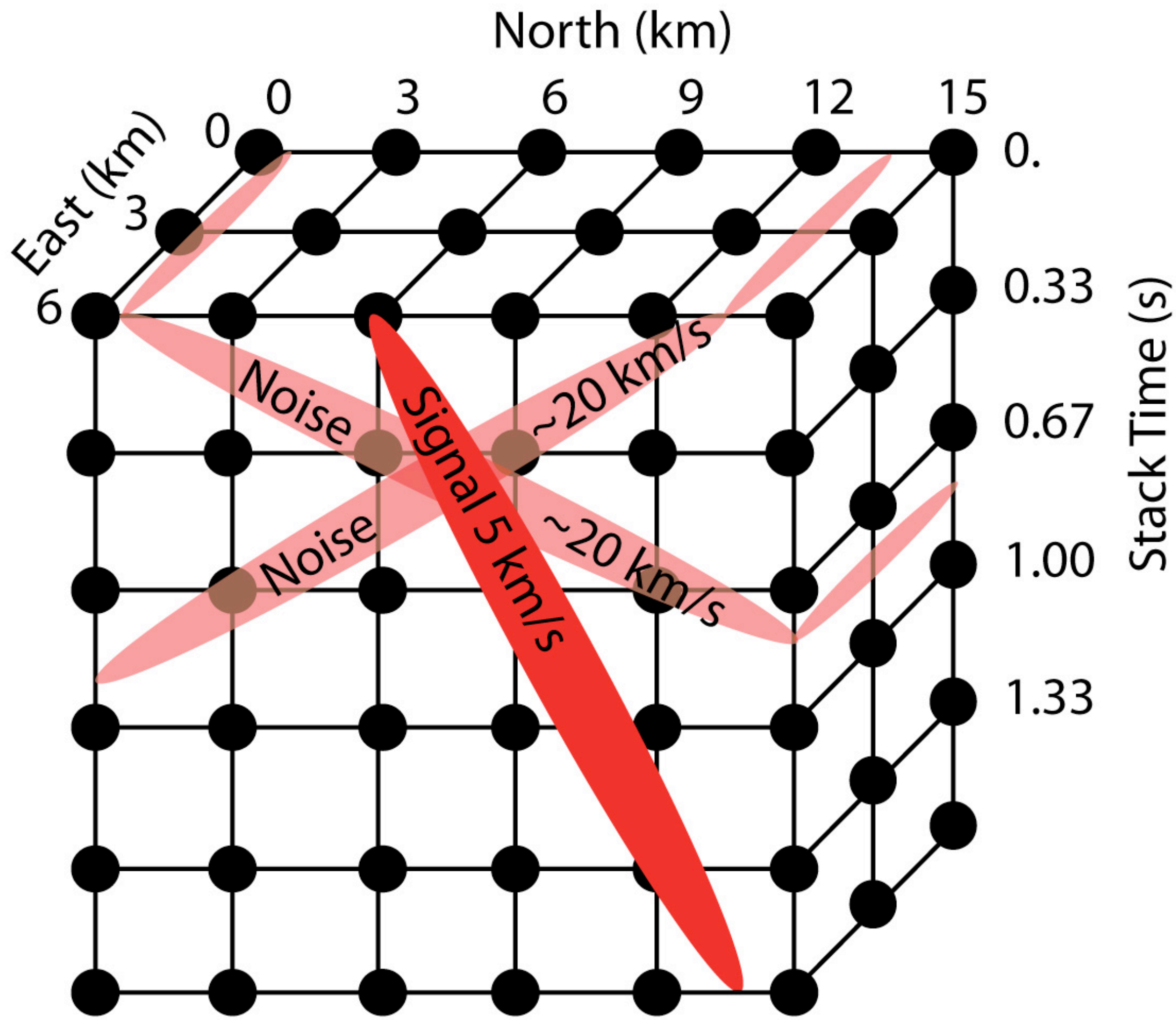

# Post-Processing $S(x,y,t)^2 \rightarrow S(x,y,t)_i^2$: Cube Integrator

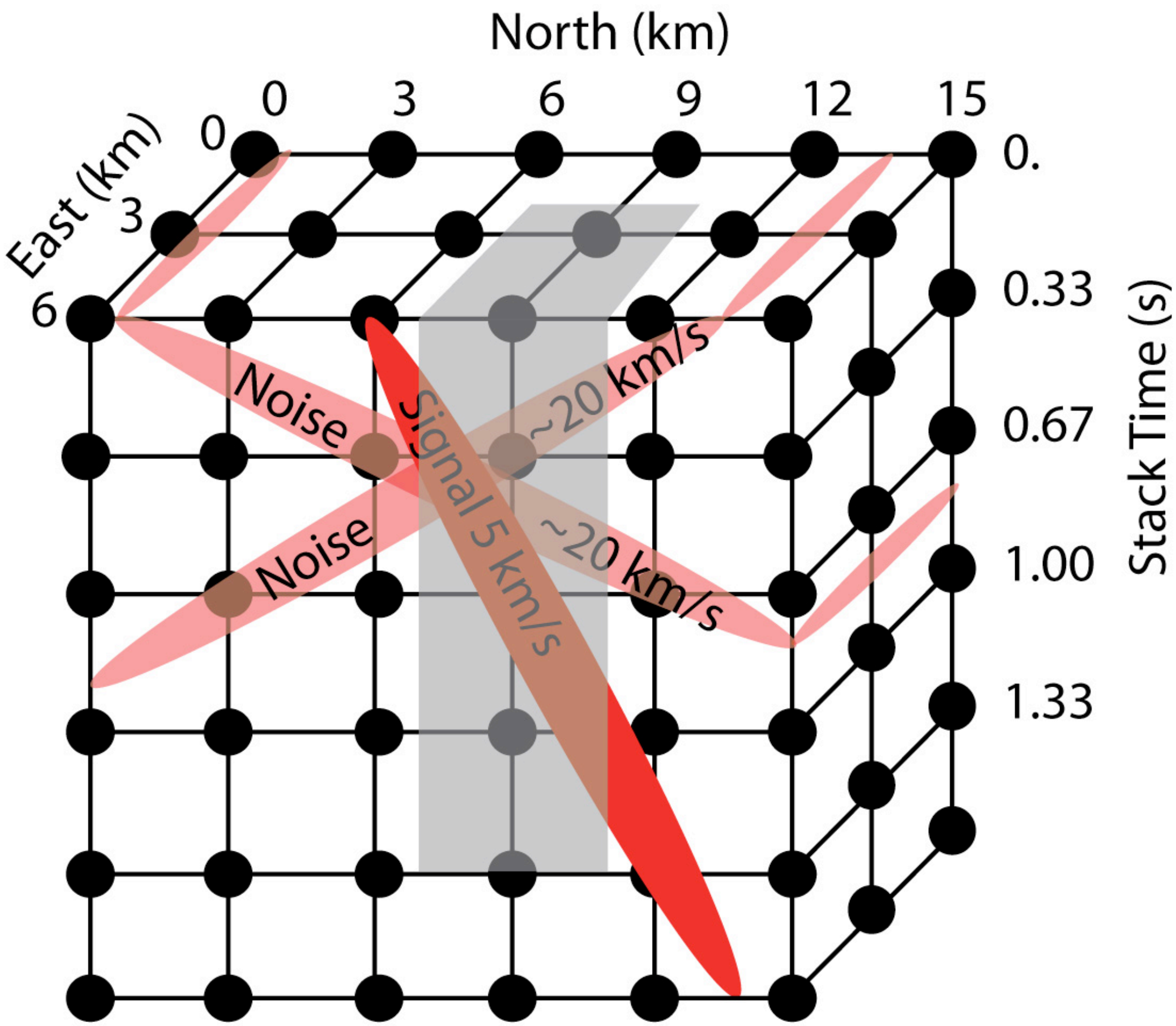


Smooth back-stacked power image with cube operator of 40 km & 20 km width for Kokoxili and Denali, respectively (using scaling velocity of 3 km/s)

# Post-processing $S(x,y,t)_i$: peak finder

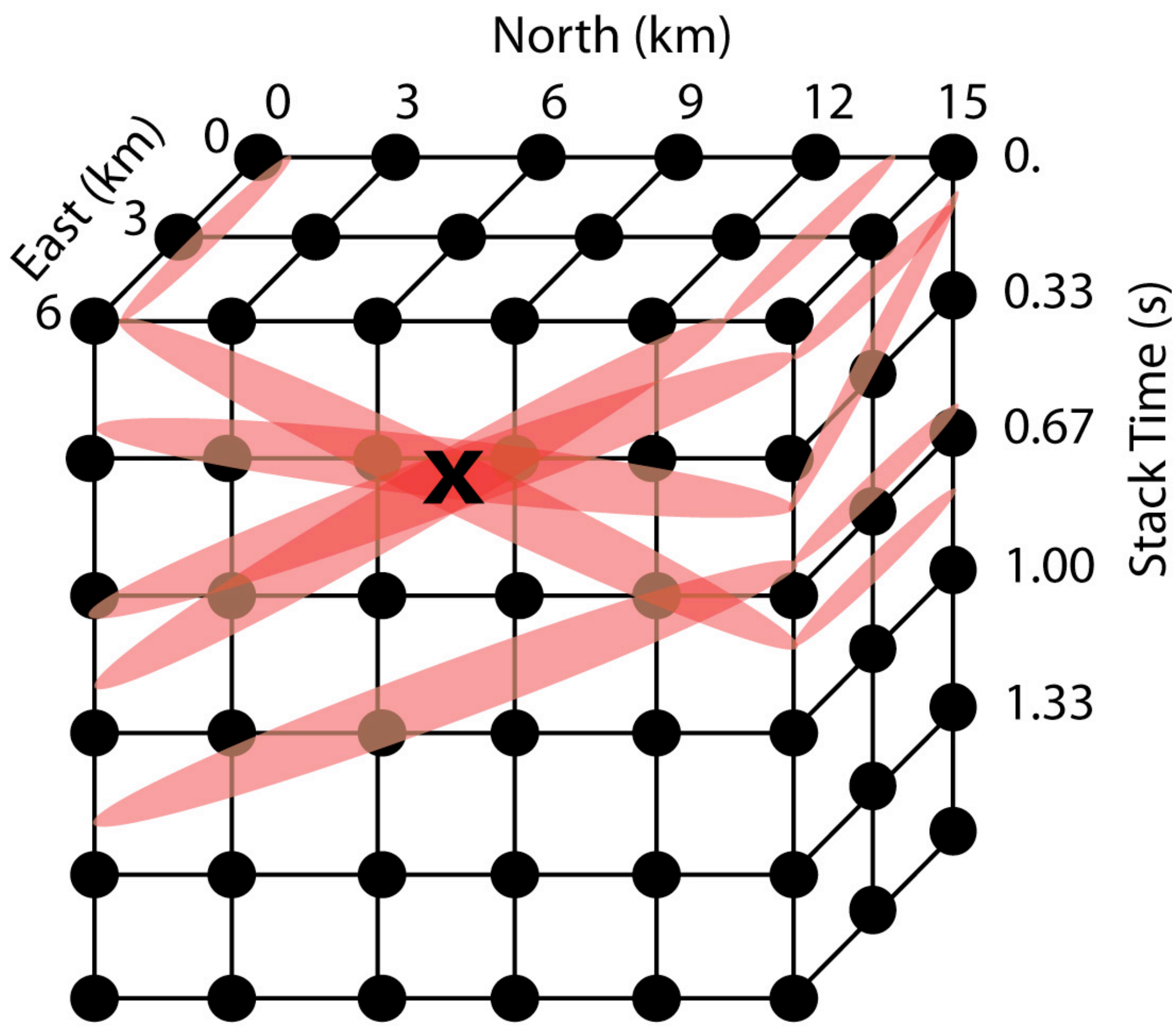


- find all local maxima greater than ~35% global maximum

- sort by decreasing amplitude

- starting with largest going down, discard maximum that are within ~32 km of larger maxima

# Kokoxili Rupture Image

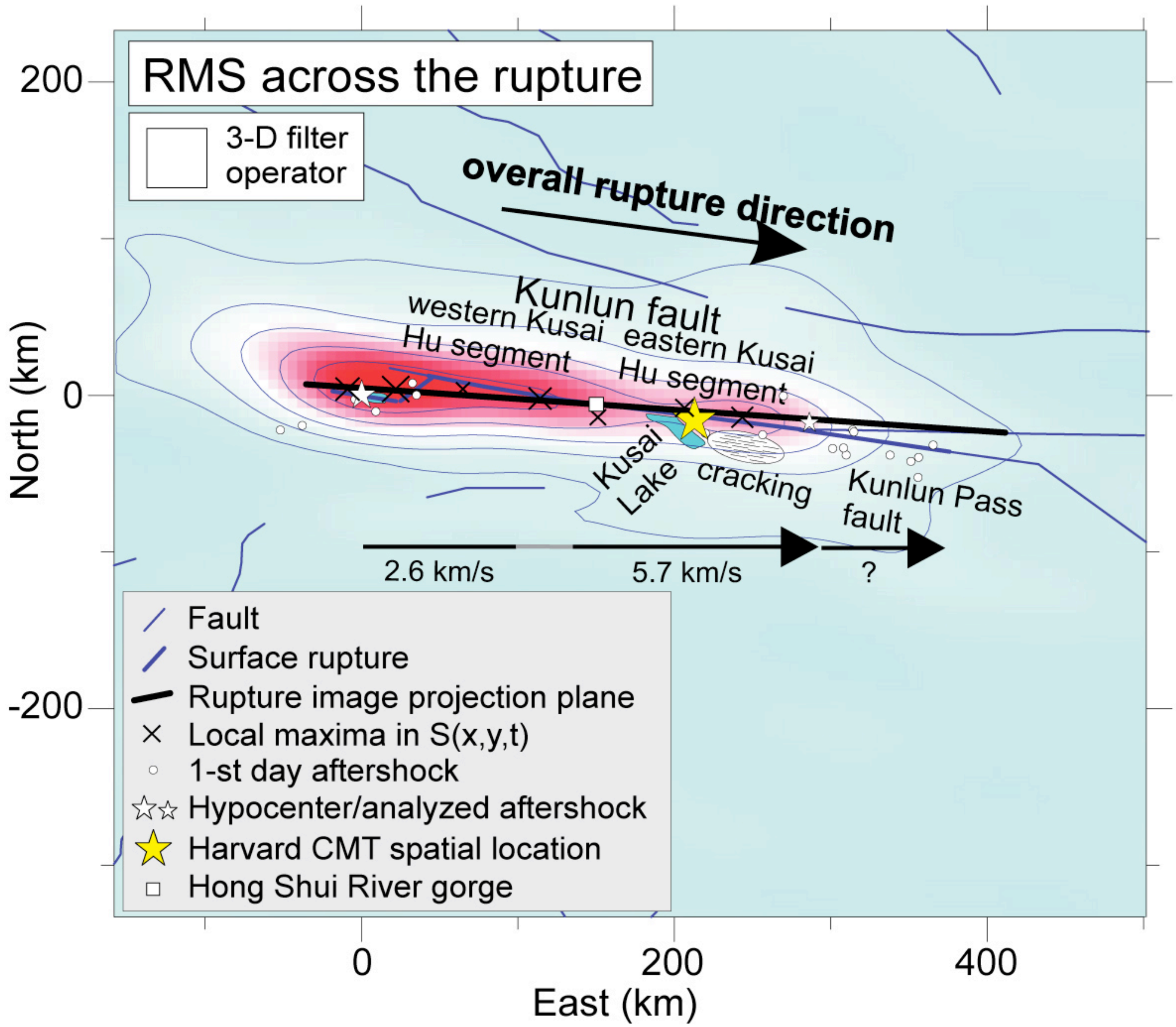


Local maxima define two rupture velocities

Coherence lost near Kunlun Pass fault

# Kokoxili Time Slices (normalized by frame max)

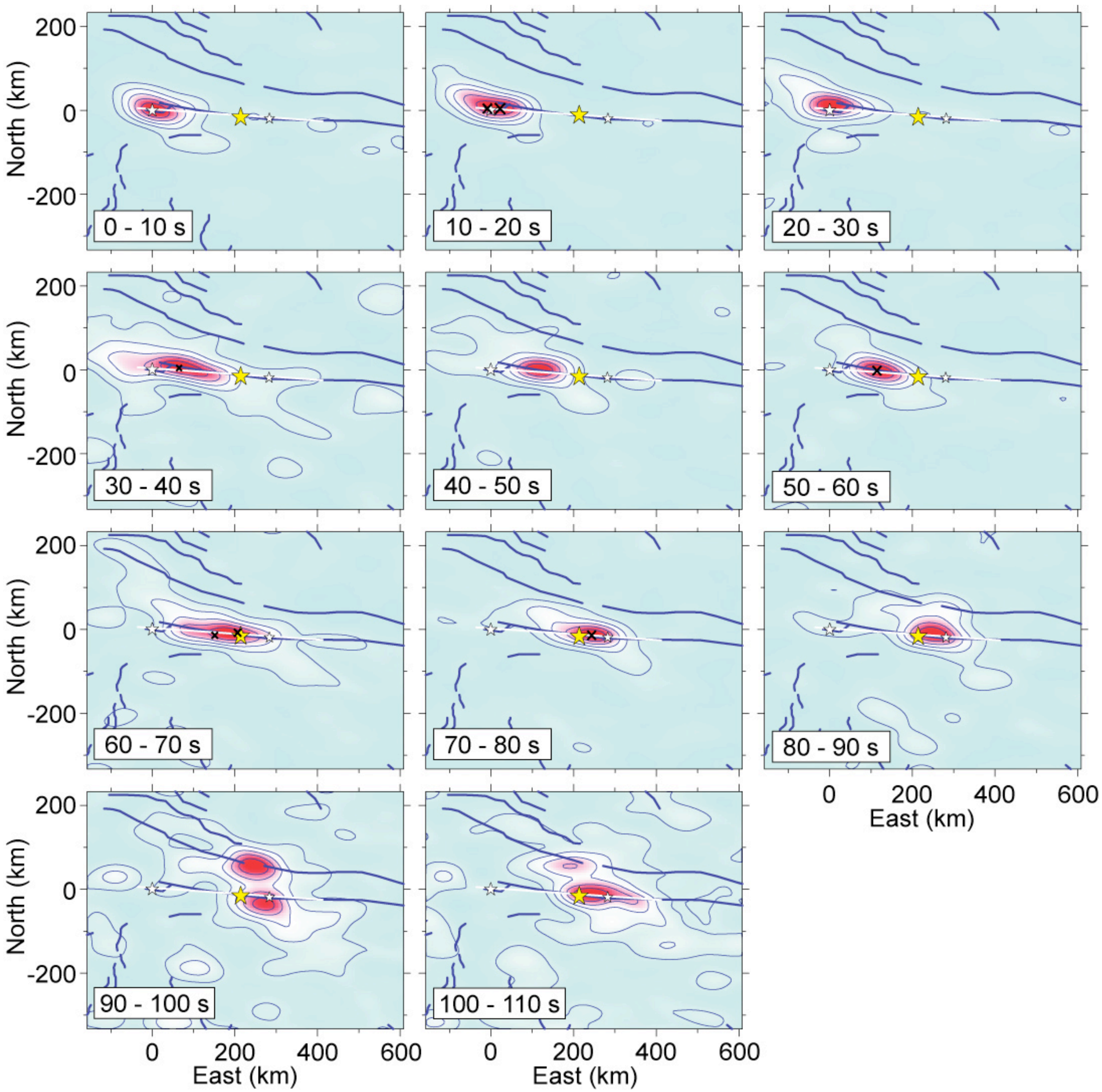


"x" marks carefully measured local maxima, which suggest two rupture velocity regimes

Rupture is well imaged out to Kunlun Pass fault

Aftershock imaging test shows apparent bifurcation is due to 3-D velocity heterogeneity

# Kokoxili Rupture Image (along-strike)

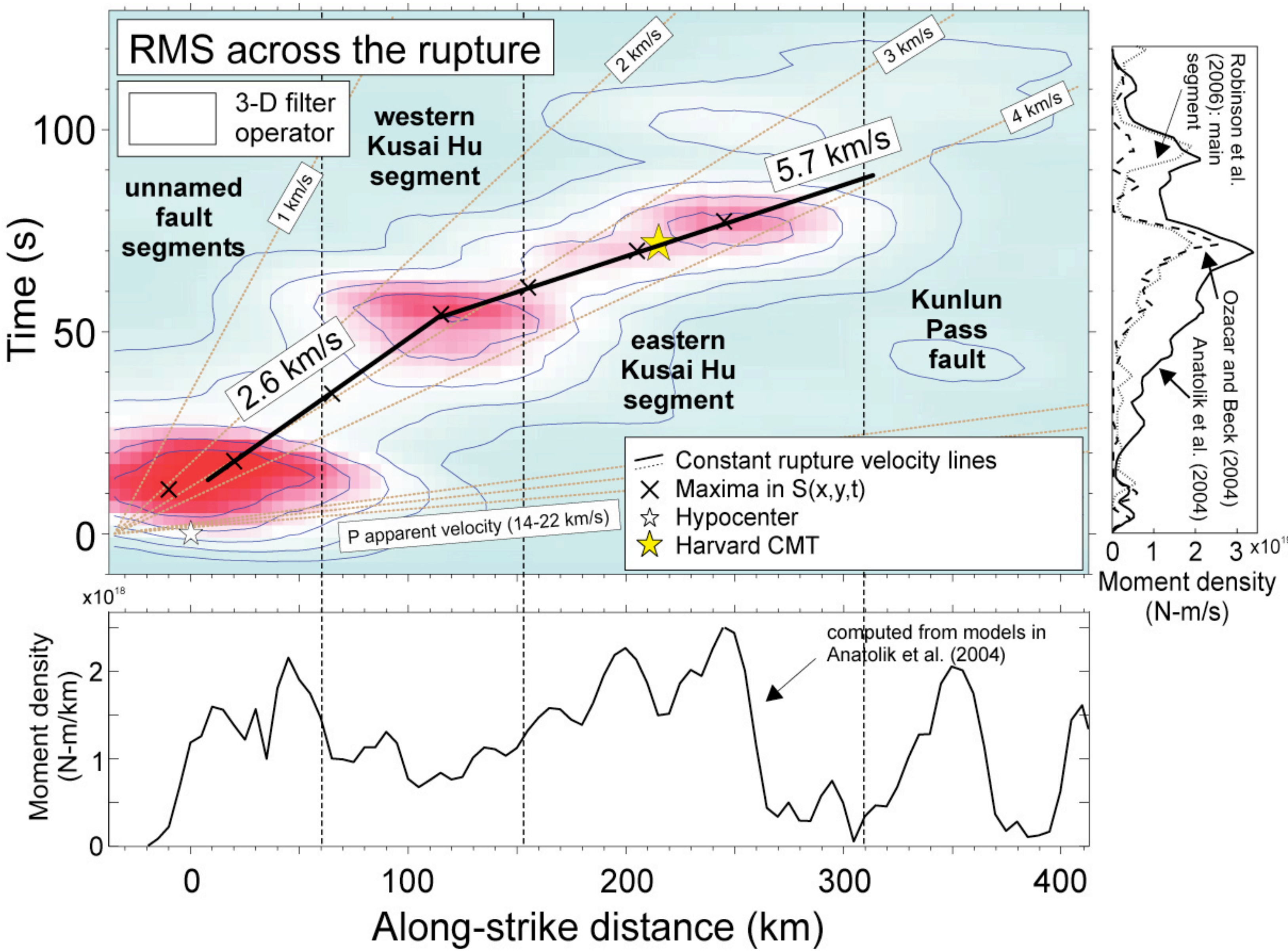

# Synthetic Imaging Tests

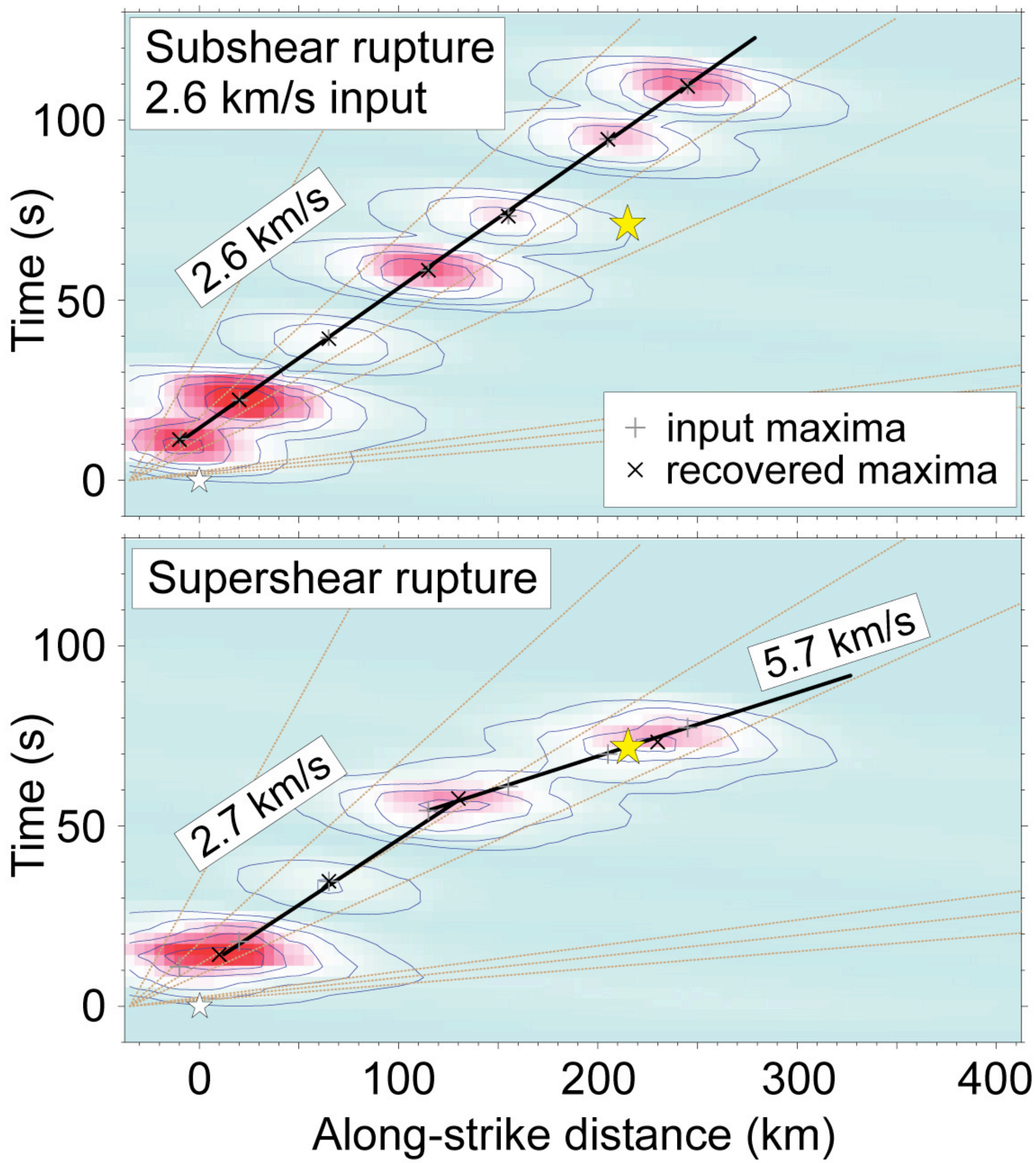


- Use maxima from real stacks as "subevents" in space. Adjust time for subshear and supershear scenarios.
- Assign to each an impulse using observed amplitudes.
- Filter impulse with same BP filter and stack as if real data.
- Recalculate maxima.
- Maxima slightly mislocated in supershear case.
- Overall supershear/subshear velocities are clearly distinguishable.

# Denali Waveforms

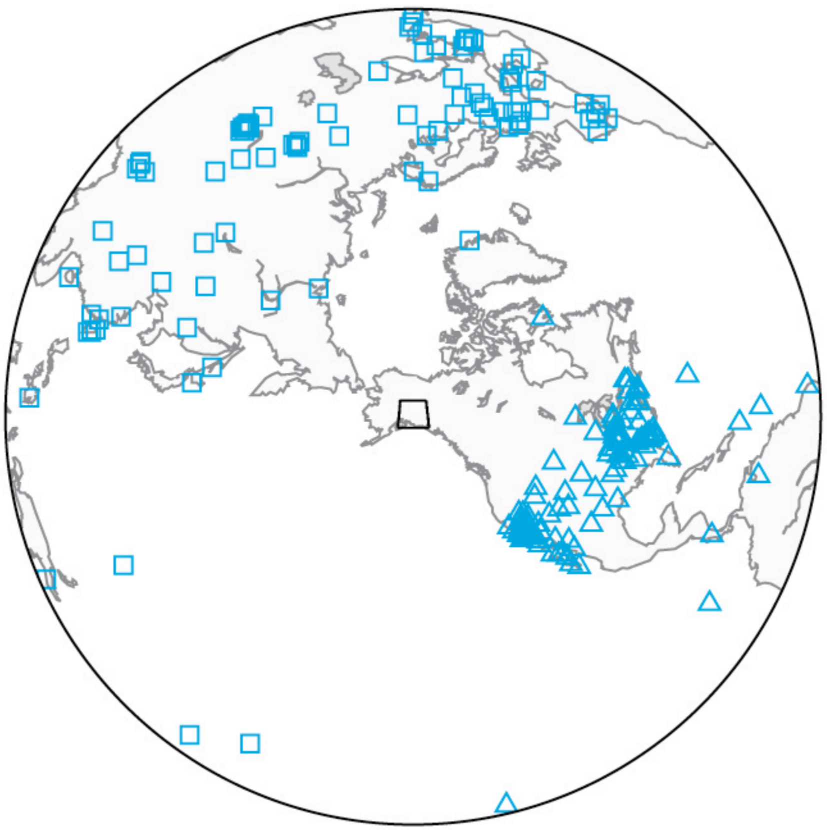

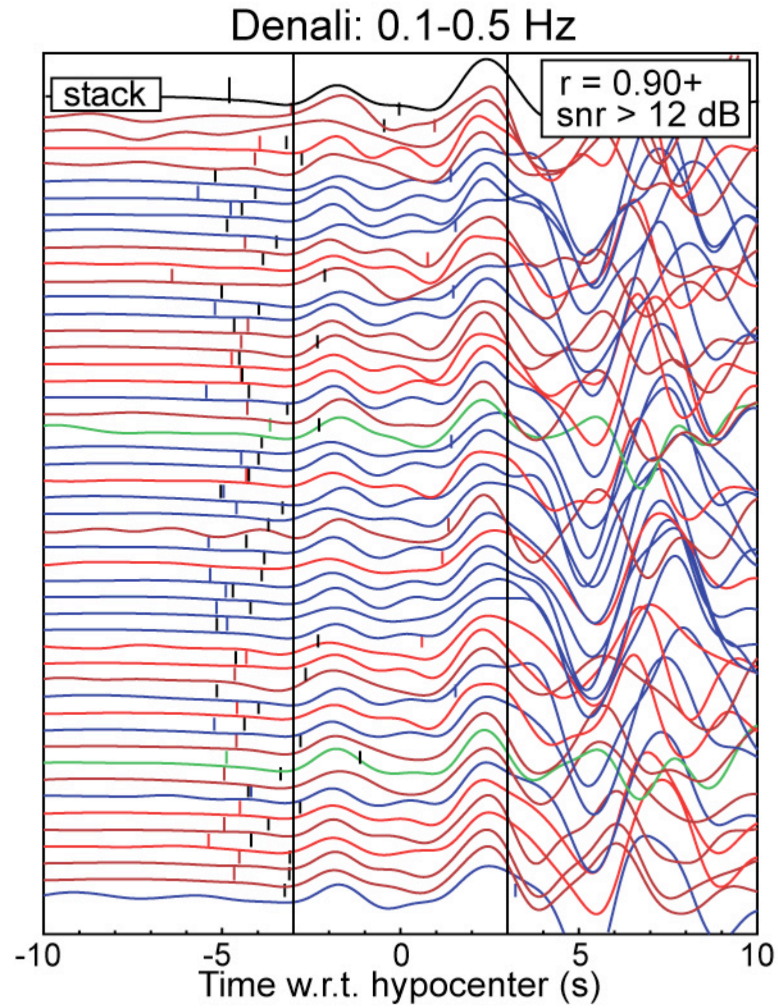

# Denali Waveforms

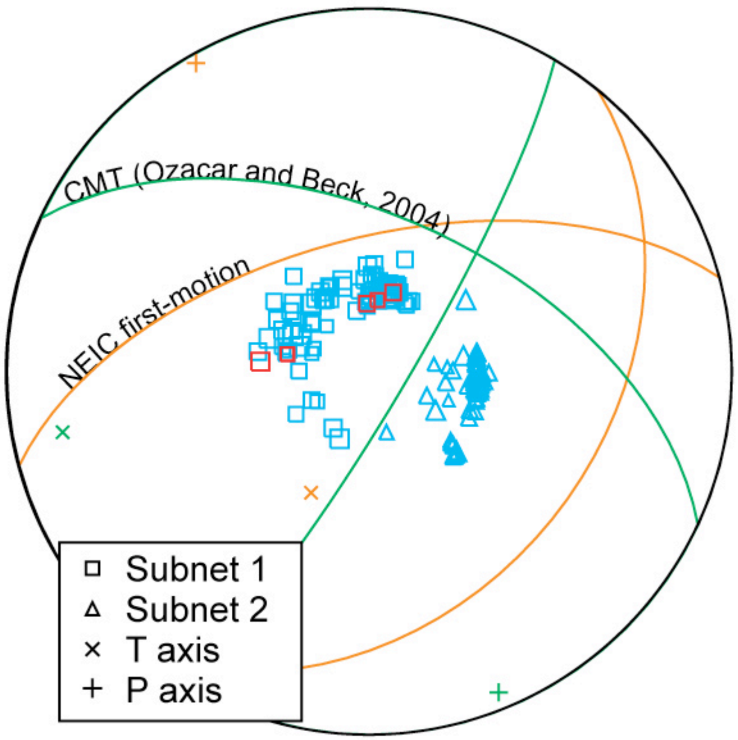


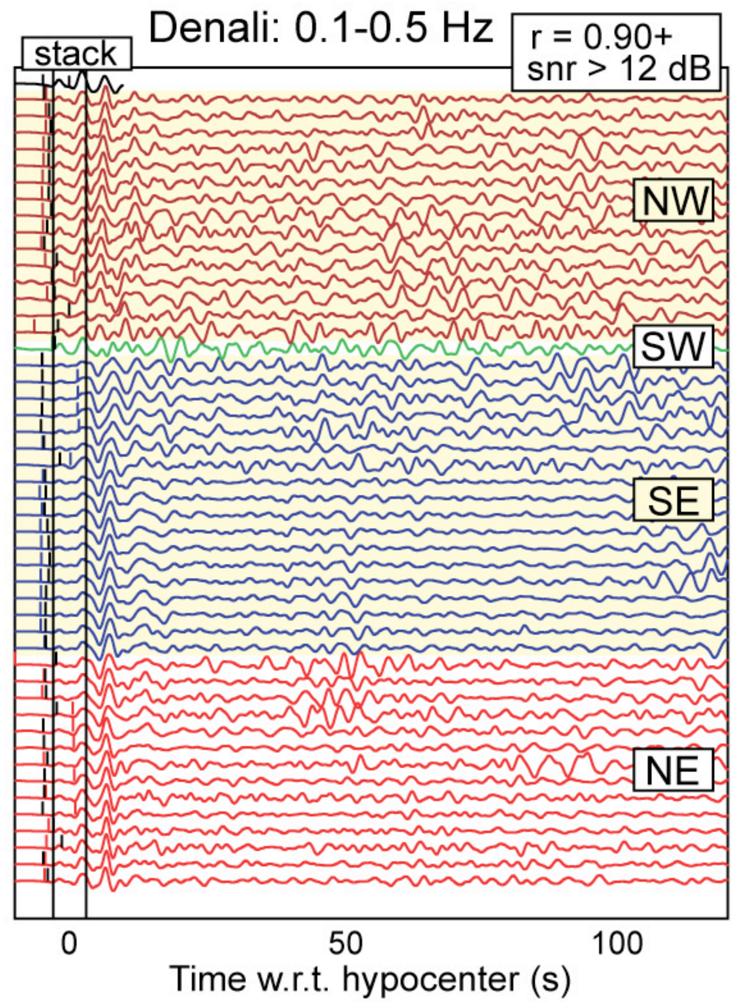


- Only a few polarity flips required
- Consistent with NEIC first motion
- 30+ s part of rupture needs to be imaged separately

# Denali Rupture Image

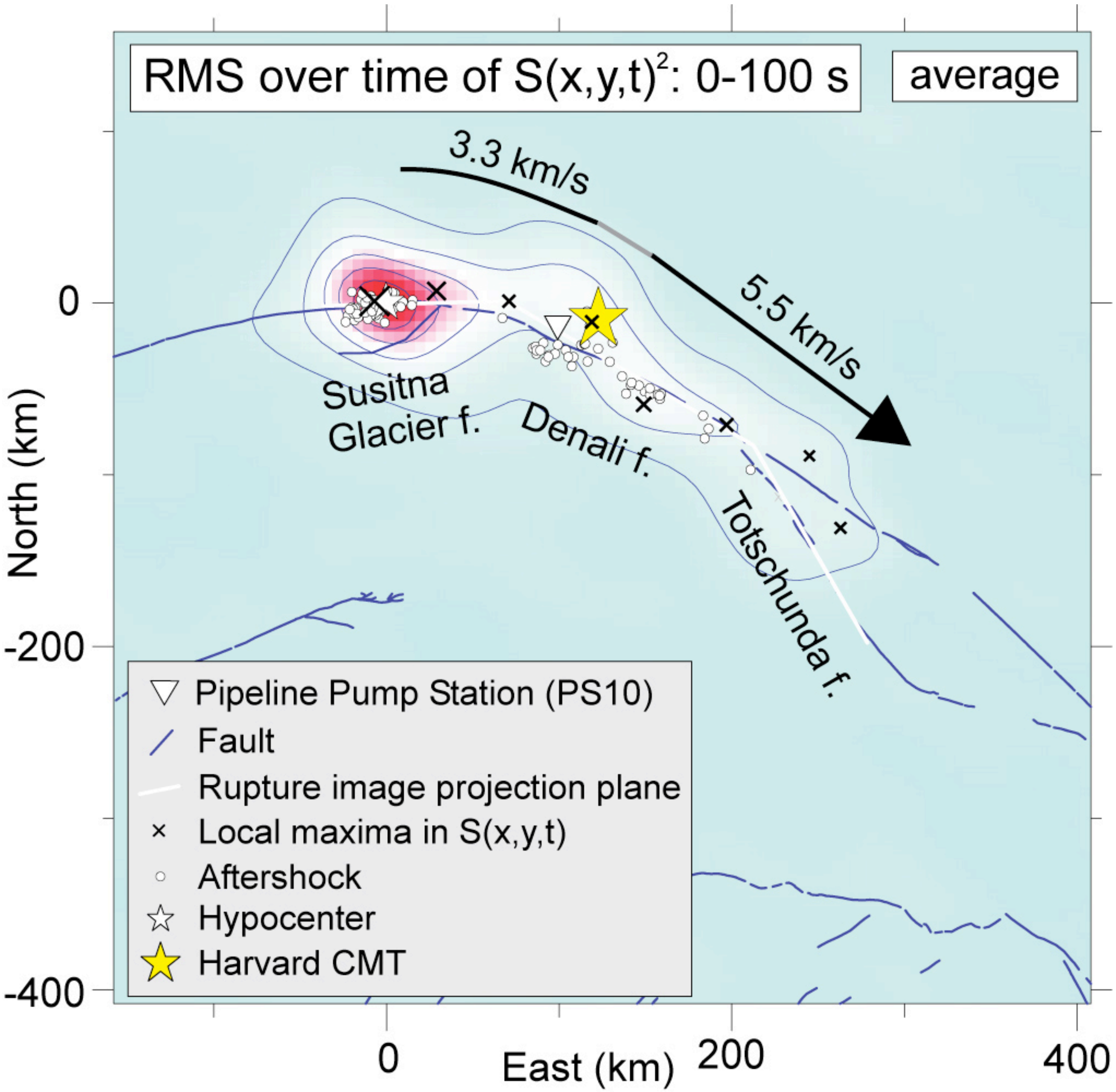

# Denali Time Slices (normalized by frame max)

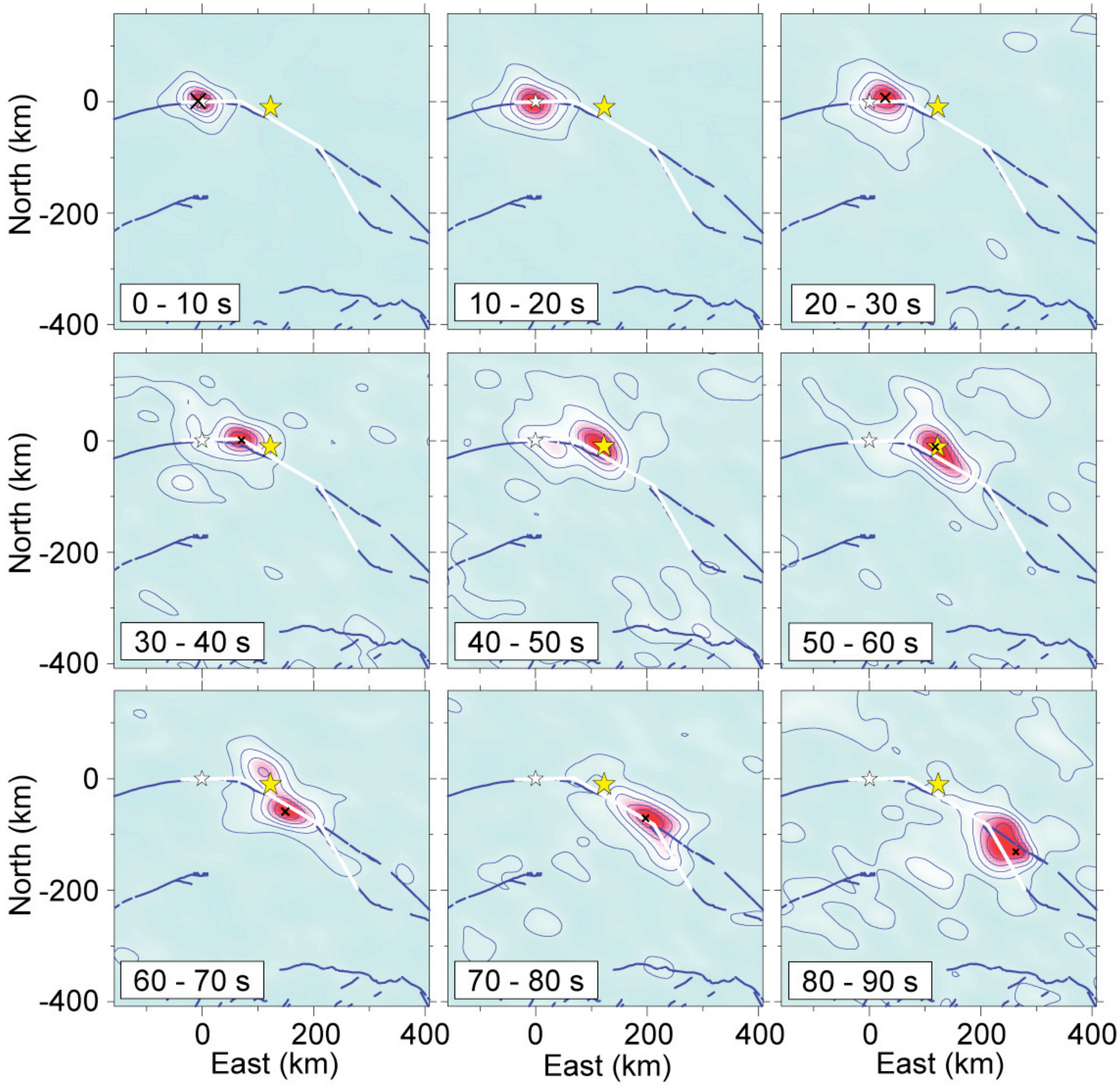

# Denali Rupture Image (along-strike)

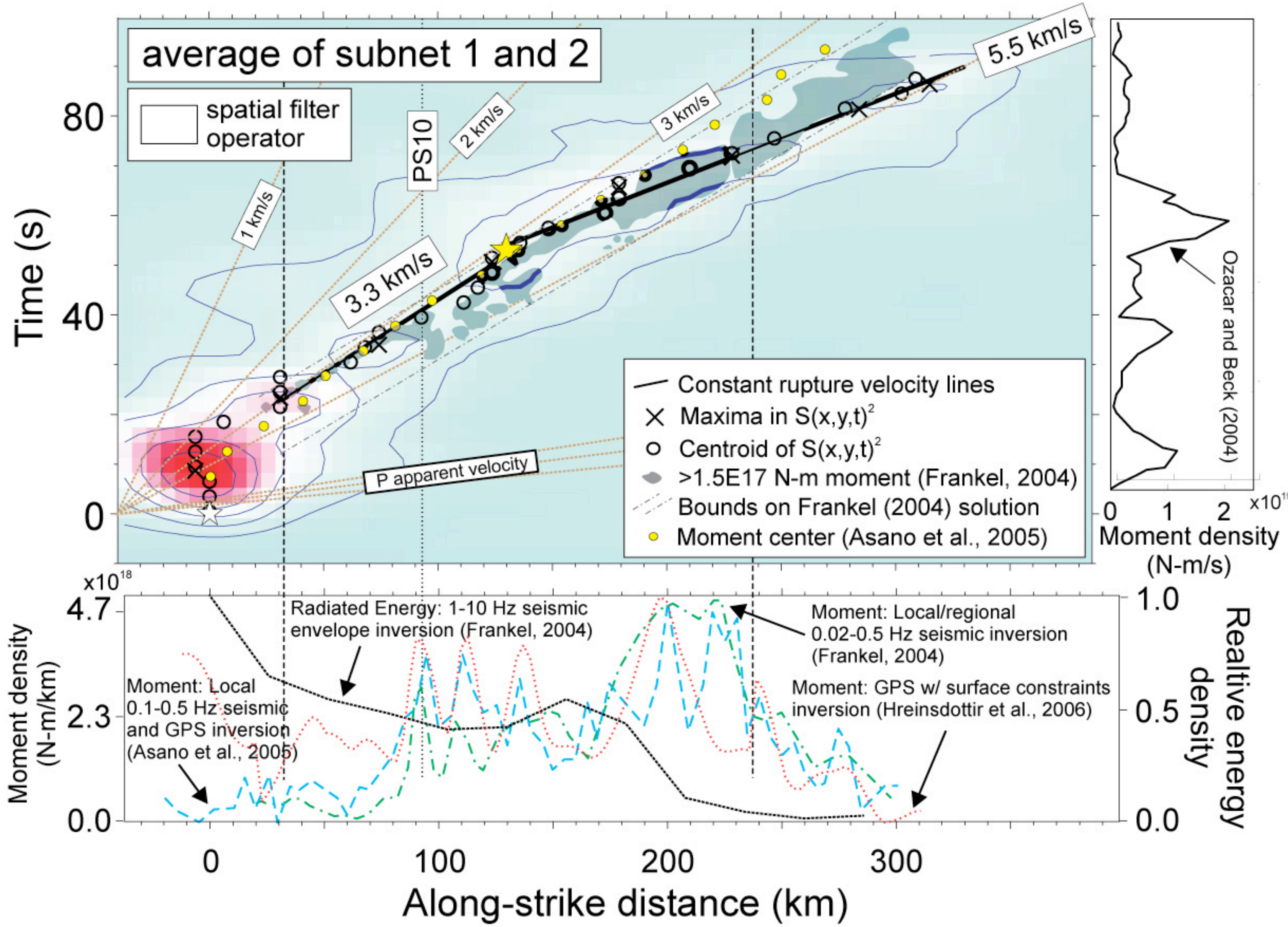

# Synthetic Imaging Tests

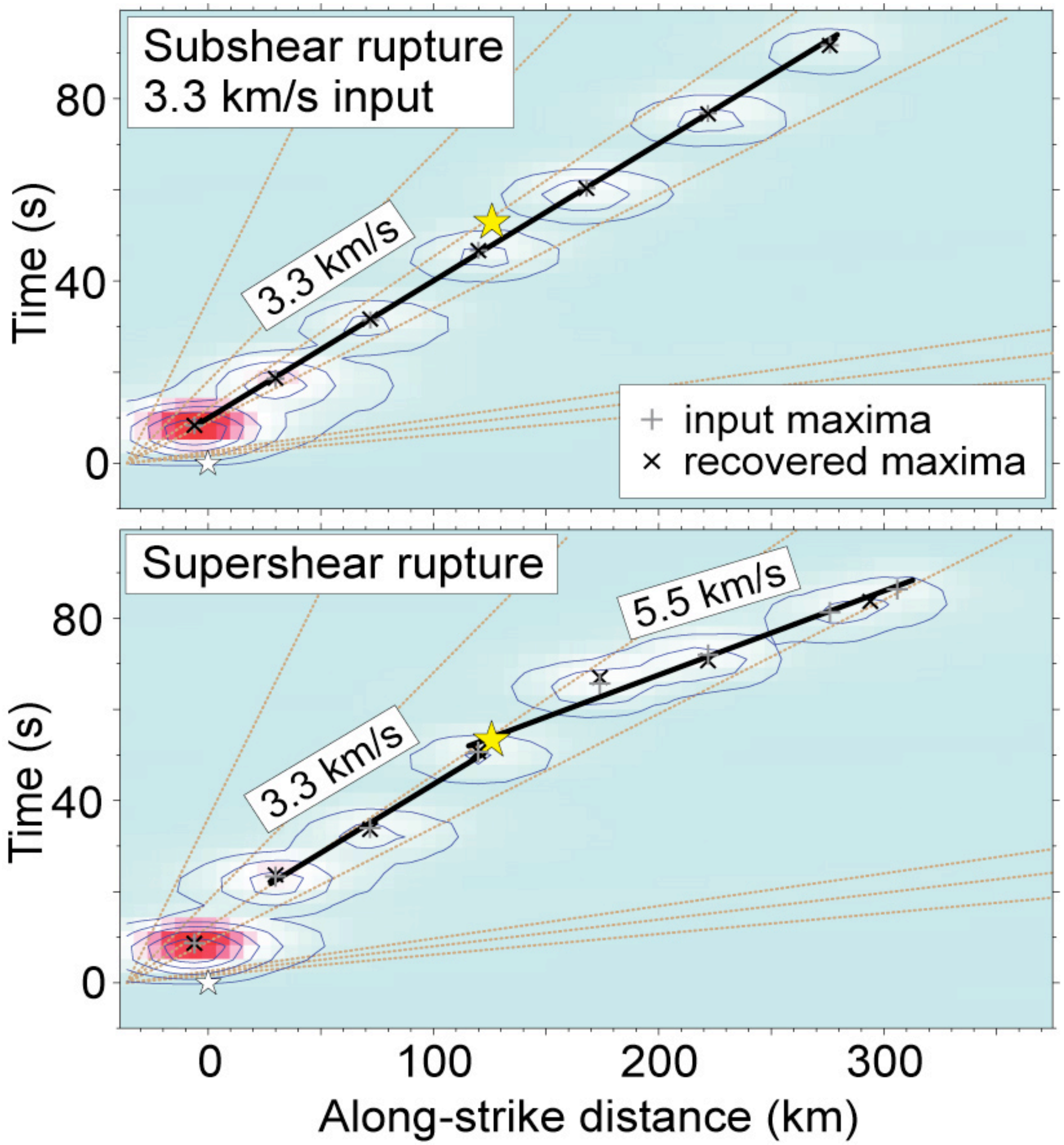


- Same strategy as with Kokoxili synthetic tests.
- Almost all maxima recovered.
- Supershear velocities are clearly distinguishable from subshear.

# Conclusions

- Both ruptures are remarkably similar, accelerating from roughly subshear to a near-sonic rupture speed over a transition distance no greater than 40 km after rupturing about 1/3 of the rupture length.

- Our preferred near-sonic velocity is ~5.6 km/s, but we conservatively estimate a range of 4.5-6.5 km/s based on a number of tests and methods for tracking the rupture (i.e. we **can** rule out subshear velocities along the supershear segments)

- There is an interesting burst of energy associated with the near-sonic rupture segment of the Kunlun Fault, but no such burst near the end of the Denali rupture.

- The triggering by adjacent faults, near-sonic rupture velocities, and long durations of near-sonic ruptures suggest that the main faults involved in this rupture had a generally homogeneous, weak fault strength.

- Kokoxili imaging results are consistent with those from Bouchon and Valée (2003), Robinson et al. (2006), and Vallée et al. (2008). Denali results are **not** inconsistent with those from Frankel (2004) and Dunham and Archuleta (2004).